Department of Energy
Carlsbad Field Office
P. O. Box 3090
Carlsbad, New Mexico 88221

February 20, 2025

Mr. Tom Peake, Director
Center for Waste Management and Regulations
William Jefferson Clinton Building, West
1301 Constitution Ave NW, Mail Code 6608T
Washington, D.C. 20004

Subject: Response to the U.S. Environmental Protection Agency's Request for a Twelve-Panel PA Sensitivity Study for EPA's Review of the Waste Isolation Pilot Plant Replacement Panel Planned Change Request

Reference: EPA letter from Tom Peake to Michael Gerle, dated November 26, 2024; Subject: Twelve-Panel PA Sensitivity Study for EPA's Review of the Waste Isolation Pilot Plant Replacement Panel Planned Change Request

Dear Mr. Peake:

Enclosed is the Analysis Report performed in response to the Environmental Protection Agency's (EPA) letter on November 26, 2024, requesting that the Department of Energy provide a twelve-panel PA sensitivity study to supplement the calculations provided in the Replacement Panels Planned Change Request.

If you have any questions, please contact Dr. Anderson Ward, Compliance Certification Manager, Environmental Regulatory Compliance Division, at (575) 988-5414.

Sincerely,

MICHAEL GERLE

Digitally signed by MICHAEL GERLE
Date: 2025.02.20 16:24:53 -07'00'

Michael Gerle, Director
Environmental Regulatory
Compliance Division

Enclosure

cc: w/enclosure

M. Bollinger, CBFO	* ED	R. Salness, SIMCO	ED
B. Forinash, CBFO	ED	J. Settle, SIMCO	ED
G. Basabilvazo, CBFO	ED	S. Strong, SIMCO	ED
Z. Lepchitz, CBFO	ED	A. Waldram, SIMCO	ED
M. Navarrete, CBFO	ED	M. Cook, SIMCO	ED
A. Ward, CBFO	ED	K. Day, SIMCO	ED
J. Adkins, CBFO	ED	S. Harper, SIMCO	ED
R. Chavez, SIMCO	ED	J. Haschets, SIMCO	ED
R. Flynn, SIMCO	ED	R. Hernandez, SIMCO	ED
M. Gonzales, SIMCO	ED	M. Serrano, SIMCO	ED
M. Jones, SIMCO	ED		

*ED denotes electronic distribution

CBFO:ERCD:MG:RS:25-0064

SANDIA NATIONAL LABORATORIES
WASTE ISOLATION PILOT PLANT

Analysis Report for a 12-panel PA Sensitivity Study

Revision 0

Author:	Todd R. Zeitler	TODD ZEITLER (Affiliate) Digitally signed by TODD ZEITLER (Affiliate) Date: 2025.01.13 11:23:39 -07'00'	
	Print	Signature	Date
Author:	James Bethune	James Bethune Digitally signed by James Bethune Date: 2025.01.14 15:33:14 -07'00'	
	Print	Signature	Date
Author:	Sarah Brunell	SARAH BRUNELL (Affiliate) Digitally signed by SARAH BRUNELL (Affiliate) Date: 2025.01.14 08:15:46 -07'00'	
	Print	Signature	Date
Author:	Paul Docherty	PAUL DOCHERTY (Affiliate) Digitally signed by PAUL DOCHERTY (Affiliate) Date: 2025.01.14 08:29:04 -07'00'	
	Print	Signature	Date
Author:	Sungtae Kim	SUNGTAE KIM (Affiliate) Digitally signed by SUNGTAE KIM (Affiliate) Date: 2025.01.14 08:38:56 -07'00'	
	Print	Signature	Date
Author:	Seth King	SETH KING (Affiliate) Digitally signed by SETH KING (Affiliate) Date: 2025.01.14 07:12:17 -07'00'	
	Print	Signature	Date
Author:	Justin Wilgus	Justin Wilgus Digitally signed by Justin Wilgus Date: 2025.01.14 08:57:55 -07'00'	
	Print	Signature	Date
Technical Review:	Clifford Hansen	CLIFFORD HANSEN (Affiliate) Digitally signed by CLIFFORD HANSEN (Affiliate) Date: 2025.01.14 09:33:03 -07'00'	
	Print	Signature	Date
QA Review:	Shelly Nielsen	Shelly R. Nielsen Digitally signed by Shelly R. Nielsen Date: 2025.01.14 09:46:25 -07'00'	
	Print	Signature	Date
Management Review:	Steve Wagner	STEPHEN WAGNER (Affiliate) Digitally signed by STEPHEN WAGNER (Affiliate) Date: 2025.01.14 10:16:39 -07'00'	
	Print	Signature	Date

This page intentionally left blank.

Executive Summary

The Department of Energy (DOE) has submitted a Planned Change Request (PCR) for use of two new panels at the Waste Isolation Pilot Plant (WIPP), termed replacement panels, to provide disposal capability equivalent to the unused volume in the current 10-panel design. The DOE may consider excavating up to seven panels beyond the two replacement panels, defined here as additional panels. The Replacement Panels Planned Change Request (RPPCR) PA was executed by Sandia National Laboratories (SNL) to quantify the long-term performance of the repository with both replacement and additional panels.

As part of their review of the PCR, the Environmental Protection Agency (EPA) has requested an analysis of repository performance with only the replacement panels and not the additional panels. This report details the results of that analysis (CRA19_12P) and compares the CRA19_12P results with those of the CRA19 PA conducted for the 2019 compliance recertification application. The CRA19_12P PA was performed in accordance with the SNL WIPP QA procedure NP 9-1.

The CRA19_12P PA calculations differ from the CRA19 calculations by considering the two replacement panels that increase the assumed repository volume and footprint. In general, differences between the results of the CRA19 and CRA19_12P calculations are minor. A slight increase in early time repository pressures and a slight decrease in late time pressures is observed. The expanded volume of the repository is seen as the driver for a decrease in late time pressures. A general decrease in brine saturation is also observed. As a result, direct brine release volumes are smaller in the CRA19_12P analysis.

With an increased repository footprint, the number of intrusions also increases. The assumed radionuclide inventory is the same for the CRA19 and CRA19_12P calculations. However, by spreading that inventory over a larger repository volume and footprint, solid waste volume concentration decreases. With increased intrusions and decreased solid waste volume concentration, there is little resulting difference in cuttings and cavings releases. Mobile radionuclide concentrations are generally unchanged. An additional point of release for radionuclides traveling from the repository to the Culebra was implemented above Panels 11 and 12; the travel times from this second release point were longer than for the original point above Panels 1-10. Spallings releases and DBRs are slightly decreased and releases from the Culebra are slightly increased at lower probabilities.

Total mean normalized releases are similar between the CRA19 and CRA19_12P analyses at the highest probabilities. At lower probabilities, releases are slightly lower in the CRA19_12P than in the CRA19. The total mean normalized releases are shown to be less than the release limits specified by the Certification Criteria in Title 40 CFR Part 194. Overall, the impact of two additional waste panels on the long-term performance of the repository is minimal.

Sandia National Laboratories is a multimission laboratory managed and operated by National Technology & Engineering Solutions of Sandia, LLC, a wholly owned subsidiary of Honeywell International Inc., for the U.S. Department of Energy's National Nuclear Security Administration under contract DE-NA0003525. This research is funded by WIPP programs administered by the Office of Environmental Management (EM) of the U.S. Department of Energy.

Table of Contents

List of Figures

List of Tables

This page intentionally left blank.

1 Introduction and Objectives

The Waste Isolation Pilot Plant (WIPP), located in southeastern New Mexico, has been developed by the U.S. Department of Energy (DOE) for the geologic (deep underground) disposal of defense-related transuranic (TRU) waste. Containment of TRU waste at the WIPP facility is derived from standards set forth in Title 40 of the Code of Federal Regulations (CFR), Part 191. The DOE assesses compliance with the containment standards according to the Certification Criteria in Title 40 CFR Part 194 by means of Performance Assessment (PA) calculations performed by Sandia National Laboratories (SNL). WIPP PA calculations estimate the probability of radionuclide releases from the repository to the accessible environment for a regulatory period of 10,000 years after facility closure.

As currently approved by the Environmental Protection Agency (EPA), the WIPP includes ten excavated panels for the placement of waste. For operational reasons, not all of the volume of the ten excavated panels will be used for waste disposal. The DOE has submitted a Planned Change Request (PCR) for use of two new panels, termed replacement panels, to provide disposal capability equivalent to the unused volume. The DOE may consider excavating up to seven panels beyond the two replacement panels, defined here as additional panels. The Replacement Panels Planned Change Request (RPPCR) PA was executed by SNL to quantify the long-term performance of the repository with both replacement and additional panels (Brunell et al. 2024). The RPPCR PA followed the PA submitted for the 2019 compliance recertification application (CRA), called CRA19, and the PA for the additional panels peer review, called APPA (Additional Panels Performance Assessment).

As part of their review of the PCR, the EPA has requested a sensitivity analysis that does not include the additional panels (Ward 2024a and 2024b)[1]. This report details the results of a long-term performance analysis (CRA19_12P) in response to EPA's request. The analysis is intended to supplement the RPPCR and demonstrates the impact to the most recent compliance PA (CRA-2019 PA) of using two replacement panels for waste disposal. The approach taken for the CRA19_12P PA is summarized in Section 2 and detailed in Zeitler (2024). This assessment was performed in accordance with the SNL WIPP QA procedure NP 9-1 (Nielsen 2024).

[1] Note that a previous analysis estimated releases from a 12-panel repository (Hansen et al. 2023). However, that analysis was based on the RPPCR PA which included several substantial changes to parameters and process models in addition to the replacement and additional waste panels, and used scaling rules to estimate the releases attributable to Panels 1-12.

This page intentionally left blank.

2 Analysis Approach

The analysis approach consists of performing a PA calculation and comparing results to the CRA 2019 PA (CRA19 analysis). The CRA19 analysis assumed a 10-panel design, while the current analysis assumes a 12-panel design based on a reduced version of a proposed 19-panel repository design. Details on the planned analysis can be found in Zeitler (2024).

2.1 CRA19 12-Panel (CRA19_12P) Analysis

The CRA19_12P analysis differs from the CRA19 analysis in the assumed number of panels in which waste is distributed. This assumption impacts various model inputs which are discussed below. The details of the key inputs and assumptions for the PA calculations are provided in this section. Results of the PA calculations are discussed in Sections 3 through 11.[2]

2.1.1 Reference Calculation and Inventory

The CRA-2019 PA (CRA19 analysis) was performed as part of the CRA-2019 submitted by the DOE to the EPA in 2019 (DOE 2019). The CRA19 analysis assumed a 10-panel repository design. The inventory used in the CRA19 analysis was based on the Performance Assessment Inventory Report – 2018 (PAIR-2018), which included inventory data collected through December 2017 (Van Soest 2018) and considered estimated future waste generation through calendar year 2033. The inventory input included scaling factors that resulted in a total waste inventory volume equal to the disposal limits (i.e., 168,485 m^3 for contact-handled (CH)-TRU and 7,079 m^3 for RH-TRU). An assumption was made in that analysis that the entire waste volume would fit into a 10-panel repository footprint. The inventory did not include a later change to the way in which waste volume is calculated for some disposal containers (NMED 2023).

The results of the CRA19_12P analysis are also compared with the results of the APPA. The APPA utilized the same inventory and input parameters as the CRA19 with a 19-panel repository layout. This consistency in inventory and input parameters allows for a direct evaluation of how variations in the number of waste panels – 10 in the CRA19, 12 in the CRA19_12P, and 19 in the APPA – impact performance outcomes. By analyzing these three scenarios, we can gain valuable insights into the relationship between panel quantity and overall system performance, thereby enhancing our understanding of repository behavior under different configurations.

2.1.2 Modeling Modifications for the CRA19_12P

A proposed design for the WIPP repository includes an expanded repository footprint and a total of 19 waste panels (Figure 2-1; Sjomeling 2019). The PCR (Bollinger 2024) seeks EPA approval for Panels 11 and 12 of this proposed design (Figure 2-2).

[2] Analysis files and post-processing scripts are archived in the WIPP PA CVS repository at: /data/cvs/CVSLIB/WIPP_EXTERNAL/CRA19_12P

As described in Brunell et al. (2024), the nine new waste panels in the 19-panel design consist of two replacement panels and seven additional panels to the west of the current repository. The proposed 19-panel design was considered in the APPA analysis (Brunell et al. 2021). A similar representation was used in the RPPCR analysis (Brunell et al. 2024). Only Panels 1-12 are considered in the CRA19_12P analysis. It is assumed that the modified design of 12 waste panels provides sufficient floorspace to accommodate the inventory.

Panels 11 and 12 will be similar to Panels 1 through 8, except that the abutment pillar widths (between the waste rooms and the access drift) are increased from 61.0 m (200 ft) to 122 m (400 ft) and the isolation pillar widths (separating any two panels) are increased from 61.0 m (200 ft) to 91.5 m (300 ft).

The area of a replacement panel is assumed to be the same as Panels 1-8, 11,642.12 m^2. The sum of the areas of the 12 panels is 135,456.84 m^2, which is represented in the calculations by parameter REFCON:AREA_CH. In the PCR, an approximate footprint of the berm area surrounding the footprint of the repository was represented as two rectangular footprints, one for the current 10-panel footprint and one for the footprint of the two replacement panels (Bollinger 2024). The sum of the areas of the two rectangles is 746,973 m^2. This area is rounded up to 750,000 m^2 for the CRA19_12P and is represented in the calculations by parameter REFCON:ABERM.

The volume of a replacement panel is assumed to be the same as Panels 1-8, 46,097.57 m^3. The sum of the volumes of the 12 panels is 530,600.50 m^3, which is represented in the calculations by parameter REFCON:VREPOS. The fraction of repository volume occupied by CH waste (parameter REFCON:FVW) is calculated as the ratio of the Land Withdrawal Act CH waste maximum volume (168,500 m^3) to REFCON:VREPOS; for the CRA19_12P, REFCON:FVW has a value of 0.318. Parameter changes are summarized in Section 2.1.5.

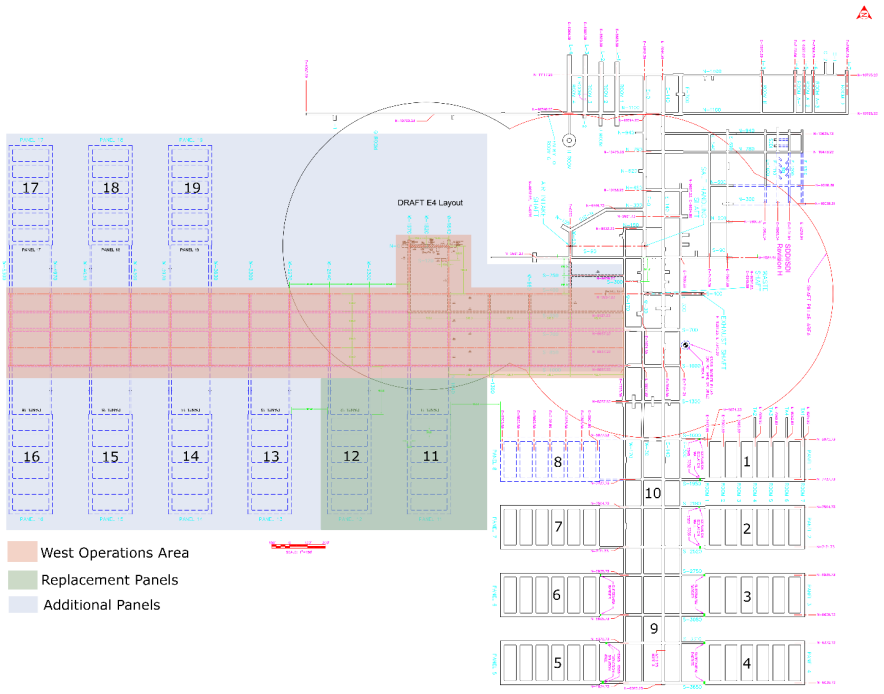

Figure derived from Sjomeling, (2019).

Figure 2-1: Current Repository Footprint, Replacement Panels and Additional Waste Panels.

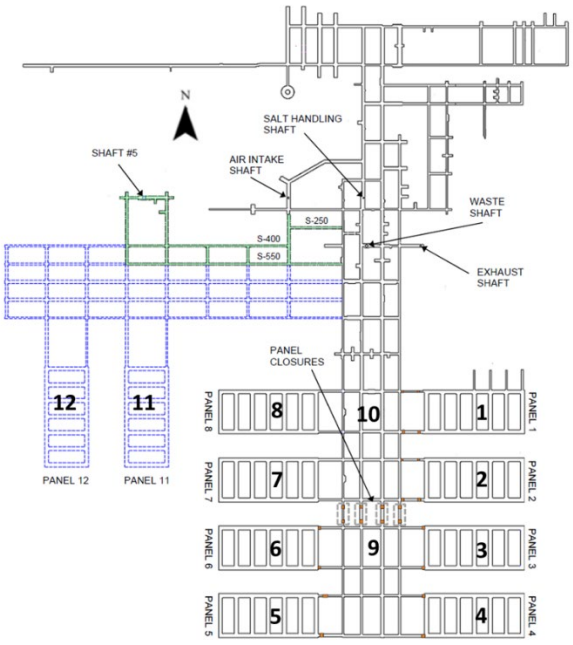

Figure 2-2: Repository Footprint for CRA19_12P (adapted from Figure 1 of Bollinger (2024).

2.1.2.1 Two-Phase Flow Computational Grid

The CRA19 BRAGFLO grid represented the repository with three waste areas: (1) the "waste panel" (WP) representing Panel 5; (2) the "south rest-of-repository" (SROR) representing Panels 3, 4, 6, and 9; and (3) the "north rest-of-repository" (NROR) representing Panels 1, 2, 7, 8, and 10.

For the CRA19_12P analysis, a repository representation is used which incorporates the excavated volume of 12 panels (Figure 2-3). With the inclusion of western panels, the repository floor plan assumes an "L" shape rather than the generally linear, north-south geometry in the current (i.e., CRA19) repository floor plan. To represent this geometry in a 2D grid, the L shape is unbent to a linear arrangement of panel groups as depicted in Figure 2-3. The general regional dip of the Salado Formation is applied to the linear grid in the same way as was done for the APPA (Brunell et al. 2021). The rectangular flaring of the CRA19 grid is recalculated for the CRA19_12P analysis. A single representative borehole continues to be used as a conservative representation of an intrusion into any waste panel; the borehole is located in the South Waste Panel, which tends to have higher saturation than the other panels.

The CRA19_12P BRAGFLO grid differs from the RPPCR grid in the volumes of the West Operations and West Rest-of-Repository areas, which have been scaled down from the 19-panel representation to the 12-panel representation. One remnant from the RPPCR grid is retained as a matter of convenience: the Castile brine reservoir is represented with the same grid cells as in the RPPCR because the CRA19_12P grid was developed from the RPPCR grid. The properties of the Castile Brine Reservoir are recalculated to match the reservoir brine volumes in the CRA19 analysis and the difference in grid cell volume is expected to be inconsequential.

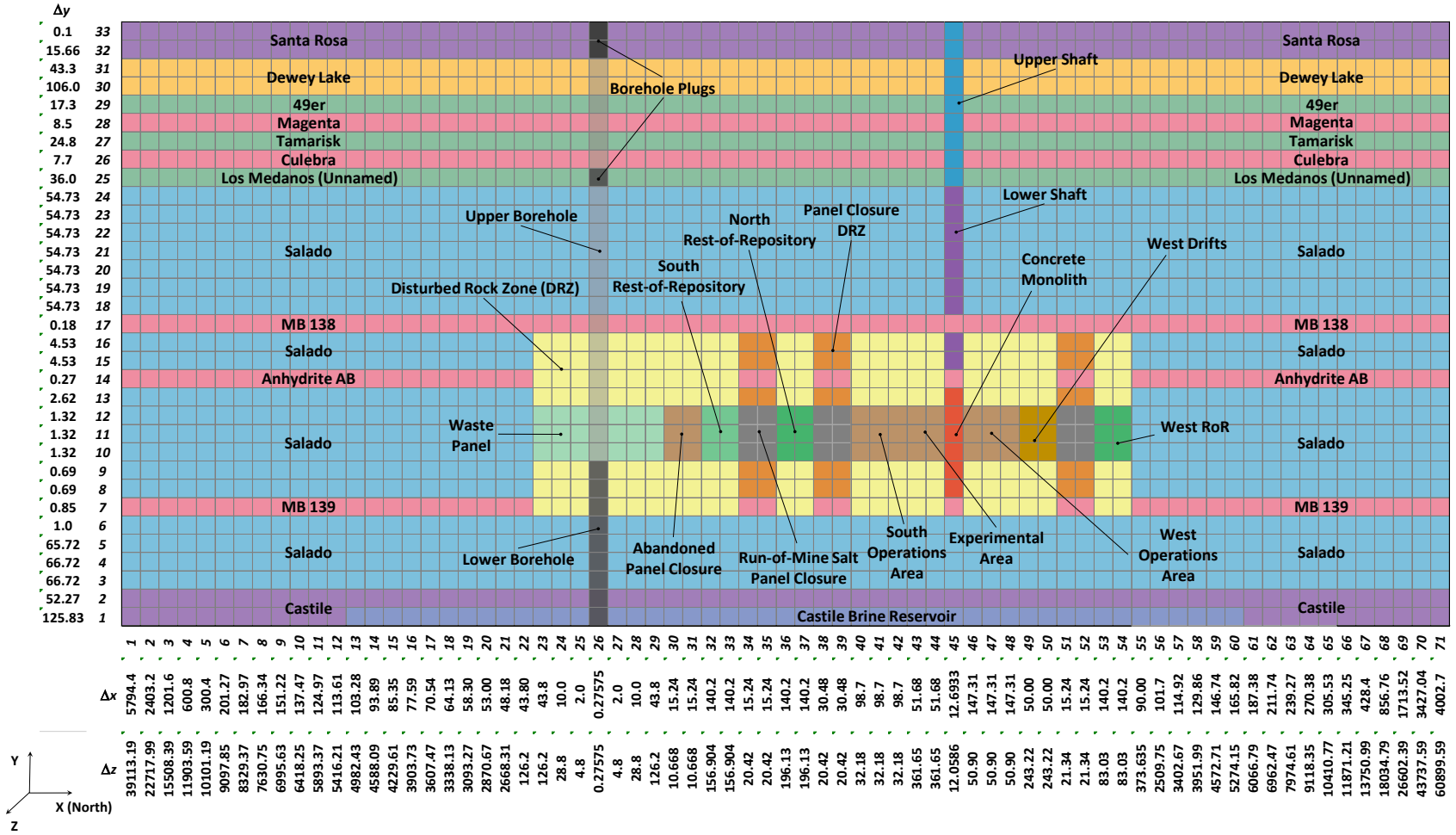

Figure 2-3: BRAGFLO Grid used in CRA19_12P Calculations with Modeled Area Descriptions (Δx, Δy, and Δz Dimensions in Meters)

This page intentionally left blank.

2.1.2.2 Direct Brine Release (DBR) Computational Grid

An additional computational grid is used in direct brine release (DBR) calculations. In the DBR grid, 10 panels were represented in the CRA19 analysis. For the CRA19_12P analysis, a DBR grid is used that has 11 waste areas and four possible intrusion locations (Figure 2-4). The same representation was used in the APPA (Brunell et al. 2021) and the RPPCR (Brunell et al. 2024) analyses.

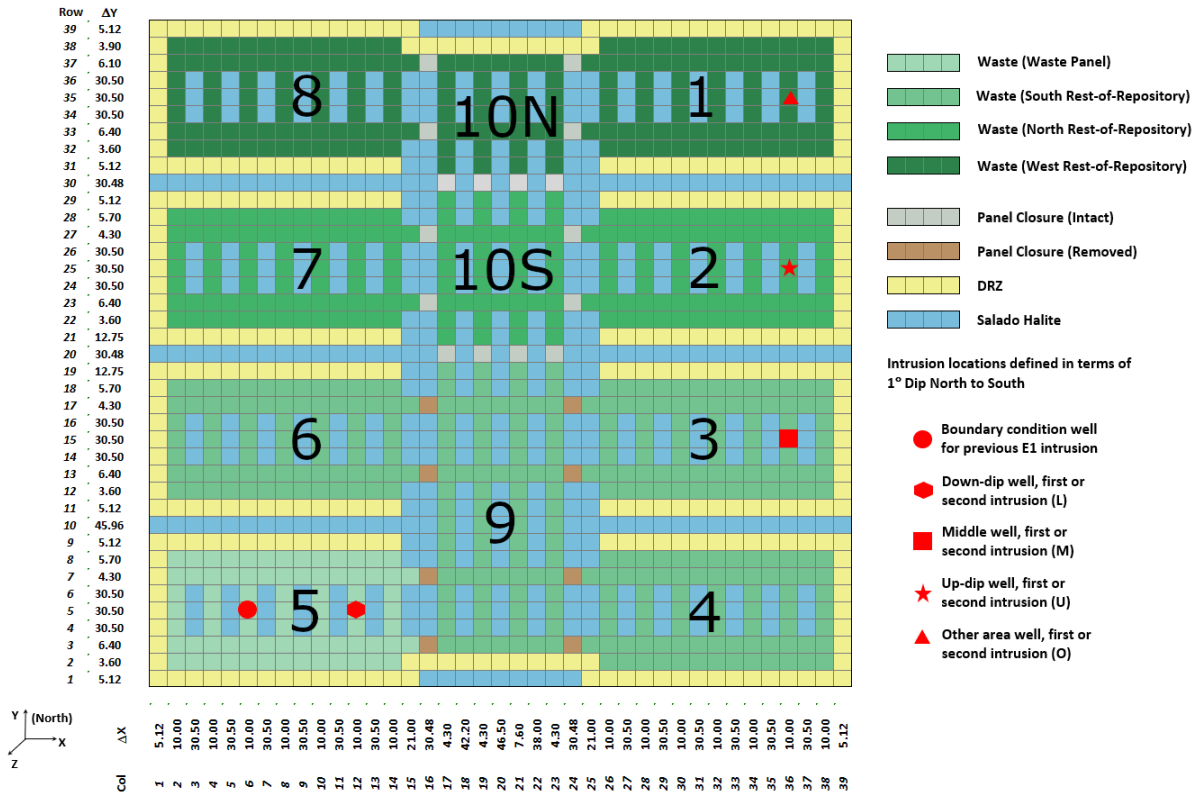

Figure 2-4: BRAGFLO Grid used in CRA19_12P DBR Calculations with Modeled Area Descriptions (Δx and Δy Dimensions in Meters)

2.1.2.3 Modeling Waste in Panels 9 and 10

For operational reasons, waste will not be emplaced in Panel 9 and only a limited amount of the volume of the planned Panel 10 will be available for waste emplacement. While there are operational plans to not emplace waste in Panel 9, the modeling of a panel with no waste but not separated from panels with waste by panel closures provides a challenge to the WIPP PA modeling framework. Areas of the repository not containing waste, but not separated from waste by panel closures, could contain radionuclide-contaminated brine that could be released to the environment if a borehole intrusion were to happen. Currently there is no mechanism in the PA to represent repository areas where intrusions could result in radionuclide releases from mobile brine but not releases from removed solid waste. This analysis assumes that waste will be emplaced in Panel 10. Since the volume of waste is fixed by the Land Withdrawal Act, modeling waste in Panel 9 and 10 reduces the concentration of waste in the other waste panels. The emplacement of waste in Panel 9 and 10 is assumed for the CRA19_12P analysis. In the CRA19_12P analysis, the waste inventory is represented as homogeneous for flow, transport,

and chemistry over the volume of the repository[3]; the repository volume (parameter REFCON:VREPOS and the total of the waste area volumes in the BRAGFLO grid) is the volume of the 12 waste panels.

2.1.2.4 Operations and Experimental Area Representations

For the CRA19_12P analysis, the operations area in the CRA19 BRAGFLO grid is renamed the South Operations area and is unchanged in dimensions. A new West Operations area represents drifts to the new panels and access drifts to the fifth shaft, as was done in the APPA and RPPCR analyses. The West Operations area is also implemented to represent drifts in the western part of the repository; the West Operations area is reduced in volume from the APPA and RPPCR analyses. The volume of the access drifts to the fifth shaft is included in the West Operations Area, rather than in the Experimental area as was done for the CRA19 analysis.

2.1.2.5 Waste Panel Neighbor Relationships

The CRA19 analysis classified panels into one of three groups as determined by the number of panel closures separating each waste panel from Panel 5: same, adjacent (i.e., zero or one intervening panel closures), and non-adjacent (i.e., two or more intervening panel closures) (Brunell 2019). For the CRA19_12P analysis, the panel neighbor groups are extended to same, connected, adjacent, and non-adjacent. Two panels are connected if there are no intervening panel closures (e.g., Panels 4 and 5 are connected). Two panels are adjacent if both panels are in the same half of the repository (i.e., south or west) but are separated by one or more intervening panel closure (e.g., Panels 1 and 5 are adjacent). Two panels are non-adjacent if the panels are in different halves of the repository (e.g., Panels 1 and 11 are non-adjacent). The path between panels is traced through excavated areas only. For Panels 1-10, the panel neighboring is the same as in the APPA and the RPPCR. For Panels 11 and 12, the panel neighboring in the CRA19_12P is changed from the APPA and the RPPCR such that these two panels are only adjacent to each other (Table 2-1).

Panel intrusion probabilities are based on the areas of the panels (note that Panels 9 and 10 are slightly smaller than the other 10 panels). Panels 1-8, 11, and 12 are assumed to have the same footprints, 11,642.12 m^2 each. The areas of Panels 9, and 10 are 9,145.52 m^2 and 9,890.15 m^2, respectively. Panel intrusion probabilities are calculated as the ratio of a panel area to the total area (REFCON:AREA_CH).

[3] Previous analyses have considered different waste emplacement schemes and determined that the mean releases were not significantly impacted by those schemes (Hansen et al. 2003, Casey et al. 2003, King et al. 2024).

Table 2-1: Panel Neighbors in the CRA19_12P Analysis

Intruded Panel	Intrusion Probability	Connected Panels	Adjacent Panels
1	0.085947056	-	2 through 10
2	0.085947056	-	1, 3 through 10
3	0.085947056	4, 5, 6, 9	1, 2, 7, 8, 10
4	0.085947056	3, 5, 6, 9	1, 2, 7, 8, 10
5	0.085947056	3, 4, 6, 9	1, 2, 7, 8, 10
6	0.085947056	3, 4, 5, 9	1, 2, 7, 8, 10
7	0.085947056	-	1 – 6, 8, 9, 10
8	0.085947056	-	1 – 7, 9, 10
9	0.067516137	3, 4, 5, 6	1, 2, 7, 8, 10
10	0.073013306	-	1 through 9
11	0.085947056	-	12
12	0.085947056	-	11

2.1.2.6 Minimum Brine Volume for a DBR and Baseline Solubilities

The minimum brine volume needed for a Direct Brine Release (DBR) event to occur (GLOBAL:DBRMINBV) is set by assuming the entire repository is at the average residual brine saturation (Clayton 2008). Baseline solubilities for An(III), An(IV), and An(V) radionuclides in Salado and Castile brines are then calculated at five integer multiples of the minimum brine volume (1X through 5X). The An(III) and An(V) baseline solubilities decrease as the brine volume increases primarily due to the reduced concentration of organic ligands. An(IV) solubilities are relatively unchanged by the brine volume.

The PANEL code is used in the PA calculation to determine total mobile radionuclide concentrations at five panel brine volumes; panel brine volumes are converted from the five repository brine volumes used in the baseline solubility calculations. When calculating direct brine releases, the radionuclide concentration in the brine in the intruded panel is linearly interpolated from the concentrations in the five panel brine volumes output from PANEL. If the volume of brine in the intruded panel is outside the range of the five panel brine volumes where concentrations are calculated, the nearest panel brine volume is used (i.e., no extrapolation is done).

The CRA19_12P analysis uses the baseline solubilities calculated for the CRA19. For consistency, the minimum brine volume for a DBR event to occur is also kept at the CRA19 value. Consequently, in the CRA19_12P, radionuclide concentrations for DBR releases are computed over a lower range of panel-scale brine volumes (1,511.7 – 7,558.4 m^3 of brine) than in the CRA19 (1,829.6 – 9,147.9 m^3 of brine) due to the increased repository volume in the CRA19_12P. The reduced range of panel-scale brine volumes could lead to more DBR events with brine volumes greater than the maximum of this range. For these events, the radionuclide concentration is the concentration at the maximum panel-scale brine volume, which for An(III) and An(V) radionuclides is expected to be higher than if the concentration was calculated at the actual brine volume. This approach ensures a conservative estimate of DBR releases in the CRA19_12P analysis.

2.1.3 Features, Events, and Processes (FEPs) Analysis

For a typical compliance calculation, an assessment is performed that identifies the features, events, and processes (FEPs) that need to be included in the PA calculations. The FEPs analysis performed for the CRA19 (Kirkes 2019) was updated for the APPA (Kirkes 2021) when considering a 19-panel repository representation. The APPA FEPs analysis resulted in no changes to FEPs screening decisions. Because the current analysis considers a 12-panel repository representation with similar treatment of the waste areas as implemented in the APPA, the Kirkes (2021) FEPs screening is sufficient for the CRA19_12P analysis.

2.1.4 Culebra Flow and Transport

The Culebra Dolomite constitutes a potential pathway for lateral migration of contaminated brine from a drilling intrusion into the repository accompanied by brine flow up the intrusion borehole. Simulations of Culebra flow and radionuclide transport evaluate the potential for radionuclides to reach the LWB from discharge locations over the WIPP repository footprint.

The CRA19_12P Culebra flow model is unchanged from the model first documented in the 2009 Performance Assessment Baseline Calculation (Kuhlman 2010) and used in subsequent CRAs, including the CRA-2019. Culebra flow calculations are performed for two potash mining scenarios, including a partial mining scenario in which all outside of the LWB is assumed to be mined, and a full mining scenario in which all potash in the model domain is assumed to be mined. The CRA19 analysis simulated the Culebra flow model with the groundwater flow software MODFLOW-2000. The CRA19_12P analysis simulates flow in the Culebra using the same model inputs as were used in the CRA19 with the updated groundwater flow software MODFLOW6. The transmissivity fields (T-fields) used in the CRA19_12P analysis are the same as were used in the CRA19. The particle tracking software DTRKMF is used to characterize the flow fields by simulating the particle travel pathway and travel time from each release point to the LWB.

In the CRA19 analysis, 1 kg of each of ^{241}Am, ^{239}Pu, ^{234}U, and ^{229}Th was released at a single point (CRP 1 in Figure 2-5) at the centroid of Panels 1 through 10 during the first 50 years after repository closure (Kuhlman 2010) and the cumulative mass discharge at the WIPP LWB over the 10,000-year regulatory period is reported. The CRA19_12P analysis retains these simulations and additionally simulates releases above the centroid of the replacement panels Panel 11 and Panel 12 (CRP 2 in Figure 2-5). In the CRA19 and APPA analyses, releases into the Culebra were modeled above the centroid of Panels 1 through 10. Radionuclide transport is simulated with the WIPP PA software SECOTP2D.

Radionuclides may be transported *to the Culebra* via boreholes or through the shaft. The assumed release points into the Culebra are dependent on the location of the panels, which are divided into two groups. Group 1 is composed of the existing waste area, Panels 1 through 10, and Group 2 is composed of the replacement panels, Panels 11 and 12. The release point for Group 1 is labeled CRP 1 and the release point for Group 2 is labeled CRP 2. The CRA19 analysis used the CRP 1 release point as the location of the Culebra release point for the *undisturbed* repository scenario (there is no random panel intrusion in this scenario). The selection is changed to CRP 2 for the CRA19_12P analysis as it is the release point closest to the shaft. The selection of this release point for the undisturbed scenario is made in the CCDFGF

code workflow. The selection is not expected to be impactful because releases in the undisturbed scenario are typically negligible.

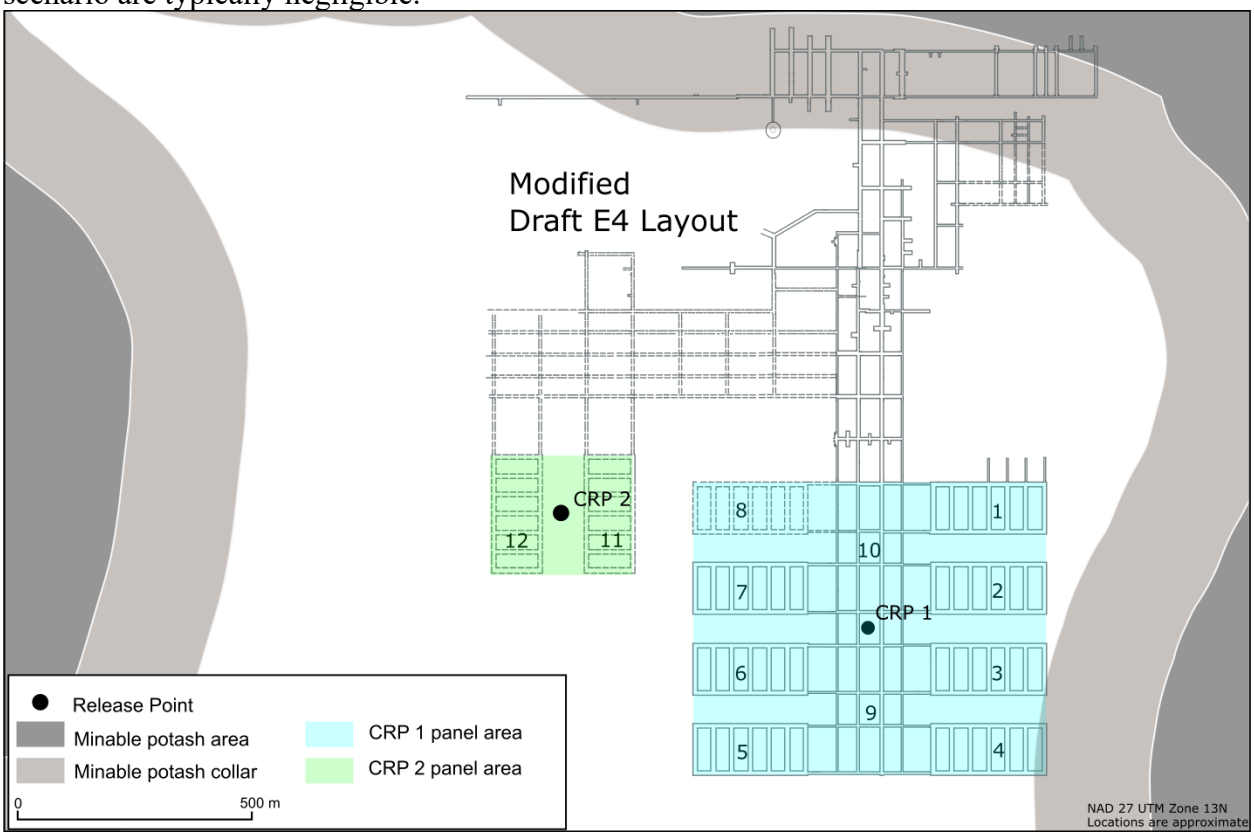

Figure 2-5: Culebra Release Point Locations

2.1.5 Summary of Parameter Changes

Table 2-2 lists parameter changes relative to the CRA19 analysis. The parameter values for the CRA19_12P analysis will be included in an unofficial version of the PA parameter database.

Table 2-2: Summary of Parameters Changed for the CRA19_12P Analysis

Material	Property	Description	CRA19 Value	CRA19_12P Value	Units
REFCON	VREPOS	Excavated storage volume of the repository	438,406.08	530,600.50	m^3
REFCON	ABERM	Area of the berm placed over waste panels	628,500	750,000	m^2
REFCON	AREA_CH	Area for contact-handled (CH) waste disposal	111,500	135,456.84	m^2
REFCON	FVW	Fraction of the repository volume occupied by waste	0.385	0.318	-

Since the running of the CRA19 analysis, all PA codes have been moved to a new hardware system, so all code versions have changed. Additionally, some codes have undergone additional changes to correct outstanding issues or improve capabilities. To facilitate an analysis in the CRA19_12P that most closely follows the CRA19 while using the most up-to-date versions of the codes, one change is necessary to the input files. The oxidation state cutoff values used to determine which radionuclide species dominate a given realization (i.e., property OXCUTOFF for materials PU, U, and NP) values were not CRA19 parameters, but are now expected by the PANEL code. The appropriate values to maintain equivalency with the CRA19 are added to the alg1_panel input file for the PANEL calculations. Also, the appropriate values are added to input files for the BRAGFLO and SECOTP2D calculations.

2.1.6 Comparison with the APPA

The APPA used the same inventory as the CRA19_12P. The APPA used a single Culebra release point while the CRA19_12P uses two release points. Changes to the CRA19 that were made for the APPA that are not included in the CRA19_12P analysis:

- Minor correction to actinide baseline solubilities.
- Modification of the Salado flow grid to accommodate the additional panels (Panels 13 through 19).

2.1.7 Comparison with the RPPCR

Changes to the CRA19 that were made for the RPPCR that are not included in the CRA19_12P analysis include:

- The updated iron surface area calculation.
- The updated porosity surface.
- The recalibrated Culebra transmissivity fields (T-fields).

- The third and fourth Culebra release points.
- The waste inventory.
- Updated baseline solubilities and solubility uncertainties.
- Updated borehole permeability distribution after cement plug degradation.
- Updated drilling rates and borehole plugging pattern probabilities.
- The updated probability of realizing Pu(III) versus Pu(IV).
- The updated Castile brine reservoir pore volume.

2.1.8 Code Execution

CRA19_12P was executed using the WIPP PA HPC/Linux Cluster. The CRA19_12P planning document specified a list of codes with versions that were planned to be used in the CRA19_12P PA. In addition to the codes in that list, the STEPWISE code (v2.23) was used to perform the parameter sensitivity analysis. The parameter database *ParamDB_ski* and results database *PA_Results_ski* were used.

This page intentionally left blank.

3 Parameter Sampling: LHS Calculations

The sampled parameters for the CRA19_12P are the same as in the CRA19. Although the results from the LHS code are unaffected by the changes made for the CRA19_12P, for simplicity in the run control process, LHS was rerun for the CRA19_12P PA using the same input as for the CRA19.

This page intentionally left blank.

4 Salado Flow: BRAGFLO Calculations

The Salado flow model calculates fluid flow in and around the repository for the 10,000-year regulatory period. The results of this model are presented in this section. Day (2019) describes the Salado flow model and results for the CRA19 in more detail.

4.1 Introduction

The PA code BRAGFLO calculates subsurface brine and gas flow in the repository and the surrounding area over a 10,000-year period using a two-dimensional, "flared" vertical cross section representation of the repository and surrounding area. In this grid representation (Figure 2-3), there are four waste areas: (1) the "waste panel" (WP) represents waste emplaced in Panel 5; (2) the "south rest-of-repository" (SROR) represents waste emplaced in Panels 3, 4, 6, and 9; (3) the "north rest-of-repository" (NROR) represents waste emplaced in Panels 1, 2, 7, 8, and 10; and (4) the "west rest-of-repository" (WROR) represents waste emplaced in Panels 11 and 12. The CRA19 analysis did not include the WROR area.

There are three non-waste areas modeled, the South operations (SOP) area, the experimental (EXP) area, and the West operations (WOP) area. In the CRA19, the SOP was referred to as the operations area (OPS), and there was no WOP area. There are also four panel closure areas (PCS): the "southernmost" PCS representation is between the WP and SROR (modeled as an abandoned panel closure with PCS_NO material properties), the "middle" PCS representation is between the SROR and NROR, the "northernmost" PCS representation is between the NROR and SOP area, and the "westernmost" PCS representation is between the WROR and the WOP area.

In the Salado flow calculations, stochastic uncertainty is addressed by defining a set of six scenarios which vary in the time and type of intrusion. The scenarios include one undisturbed scenario (S1-BF), four scenarios that include a single inadvertent future drilling intrusion into the repository during the 10,000-year regulatory period (S2-BF to S5-BF), and one scenario investigating the effect of two intrusions into a single waste panel (S6-BF).

The major assumptions used in the BRAGFLO grid for the Salado flow model for the APPA (Brunell et al. 2021) were reviewed by the APPA Changed Conceptual Models Peer Review. The peer review panel found the assumptions to be well justified and the model adequate and reasonable for its intended application (Falta et al. 2021). While the CRA19_12P analysis only includes 12 waste panels instead of the 19 waste panels used in the APPA, the CRA19_12P BRAGFLO grid uses the same major assumptions as the APPA BRAGFLO grid.

Two types of intrusions, denoted as E1 and E2, are considered. An E1 intrusion assumes the borehole passes through a waste-filled panel and into a pressurized brine pocket that may exist under the repository in the Castile formation. An E2 intrusion assumes that the borehole passes through the repository but does not encounter a brine pocket. Scenarios S2-BF and S3-BF model the effect of an E1 intrusion occurring at 350 years and 1,000 years, respectively, after the repository is closed. Scenarios S4-BF and S5-BF model the effect of an E2 intrusion at 350 and 1,000 years. Scenario S6-BF models an E2 intrusion occurring at 1,000 years, followed by an E1

intrusion into the same panel at 2,000 years. Table 4-1 summarizes the six scenarios used in this analysis.

Epistemic uncertainty in, for example, material properties, is addressed by parameter sampling. Uncertain parameters are sampled in three independent replicates each of size 100; an element in one sample is termed a vector as it comprises values for each uncertain parameter. The total number of BRAGFLO simulations executed in the CRA19_12P PA is 1,800 (3 replicates of 100 vectors times 6 scenarios).

Table 4-1: BRAGFLO Modeling Scenarios

Scenario	Description
S1-BF	Undisturbed Repository
S2-BF	E1 intrusion at 350 years
S3-BF	E1 intrusion at 1,000 years
S4-BF	E2 intrusion at 350 years
S5-BF	E2 intrusion at 1,000 years
S6-BF	E2 intrusion at 1,000 years; E1 intrusion at 2,000 years.

4.2 Results

The Salado flow model results are presented in this section. Pressure in the waste areas, brine saturation in the waste areas, and brine flow up the borehole are the drivers of radionuclide releases communicated from the Salado flow model to downstream PA codes. Gas generation results can help to understand repository pressure, brine saturation, and brine flows. These will be the results focused on in this section. Only results for the first replicate will be discussed, results for the other two replicates show the same trends.

4.2.1 Fluid Pressure

Statistics on the mean pressure in the Waste Panel are shown in Table 4-2. The mean, minimum, and maximum pressure in the waste panel through time for Scenarios S1-BF, S2-BF, S4-BF, and S6-BF are shown in Figure 4-1, Figure 4-2, Figure 4-3, and Figure 4-4 respectively. In general, there is very little change in pressure between the CRA19 and CRA19_12P calculations. There is a slight increase in early time pressures and a slight decrease in late time pressures. An increased rate of iron corrosion, due to the iron surface area being a function of repository volume, is seen as the driver for the slight increase in early time pressures. The expanded volume of the repository including the increase in excavated non-waste areas is seen as the driver for the decrease in late time pressures.

Mean pressures in the South Rest-of-Repository (SROR) through time are shown in Figure 4-5. Pressures in the SROR closely follow pressures in the Waste Panel due to the lack of panel closures separating the two waste areas. Mean pressures in the North Rest-of-Repository (NROR) are shown in Figure 4-6. As with the other waste areas, pressures in the NROR are very similar between the CRA19 and CRA19_12P results.

The mean pressures in the West Rest-of-Repository (WROR) through time are shown in Figure 4-7 for the CRA19_12P results. The WROR did not exist in the CRA19, so there is no

comparison of these results. The WROR being farthest up-dip has the lowest pressures of all the waste areas. The pressure in the WROR is increased in scenarios with an E1 intrusion and decreased in scenarios with an E2 intrusion compared to the undisturbed scenario despite being on the opposite side of the repository from the intruded waste panel.

Table 4-2: Mean Waste Panel Pressure Statistics for the CRA19 and the CRA19_12P

	Mean Value[1] (MPa)	**Mean Value[1] (MPa)**	**Maximum Value[2] (MPa)**	**Maximum Value[2] (MPa)**
Scenario	CRA19	CRA19_12P	CRA19	CRA19_12P
S1-BF	4.95	4.94	6.49	6.22
S2-BF	9.96	9.80	11.20	11.46
S4-BF	3.44	3.47	4.33	4.19
S6-BF	7.02	6.99	8.53	8.76

Notes:
1 – Average over the time interval (0-10,000 years) of the Replicate 1 mean.
2 – Maximum over the time interval (0-10,000 years) of the Replicate 1 mean.

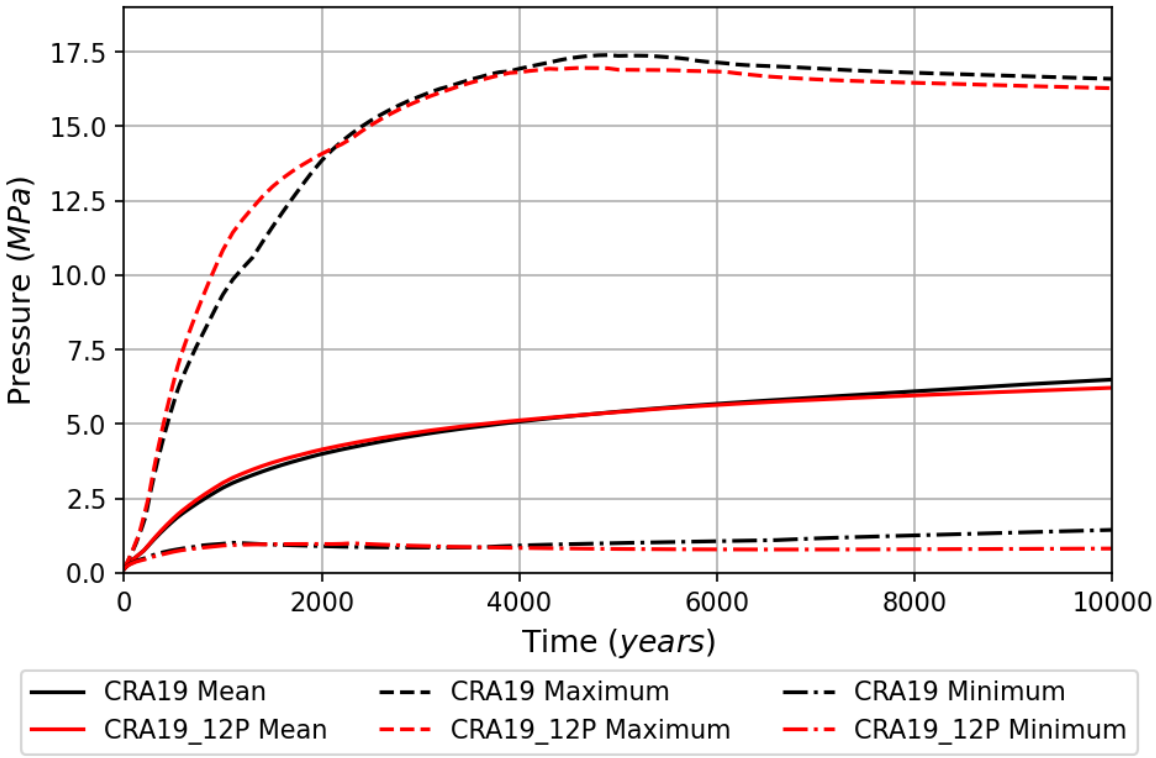

Figure 4-1: Pressure in the Waste Panel for Scenario S1-BF

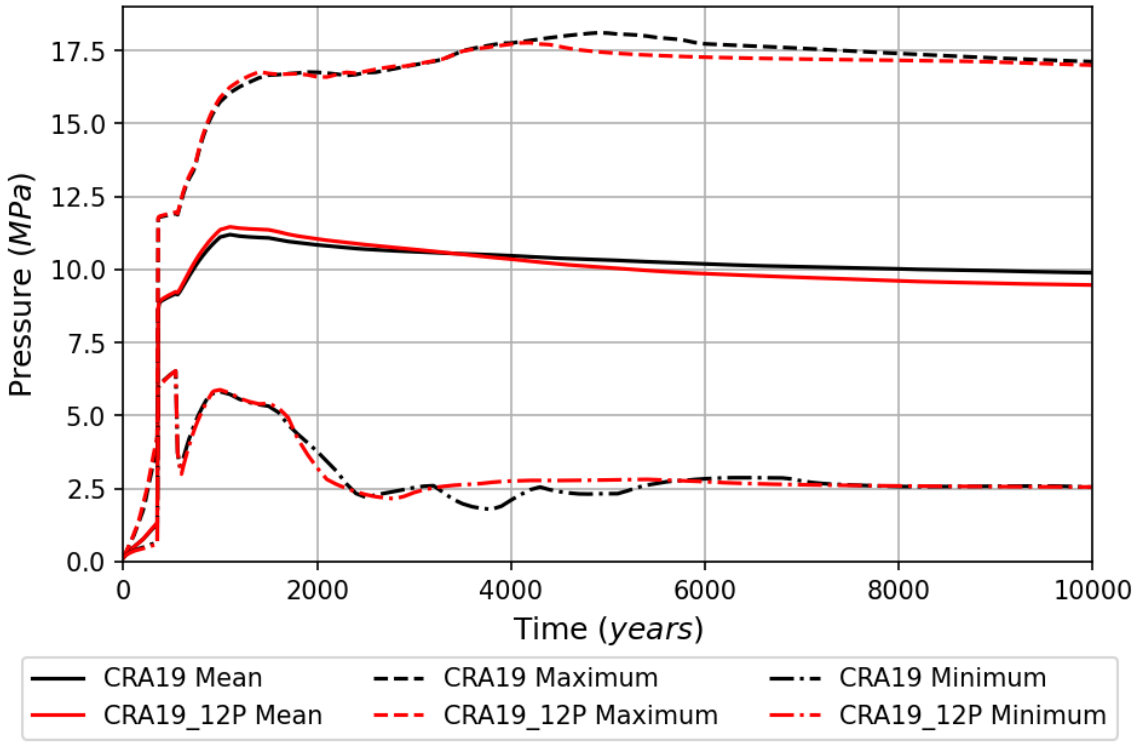

Figure 4-2: Pressure in the Waste Panel for Scenario S2-BF

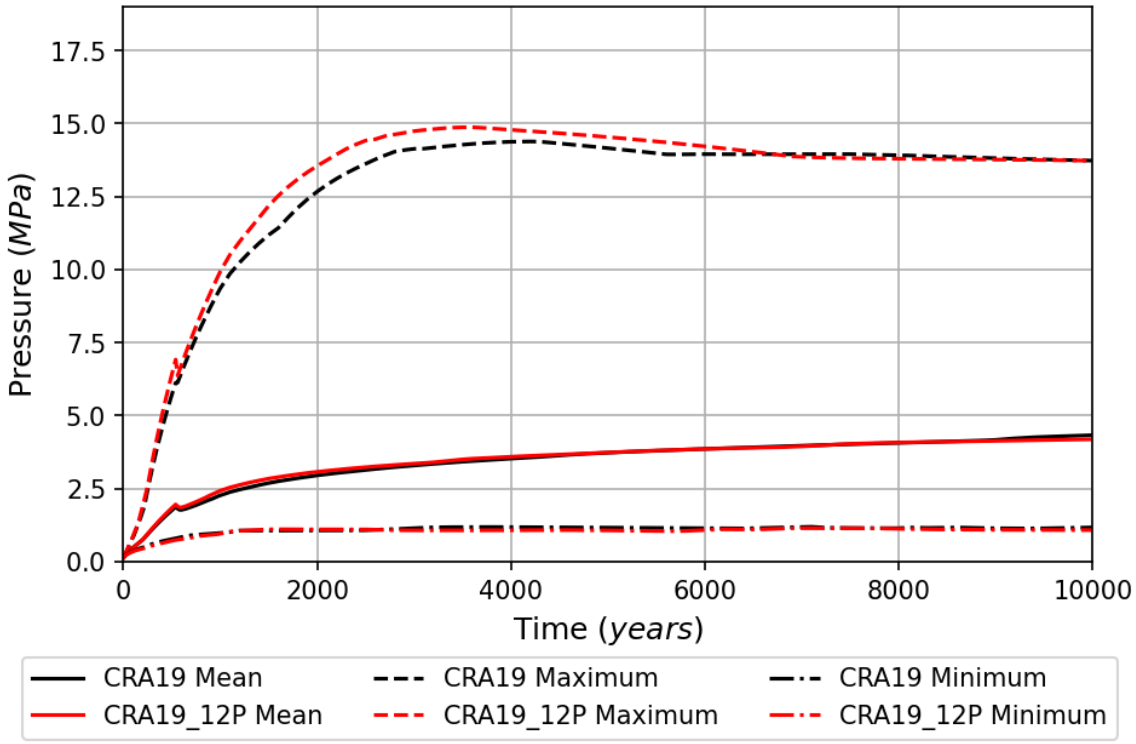

Figure 4-3: Pressure in the Waste Panel for Scenario S4-BF

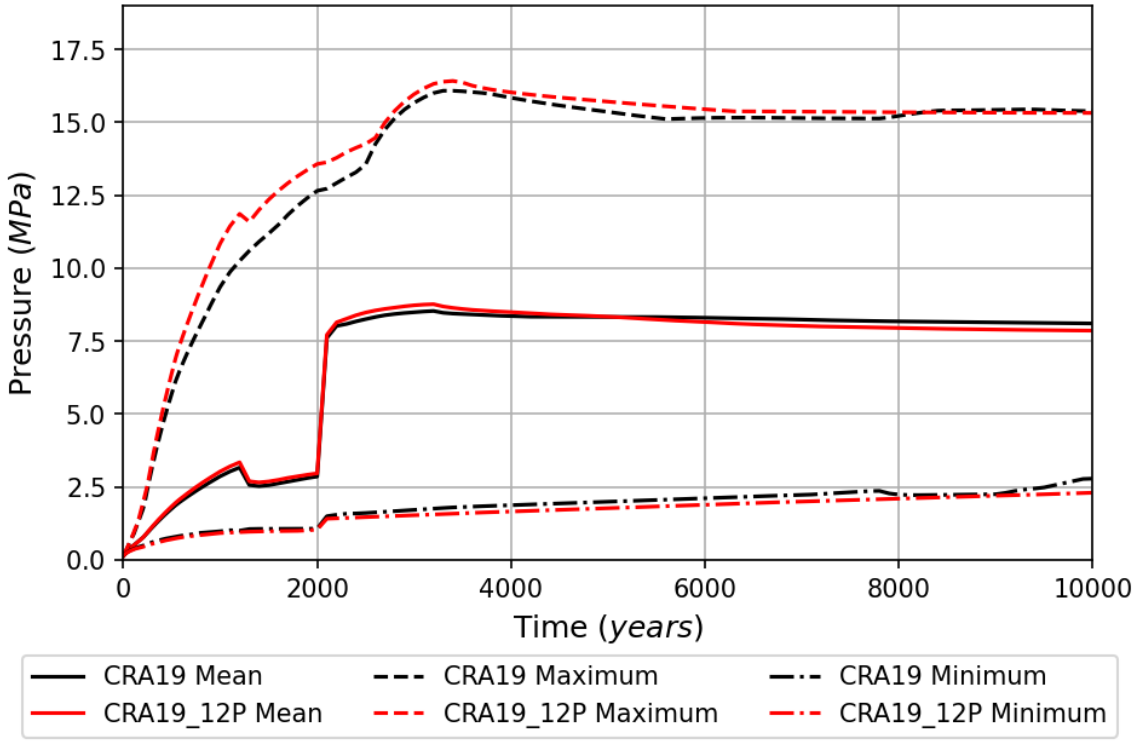

Figure 4-4: Pressure in the Waste Panel for Scenario S6-BF

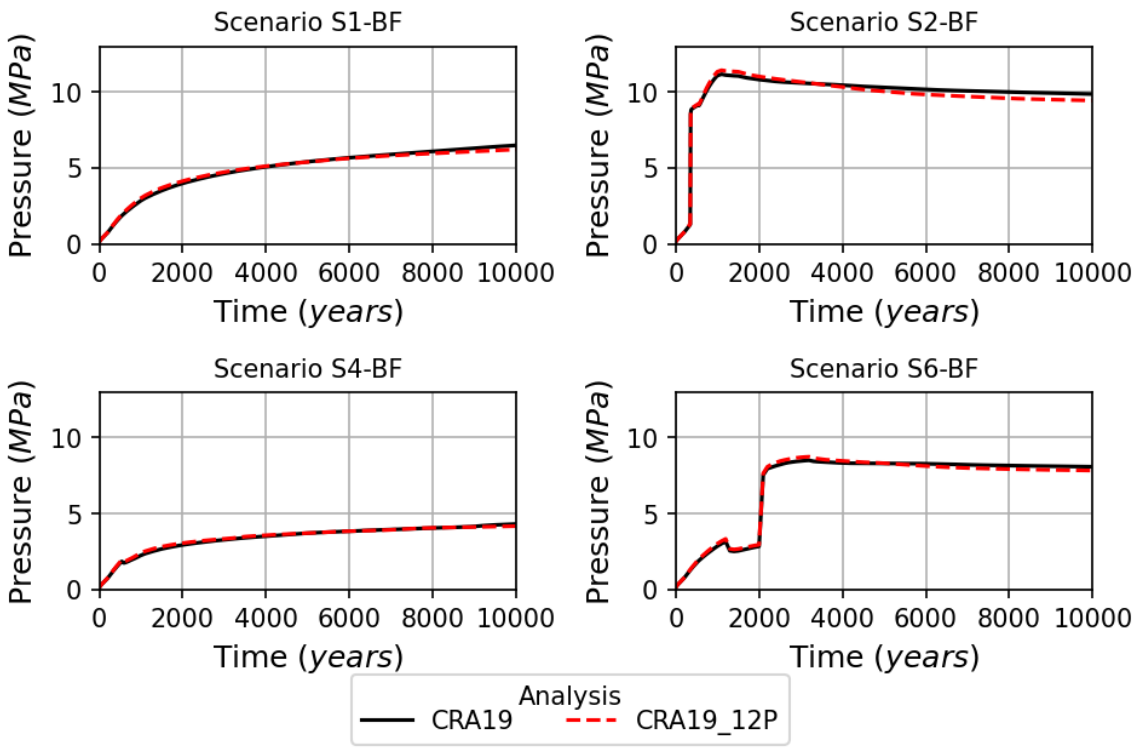

Figure 4-5: Mean Pressure in the South Rest-of-Repository

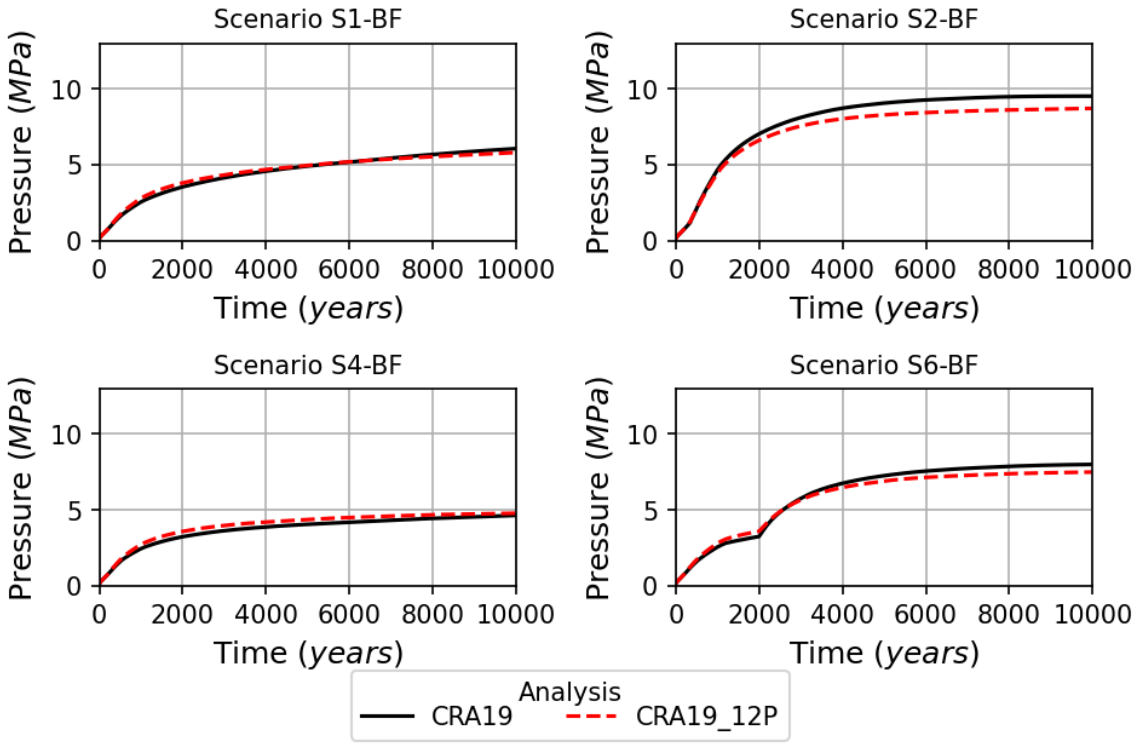

Figure 4-6: Mean Pressure in the North Rest-of-Repository

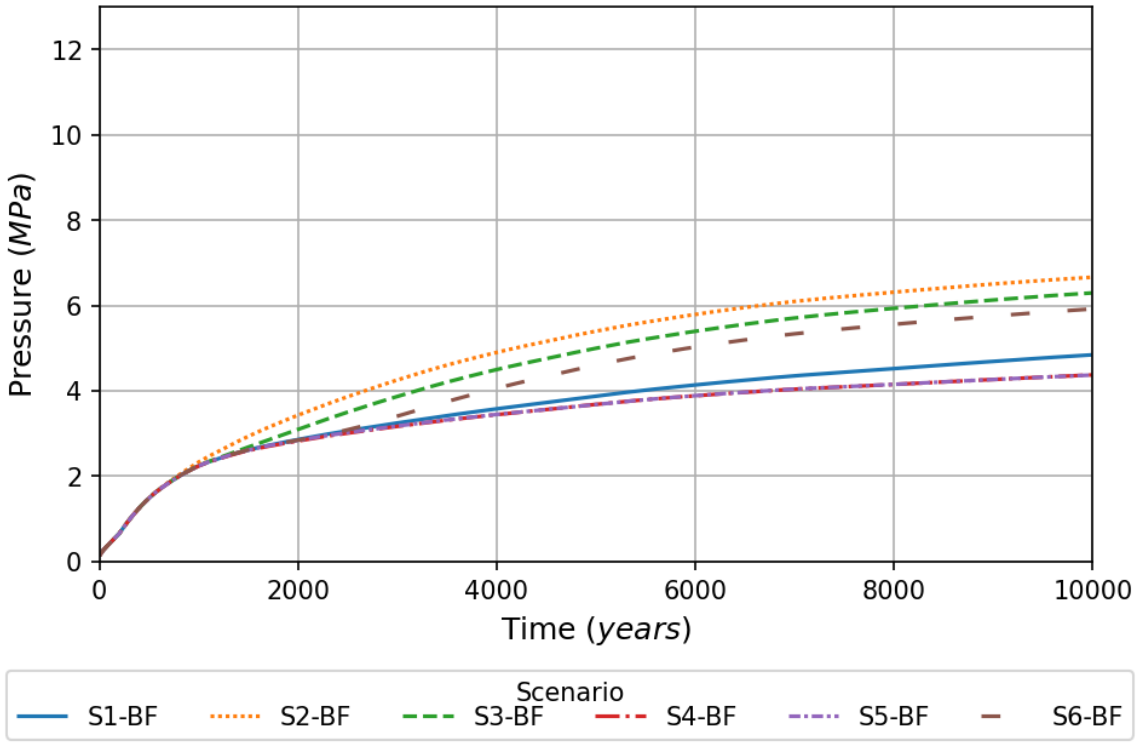

Figure 4-7: Mean Pressure in the West Rest-of-Repository for the CRA19_12P Analysis

4.2.2 Brine Saturation

Mean Waste Panel brine saturation statistics are shown in Table 4-3. Mean, minimum, and maximum brine saturations in the Waste Panel for scenarios S1-BF, S2-BF, S4-BF, and S6-BF are shown in Figure 4-8, Figure 4-9, Figure 4-10, and Figure 4-11 respectively. Brine saturations in the Waste Panel are slightly decreased in scenarios without an E1 intrusion and largely the same in scenarios with an E1 intrusion. Despite the increased repository volume being able to drain a larger volume of the brine in the Salado formation, the extra panel closure between the up-dip formation and the waste panel tends to inhibit brine flow down-dip into the waste panel leading to a decrease in brine saturation in scenarios without an E1 intrusion. Waste Panel brine saturation in scenarios with an E1 intrusion is controlled by brine flow from the Castile and is largely unchanged by the addition of up-dip repository volume.

Mean brine saturations in the SROR are shown in Figure 4-12. The SROR shows a slight increase in brine saturations after an E1 intrusion and little change in the other scenarios. Mean brine saturations in the NROR are shown in Figure 4-13. Mean brine saturations for the NROR are slightly increased in the CRA19_12P compared to the CRA19 results.

Figure 4-14 shows the mean brine saturations in the WROR for the CRA19_12P. As this waste area did not exist in the CRA19 calculation, there is no comparison of these results to the CRA19 results. The WROR is farthest up-dip and has lower mean brine saturations than the down-dip panels. There is little to no difference in the brine saturations in the WROR between the different scenarios.

Table 4-3: Mean Waste Panel Brine Saturation Statistics for the CRA19 and the CRA19_12P

	Mean Value[1] (-)	**Mean Value[1] (-)**	**Maximum Value[2] (-)**	**Maximum Value[2] (-)**
Scenario	CRA19	CRA19_12P	CRA19	CRA19_12P
S1-BF	0.21	0.17	0.23	0.20
S2-BF	0.82	0.83	0.97	0.97
S4-BF	0.37	0.33	0.44	0.38
S6-BF	0.63	0.63	0.81	0.81

Notes:
1 – Average over the time interval (0-10,000 years) of the Replicate 1 mean.
2 – Maximum over the time interval (0-10,000 years) of the Replicate 1 mean.

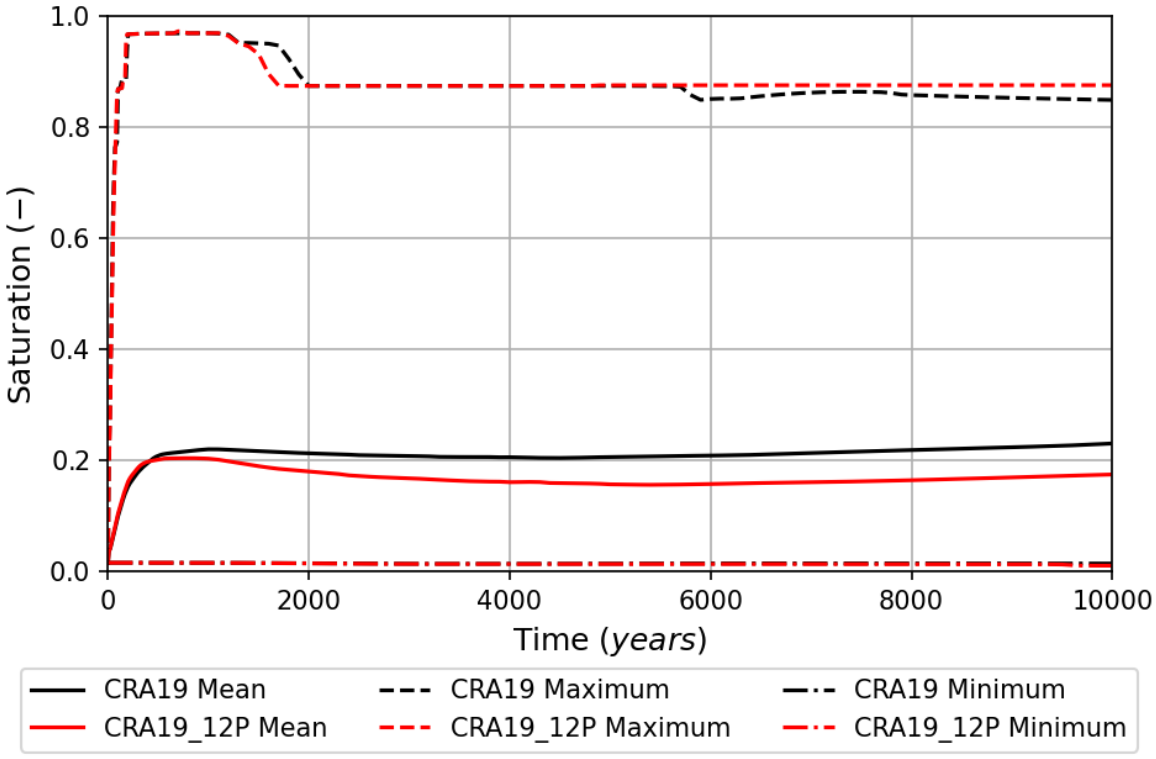

Figure 4-8: Brine Saturation in the Waste Panel for Scenario S1-BF

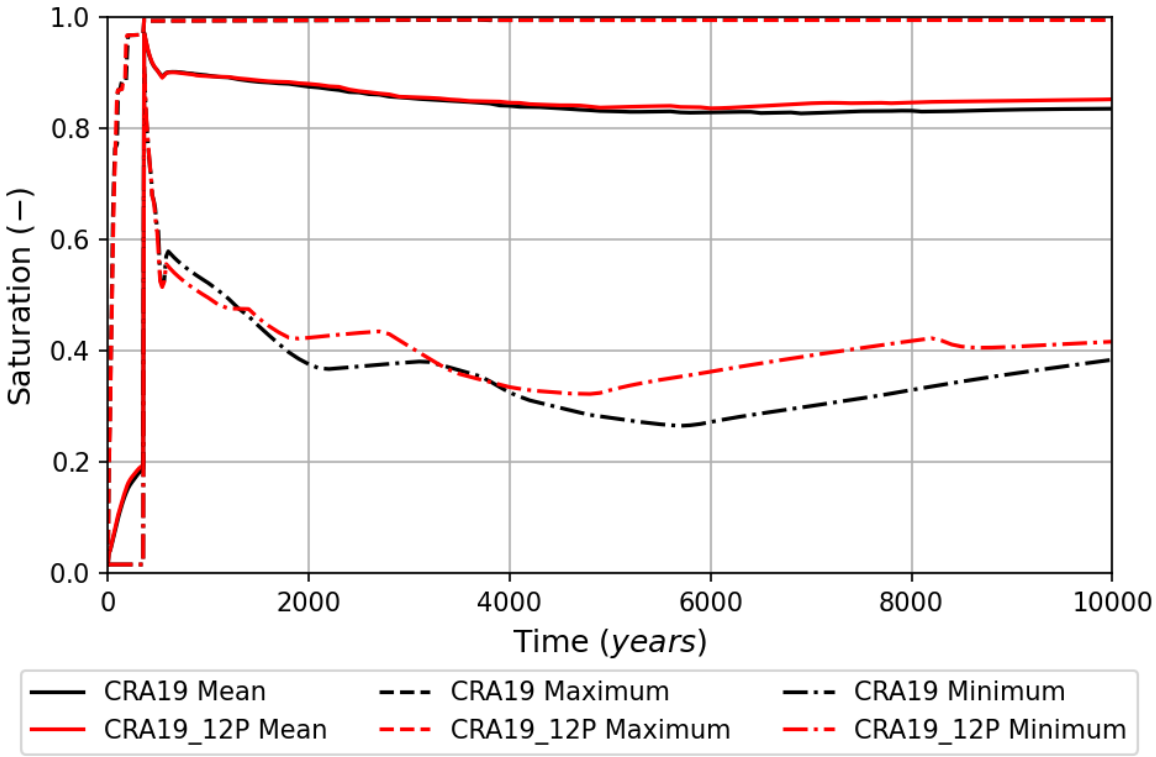

Figure 4-9: Brine Saturation in the Waste Panel for Scenario S2-BF

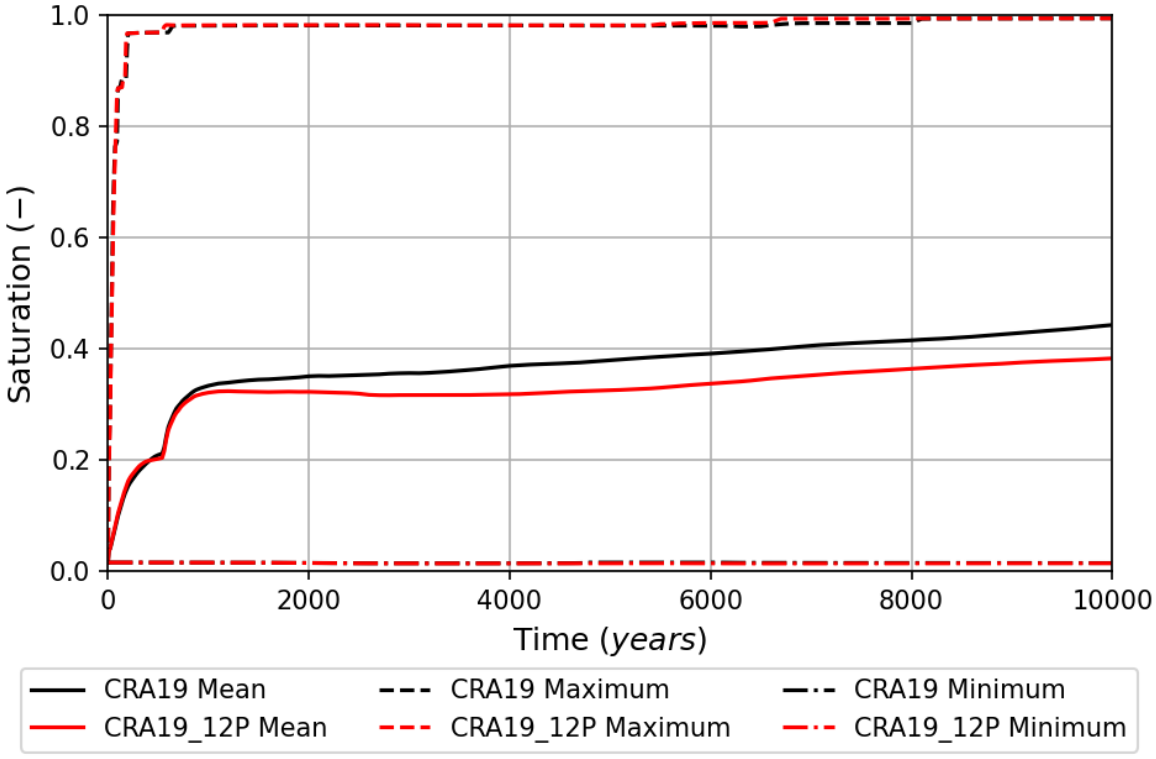

Figure 4-10: Brine Saturation in the Waste Panel for Scenario S4-BF

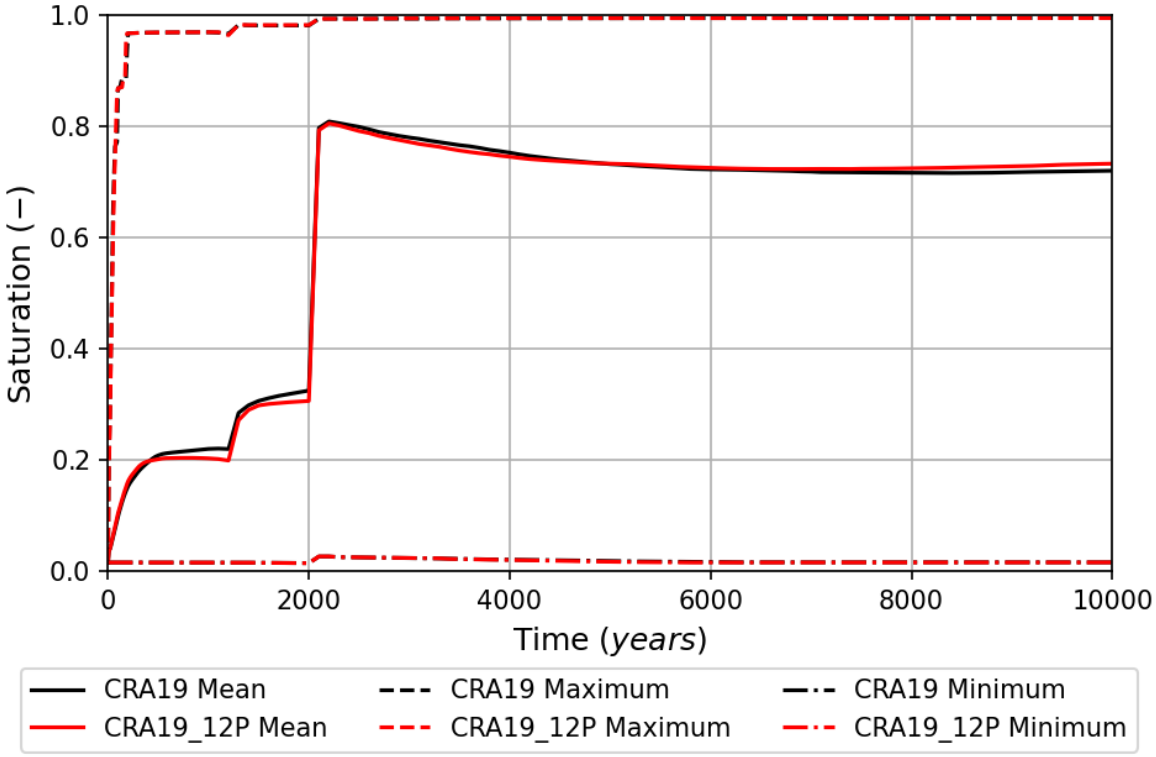

Figure 4-11: Brine Saturation in the Waste Panel for Scenario S6-BF

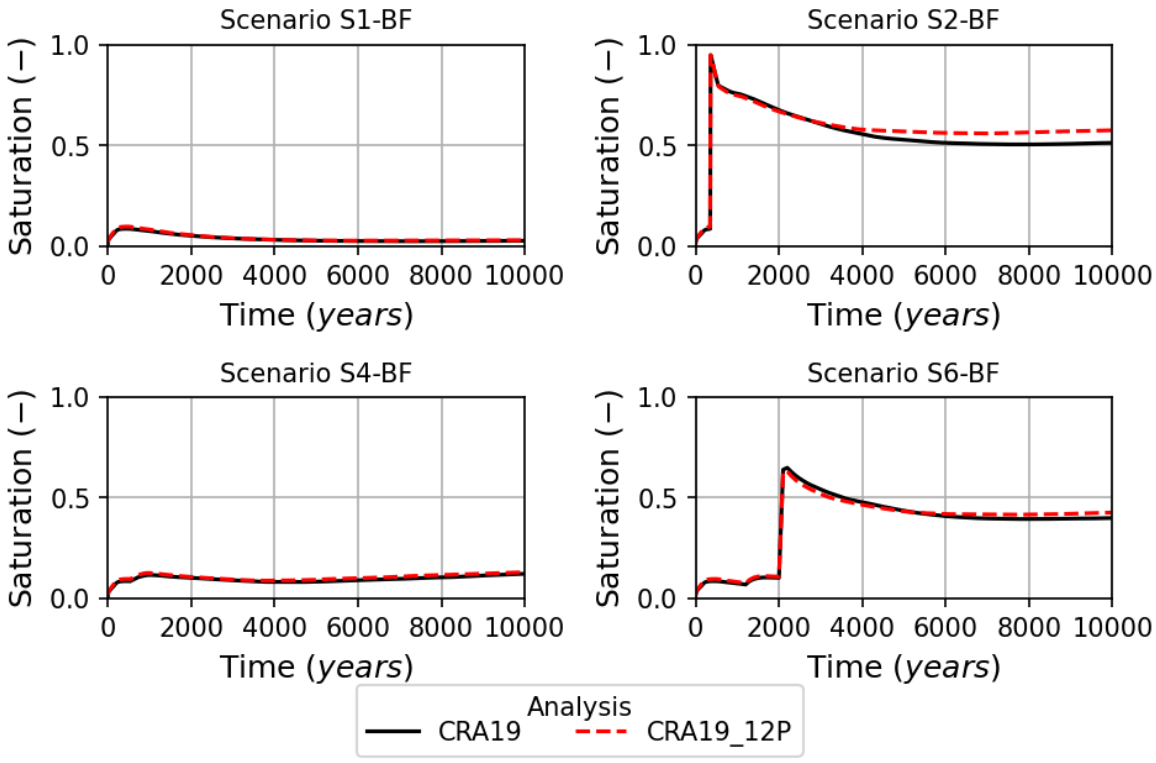

Figure 4-12: Mean Brine Saturation in the South Rest-of-Repository

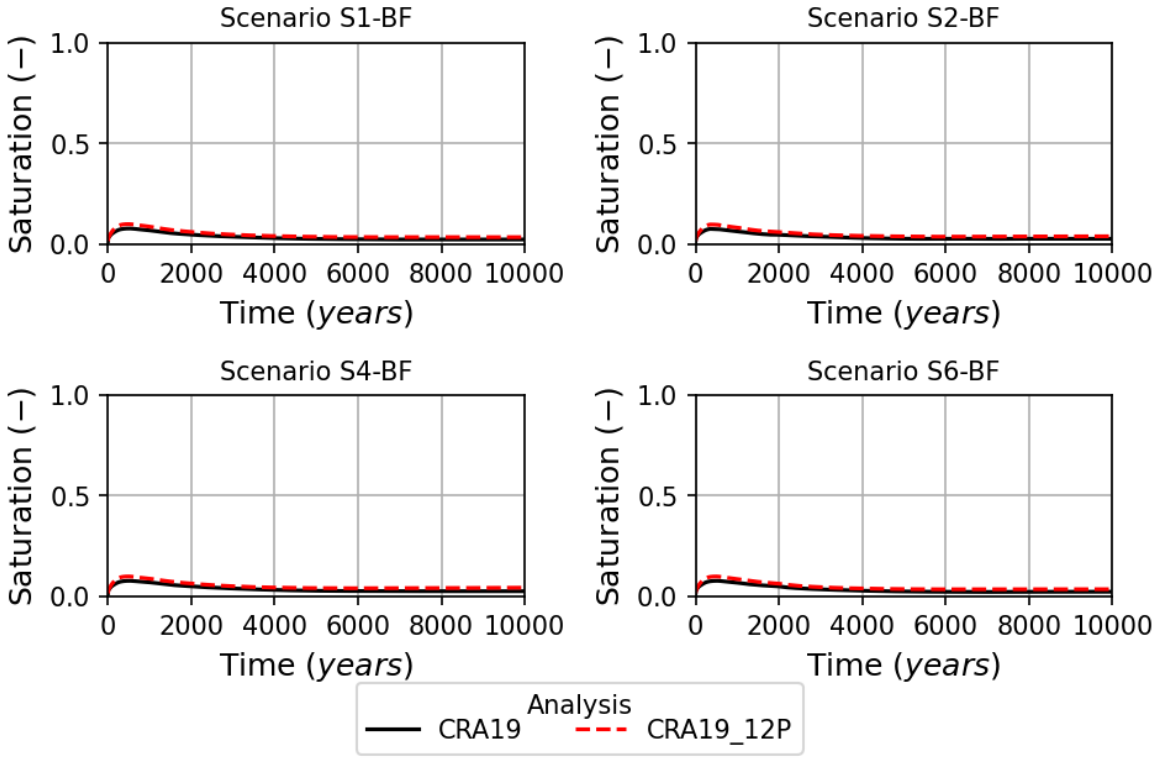

Figure 4-13: Mean Brine Saturation in the North Rest-of-Repository

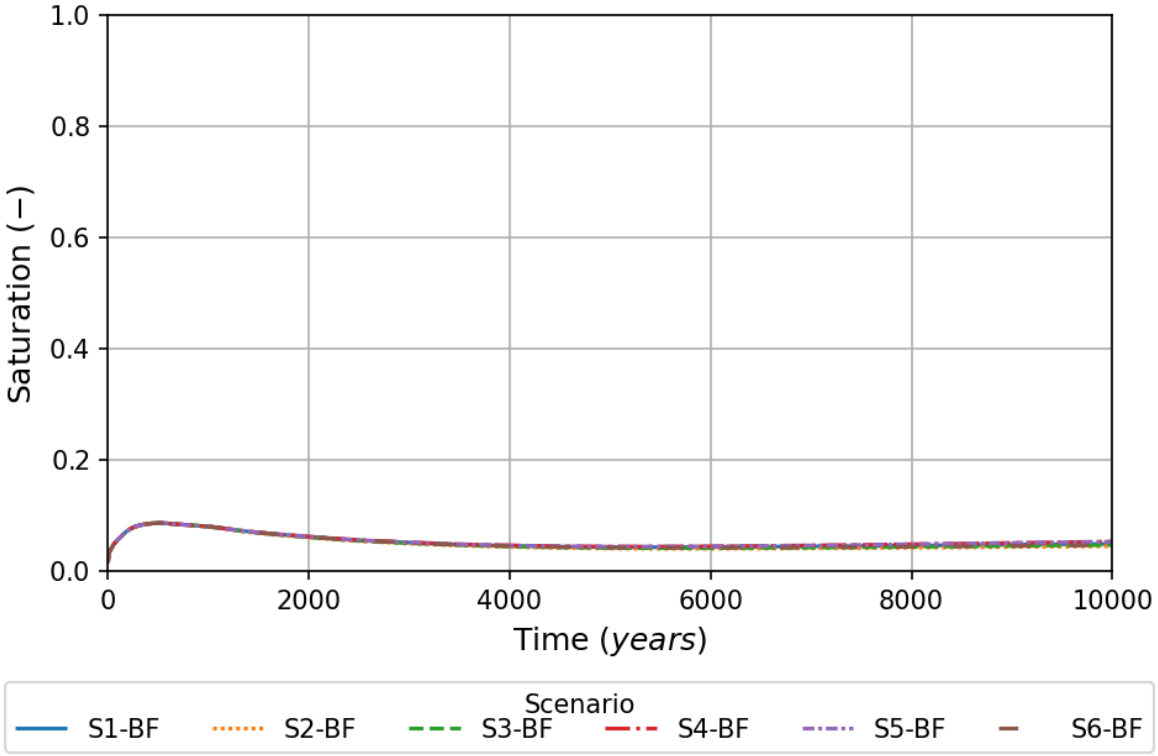

Figure 4-14: Mean Brine Saturation in the West Rest-of-Repository

4.2.3 Brine Flow up the Borehole

Cumulative brine flow up the borehole at 10,000 years is shown in Figure 4-15[4]. There is a slight increase in brine flow up the borehole in the CRA19_12P compared to the CRA19 in scenarios with an E1 intrusion. Scenarios with an E1 intrusion saw slight increases in pressure with little change in the brine saturation, leading to the slight increase in brine flow up the borehole.

[4] Box and whisker plots are used to display results throughout Sections 5-9. Boxes extend from the 25th percentile to the 75th percentile, also known as the interquartile range. Whiskers extend from the 25th percentile to the 25th percentile minus 1.5 times the interquartile range and from the 75th percentile to the 75th percentile plus 1.5 times the interquartile range. Outliers are defined as data points beyond the extent of the whiskers. Outliers are plotted as diamonds. The black center line in the box is the median value; the mean value is denoted with a white square.

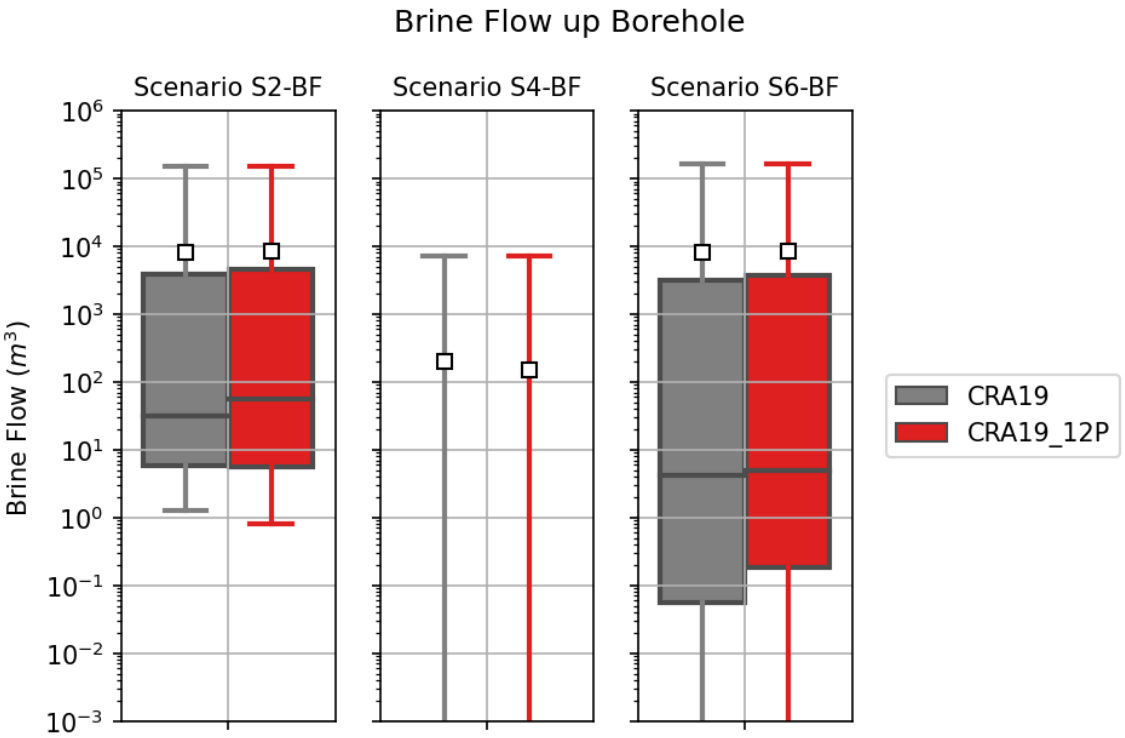

Figure 4-15: Cumulative Brine Flow up the Borehole at 10,000 years

4.2.4 Gas Generation

Mean total cumulative gas generation through time is shown in Figure 4-16. Mean cumulative gas generation by mechanism for Scenarios S1-BF, S2-BF, S4-BF, and S6-BF is shown in Figure 4-17, Figure 4-18, Figure 4-19, and Figure 4-20, respectively.

Mean gas generation is increased in Scenarios S1-BF and S4-BF at all time points. Mean gas generation is increased in early time and decreased in late time in Scenarios S2-BF and S6-BF. Total gas generation is dominated by gas generation from iron corrosion in all scenarios.

In both the CRA19 and the CRA19_12P, the initial surface area concentration of steel in the repository is 11.2 m^2 surface area per m^3 disposal volume. With the increase in disposal volume for the CRA19_12P analysis and the assumption that the waste is distributed over all 12 panels, the total surface area of steel increases to 5.94 × 10^6 m^2 from the 4.91× 10^6 m^2 value of the CRA19. This increase in total iron surface area increases the rate of gas generation from iron corrosion.

For scenarios without an E1 intrusion, this iron corrosion rate increase leads to a gas generation increase at all times. For scenarios with an E1 intrusion, the rate increase leads to an early time gas generation increase, however with the concentration of iron in the down-dip waste panel being reduced due to the increased disposal area, the iron in the down-dip panels with high brine saturations is more easily depleted leading to a late time decrease in gas generation.

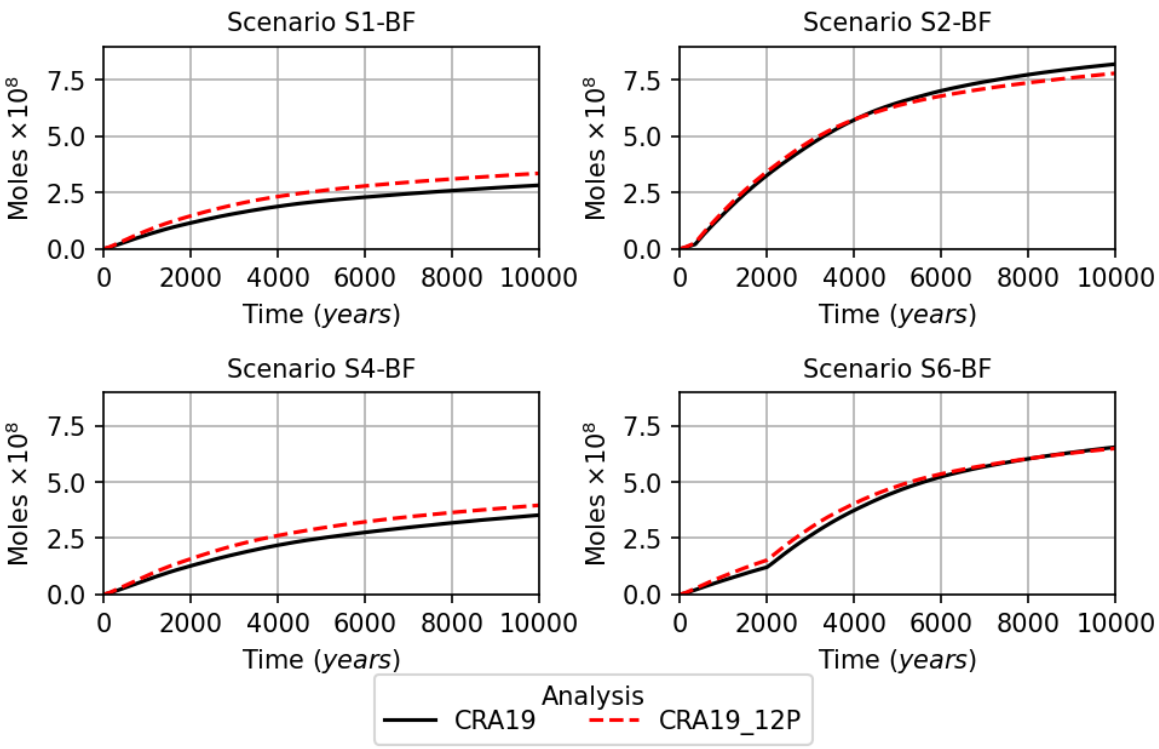

Figure 4-16: Mean Cumulative Total Gas Generation over 10,000 years

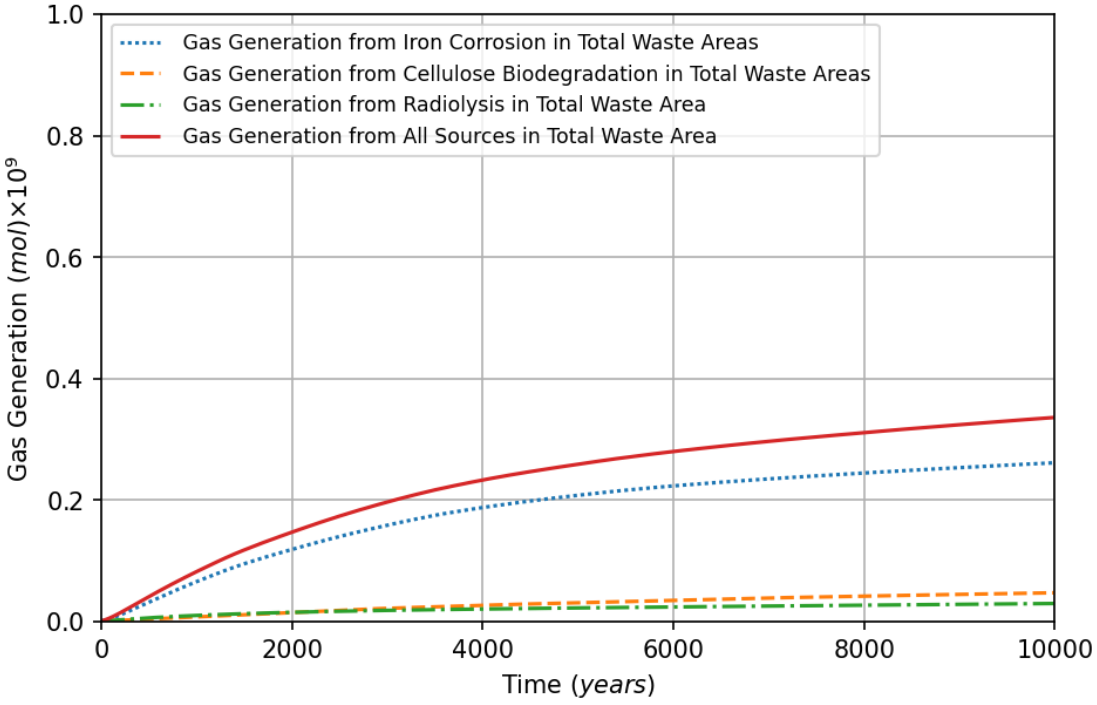

Figure 4-17: Mean Cumulative Gas Generation by Mechanism for Scenario S1-BF in the CRA19_12P

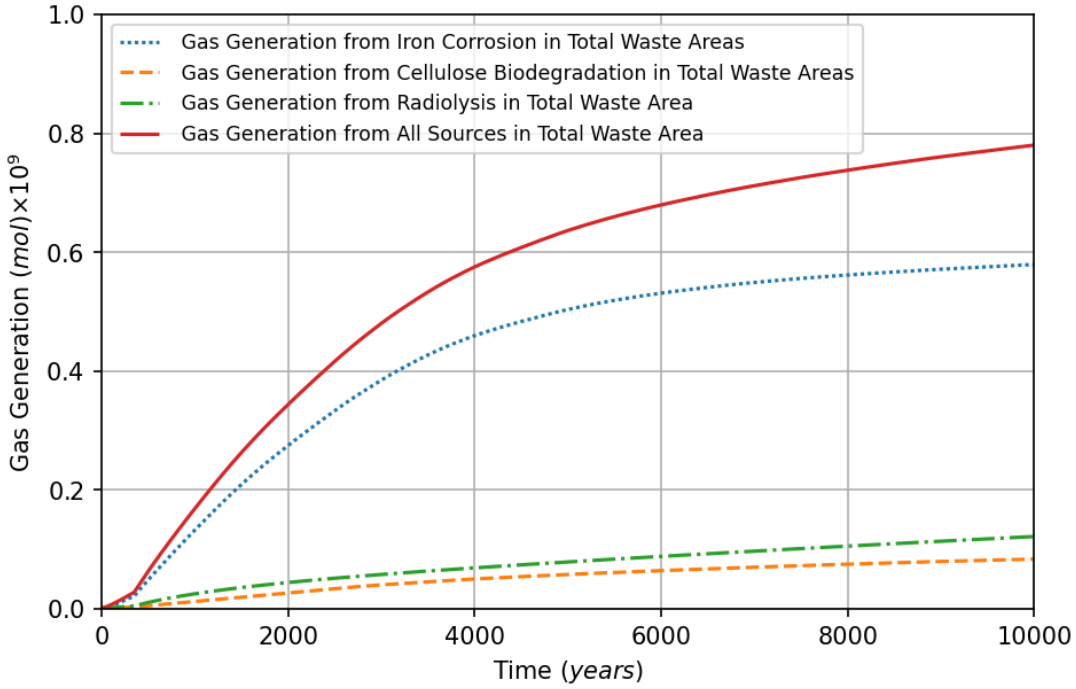

Figure 4-18: Cumulative Gas Generation by Mechanism for Scenario S2-BF in the CRA19_12P

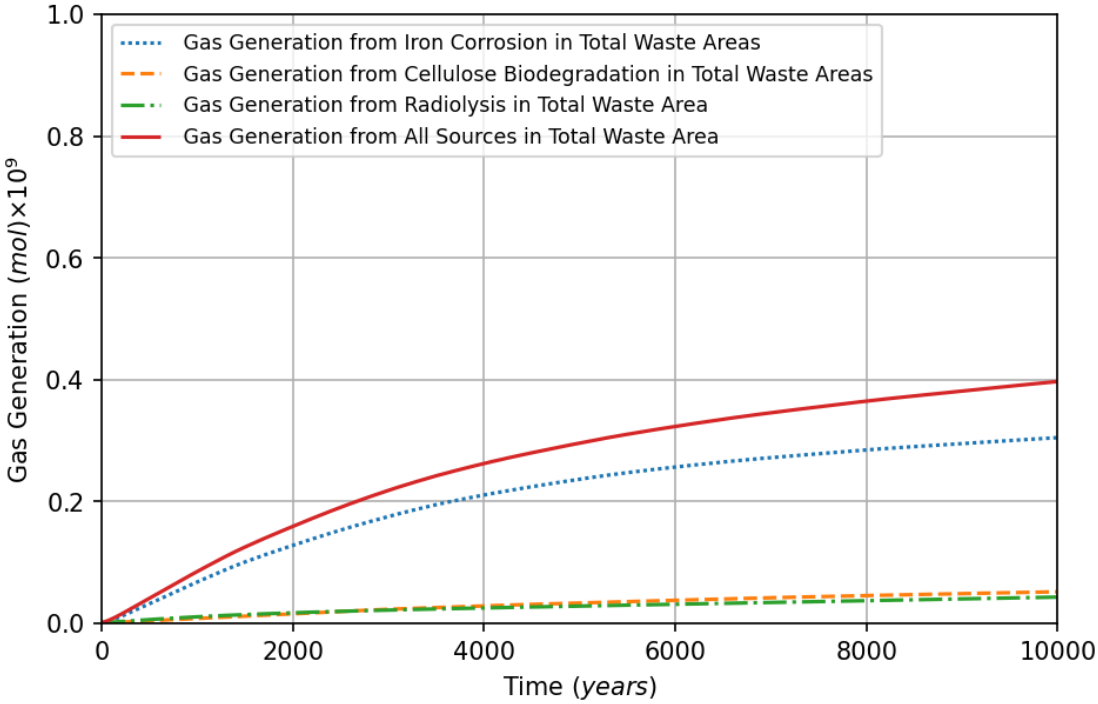

Figure 4-19: Cumulative Gas Generation by Mechanism for Scenario S4-BF in the CRA19_12P

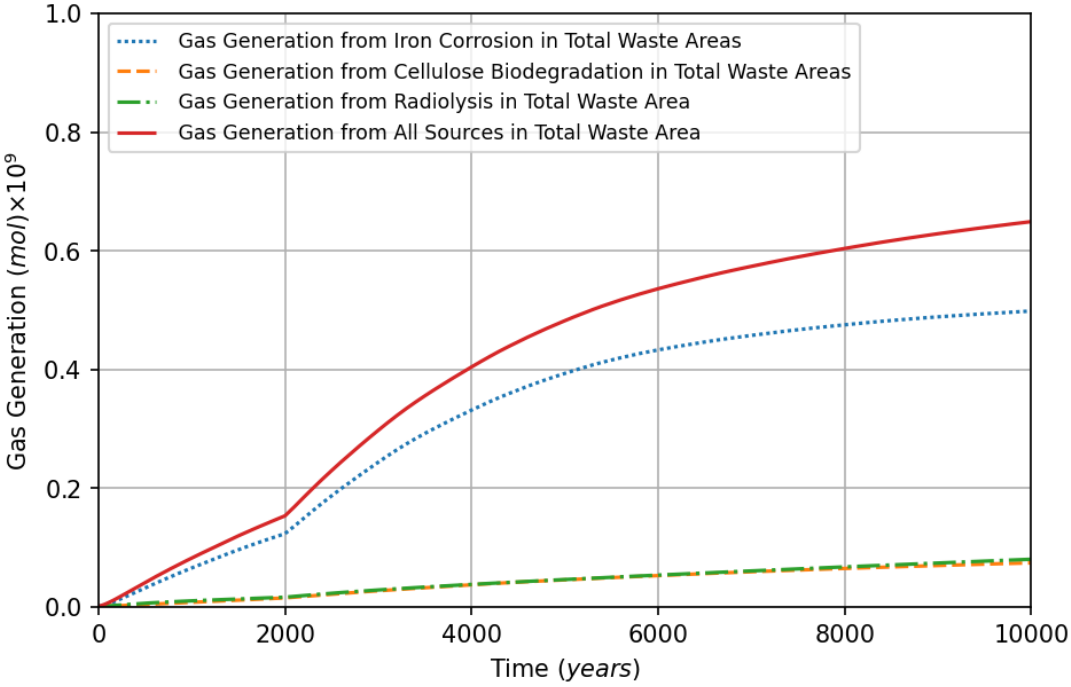

Figure 4-20: Cumulative Gas Generation by Mechanism for Scenario S6-BF in the CRA19_12P

5 Direct Brine Release Volumes: BRAGFLO_DBR Calculations

This section describes the Direct Brine Release (DBR) volume calculations for the CRA19_12P PA. For more information on the development, history, and implementation details of the DBR model, see Stoelzel and O'Brien (1996) and King (2021).

5.1 Introduction

If the WIPP repository were to be penetrated by a borehole while under conditions of sufficient repository brine pressure and saturation, brine could flow up the intruding borehole to reach the land surface. Such an event is defined as a DBR. The code BRAGFLO_DBR is used to evaluate DBR volumes for a suite of simulations, comprising variations in initial conditions, intrusion location and intrusion time, and three replicates of 100 parameter vectors. The DBR scenarios are summarized in Table 5-1.

Table 5-1: Intrusion Scenarios Used in Calculating Direct Brine and Spallings Releases

Scenario	Description
S1-DBR	Initially undisturbed repository (E0 conditions). Intrusion at the L, M, U, or O location at 100; 350; 1,000; 3,000; 5,000; or 10,000 years: 24 combinations.
S2-DBR	Initial E1 intrusion at 350 years followed by a second intrusion at the L, M, U, or O location at 550; 750; 2,000; 4,000; or 10,000 years: 20 combinations.
S3-DBR	Initial E1 intrusion at 1,000 years followed by a second intrusion at the L, M, U, or O location at 1,200; 1,400; 3,000; 5,000; or 10,000 years: 20 combinations.
S4-DBR	Initial E2 intrusion at 350 years followed by a second intrusion at the L, M, U, or O location at 550; 750; 2,000; 4,000; or 10,000 years: 20 combinations.
S5-DBR	Initial E2 intrusion at 1,000 years followed by a second intrusion at the L, M, U, or O location at 1,200; 1,400; 3,000; 5,000; or 10,000 years: 20 combinations.

The two-dimensional, rectilinear BRAGFLO_DBR grid explicitly represents individual panels and other specific repository features (Figure 2-4). The same grid was used in the APPA. As described by King (2021), volume-averaged pressures and saturations are mapped from the BRAGFLO grid's Waste Panel (WP), South Rest-of-Repository (SROR), North Rest-of-Repository (NROR), and West Rest-of-Repository (WROR) lumped waste regions onto the BRAGFLO_DBR grid panels containing the Lower (L), Middle (M), Upper (U), and Other (O) intrusion locations, respectively. Like the BRAGFLO Salado model, the BRAGFLO_DBR grid dips 1º to the south, placing the L intrusion location farthest down-dip to the south, and the O intrusion farthest up-dip to the north. Note that the addition of the O intrusion location in the CRA19_12P results in a total of 31,200 DBR simulations. In the CRA19, with only L, M and U intrusion locations, there were 23,400 DBR simulations.

Minimum pressure and saturation conditions must exist within the waste panel for brine to flow to the surface during an intrusion and produce a DBR. Pressure in the intruded waste panel must be great enough to overcome the static pressure exerted by a column of drilling fluid at the repository depth, assumed to be equal to 8 megapascals (MPa). Brine saturation in the intruded

waste panel must be above the residual brine saturation of the waste (parameter WAS_AREA:SAT_RBRN). DBR volumes are multiplied by the mobilized radionuclide concentrations (Section 7) to calculate DBR radionuclide releases (Section 10.2.3).

5.2 Results

The DBR calculation results for Replicate 1 vectors in the CRA19_12P are summarized in this section and compared to results from the CRA19. Results for the other two replicates show similar trends. Average DBR volumes are calculated as the sum of DBR volumes divided by the total number of simulations. Brine release volumes are described first, followed by initial values of brine pressure and saturation obtained from BRAGFLO.

5.2.1 Brine release volumes

Mean brine releases, fraction of simulations with non-zero releases, and mean of non-zero brine releases are summarized in Table 5-2. The number of non-zero brine releases is plotted by brine release volume for all intrusion locations in Figure 5-1, and for locations L, M, and U only in Figure 5-2. The distribution of all non-zero releases is plotted in Figure 5-3, then broken down by scenario in Figure 5-4 and by location in Figure 5-5.

Overall, DBR volumes are similar for the CRA19 and the CRA19_12P. The following observations are also noted:

(i) In the CRA19_12P, the number of smaller magnitude release volumes increased while the number of larger magnitude release volumes decreased slightly, compared to the CRA19 (Figure 5-1 and Figure 5-2). Stated differently, there is a shift towards smaller release volumes in the CRA19_12P.

(ii) Releases from the Other (O) location in the CRA19_12P, of which there are 39 in total, were among the smallest releases: Figure 5-1 and Figure 5-2 are identical except for the leftmost red bar in each plot.

(iii) Overall mean and median non-zero release volumes decreased by small amounts for the CRA19_12P compared to the CRA19 (Table 5-2 and Figure 5-3).

(iv) For both the CRA19 and the CRA19_12P, the greatest frequency of non-zero releases and the largest mean release volume occurred for scenario S2-DBR, followed by scenario S3-DBR (Table 5-2 and Figure 5-4). These are scenarios with an initial E1 intrusion.

(v) For both the CRA19 and the CRA19_12P, the greatest frequency of non-zero releases and the largest mean release volume occurred at intrusion location L, followed by location M (Table 5-2 and Figure 5-5). These are down-dip intrusion locations; in addition, they are closest to where previous intrusions occur.

Initial brine pressure and saturation are the two most important variables that control brine release volume from a single intrusion (Clayton et al. 2008). Initial brine pressure and saturation for the CRA19 and the CRA19_12P are summarized and compared in the next section.

Table 5-2: DBR Volume Summary

Intrusion Location	Mean Brine Released (m^3)	Mean Brine Released (m^3)	Fraction of Simulations with Non-Zero Releases	Fraction of Simulations with Non-Zero Releases	Mean of Non-Zero Brine Releases (m^3)	Mean of Non-Zero Brine Releases (m^3)
	CRA19	CRA19_12P	CRA19	CRA19_12P	CRA19	CRA19_12P
S1-DBR	**0.26**	**0.26**	**2.72%**	**3.38%**	**9.65**	**7.59**
L	0.76	0.97	6.33%	7.67%	12.03	12.64
M	0.03	0.05	1.17%	2.00%	2.19	2.63
U	0	0	0.67%	2.17%	0	0.14
O	-	0	-	1.67%	-	0
S2-DBR	**8.11**	**5.69**	**46.80%**	**36.60%**	**17.34**	**15.55**
L	15.3	14.05	73.60%	74.20%	20.79	18.94
M	9.04	8.71	65.00%	67.80%	13.92	12.84
U	0	0.01	1.80%	3.00%	0.07	0.31
O	-	0	-	1.40%	-	0
S3-DBR	**5.01**	**3.41**	**38.87%**	**29.85%**	**12.89**	**11.41**
L	10.48	9.36	64.40%	64.00%	16.28	14.63
M	4.55	4.25	50.40%	50.60%	9.03	8.4
U	0	0.01	1.80%	3.20%	0	0.33
O	-	0	-	1.60%	-	0
S4-DBR	**0.04**	**0.04**	**1.07%**	**1.45%**	**4**	**2.83**
L	0.13	0.15	1.80%	2.40%	7.02	6.31
M	0	0.01	0.60%	0.80%	0.28	1.47
U	0	0	0.80%	1.40%	0	0.07
O	-	0	-	1.20%	-	0.01
S5-DBR	**0.09**	**0.11**	**1.93%**	**2.80%**	**4.91**	**4**
L	0.26	0.36	4.00%	5.00%	6.62	7.17
M	0.02	0.08	1.00%	1.60%	2	5.01
U	0	0.01	0.80%	3.00%	0	0.3
O	-	0	-	1.60%	-	0
All Scenarios						
L	**5.21**	**4.82**	**29.12%**	**29.77%**	**17.89**	**16.21**
M	**2.62**	**2.52**	**22.77%**	**23.69%**	**11.53**	**10.64**
U	**0**	**0.01**	**1.15%**	**2.54%**	**0.02**	**0.25**
O	**-**	**0**	**-**	**1.50%**	**-**	**0**
L, M, and U	**2.61**	**2.45**	**17.68%**	**18.67%**	**14.77**	**13.13**
ALL	**2.61**	**1.84**	**17.68%**	**14.37%**	**14.77**	**12.79**

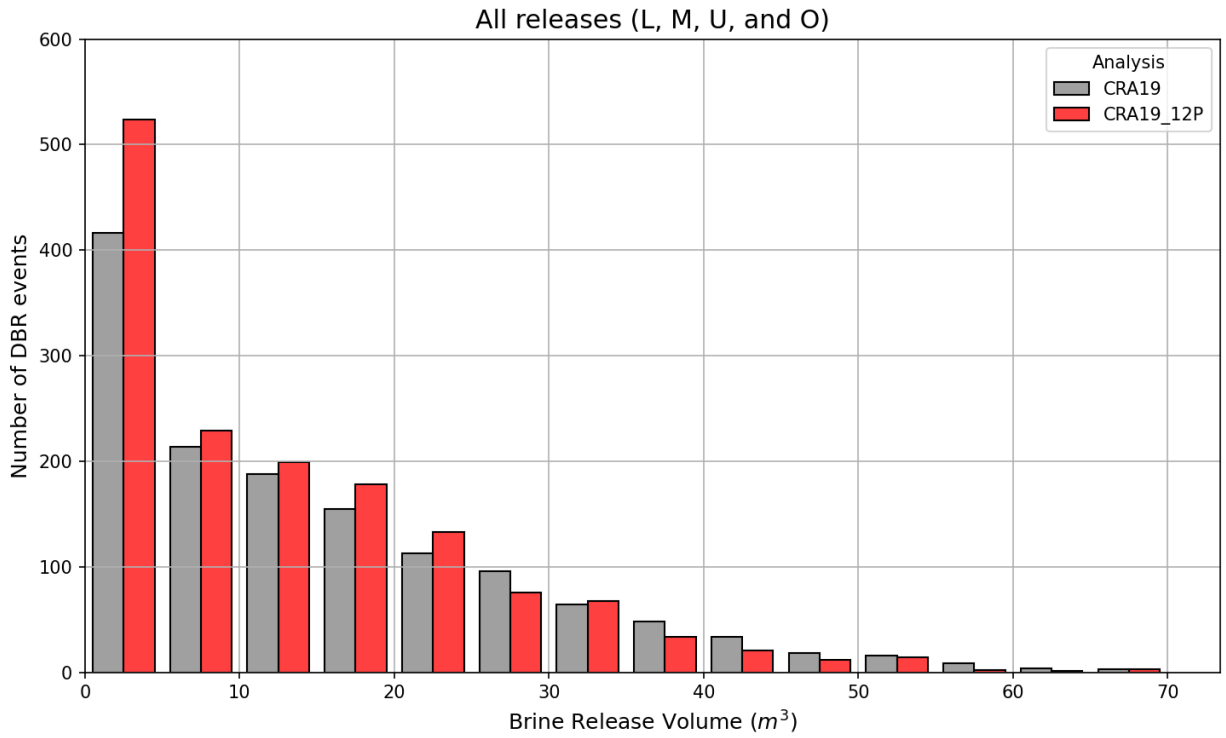

Figure 5-1: Release Volume Frequency; All Non-zero Releases

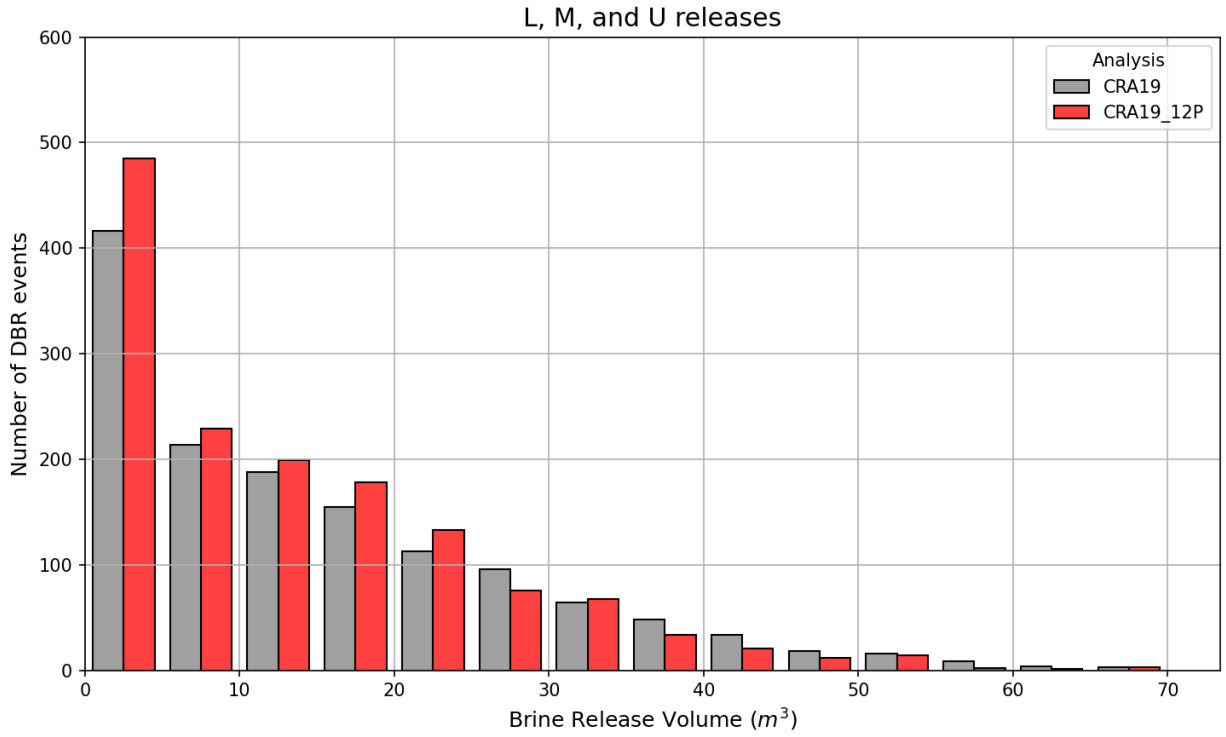

Figure 5-2: Release Volume Frequency; Only L, M, U Non-zero Releases

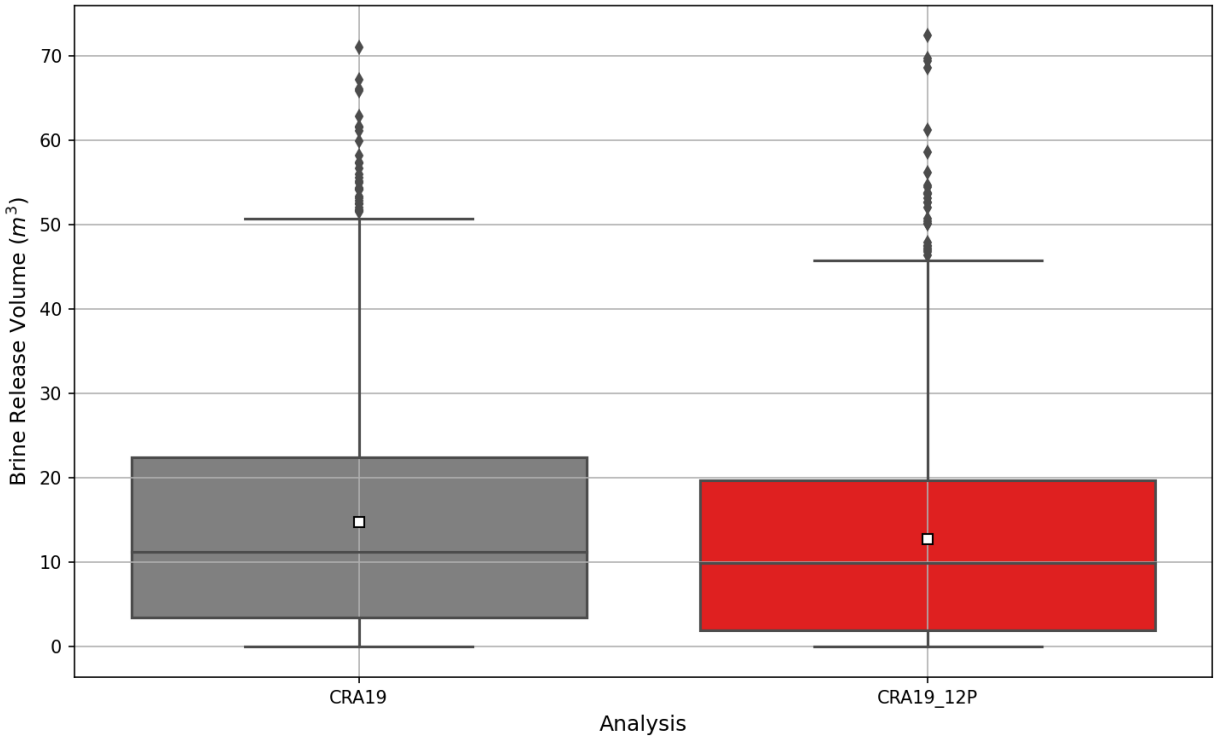

Figure 5-3: Release Volumes; All Non-zero Releases

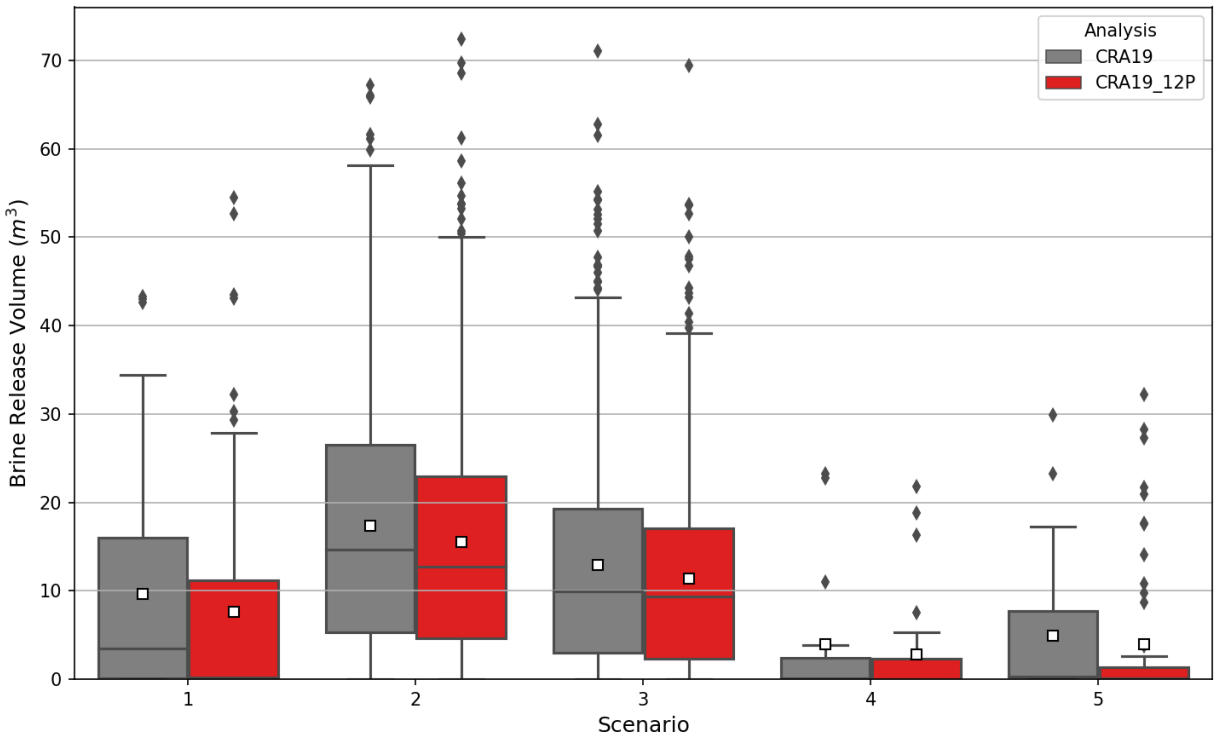

Figure 5-4: Release Volumes by Scenario; All Non-zero Releases

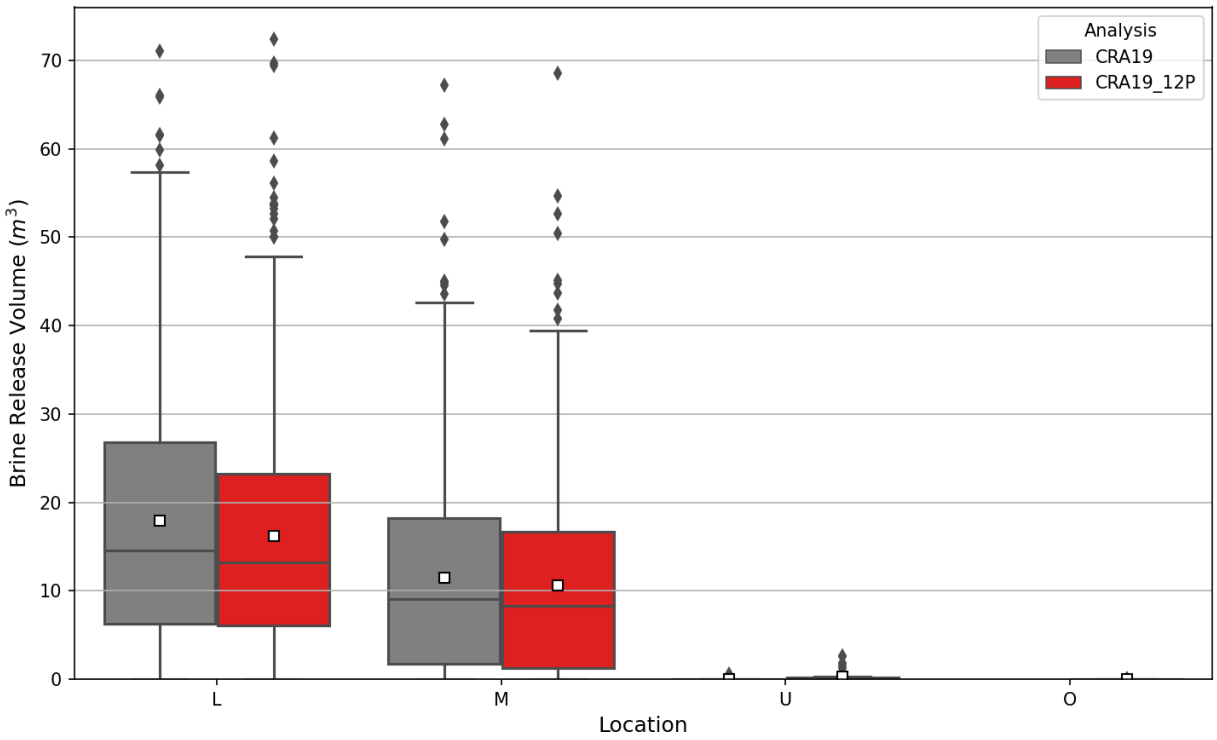

Figure 5-5: Release Volumes by Location; All Non-zero Releases

5.2.2 Initial brine pressure and saturation in the BRAGFLO_DBR grid

Volume-averaged pressures and saturations, obtained by scenario, intrusion time, and intrusion location (Table 5-1), are used as initial conditions in the BRAGFLO_DBR simulations.

Initial pressure and saturation for both the CRA19 and the CRA19_12P are summarized in Table 5-3. Distributions of initial pressure and saturation, broken down by scenario, are shown in Figure 5-6 and Figure 5-7. From the table and the figures, mean initial pressure in the CRA19_12P is seen to be decreased a small amount for all scenarios. Mean initial saturation in the CRA19_12P is also down across all 5 scenarios. (In interpreting the overall mean for each scenario, it should be noted that (i) there are more non-zero releases from the L intrusion location (Table 6.2), giving L a greater influence on the mean value; and (ii) non-zero values from the O location are affecting overall means in the CRA_12P.)

5.2.3 Summary of results

Brine release volumes in the 12-panel CRA19_12P are not much different from those in the 10-panel CRA19. There is a slight decrease in mean release volumes across all intrusion scenarios in the CRA19_12P and an overall shift towards somewhat smaller release volumes. The reduction in release volumes in the CRA19_12P can be attributed to small decreases in the mean values of initial pressure and saturation.

Table 5-3: Mean Initial Conditions; All Non-zero Releases

Intrusion Location	Brine Pressure (MPa)	Brine Pressure (MPa)	Brine Saturation	Brine Saturation
	CRA19	CRA19_12P	CRA19	CRA19_12P
S1-DBR	**10.9**	**10.74**	**0.49**	**0.42**
L	11.17	11.33	0.58	0.57
M	9.96	10.78	0.22	0.25
U	9.92	9.31	0.16	0.2
O	-	9.81	-	0.22
S2-DBR	**11.26**	**11.2**	**0.78**	**0.77**
L	11.35	11.3	0.86	0.87
M	11.15	11.14	0.7	0.7
U	11.58	10.63	0.14	0.23
O	-	10.03	-	0.2
S3-DBR	**10.79**	**10.68**	**0.73**	**0.72**
L	10.92	10.82	0.83	0.83
M	10.64	10.58	0.64	0.63
U	10.28	9.88	0.09	0.24
O	-	9.97	-	0.22
S4-DBR	**10.29**	**10.08**	**0.36**	**0.34**
L	10.99	10.64	0.52	0.54
M	9.71	9.82	0.14	0.22
U	9.15	9.25	0.15	0.17
O	-	10.11	-	0.21
S5-DBR	**10.23**	**9.95**	**0.44**	**0.38**
L	10.54	10.49	0.55	0.54
M	9.65	9.7	0.25	0.29
U	9.43	9.19	0.15	0.23
O	-	9.94	-	0.22
All Scenarios				
L	**11.13**	**11.06**	**0.82**	**0.82**
M	**10.9**	**10.88**	**0.66**	**0.65**
U	**10.36**	**9.71**	**0.13**	**0.22**
O	**-**	**9.96**	**-**	**0.21**
LMU	**11.02**	**10.92**	**0.74**	**0.72**
ALL	**11.02**	**10.9**	**0.74**	**0.71**

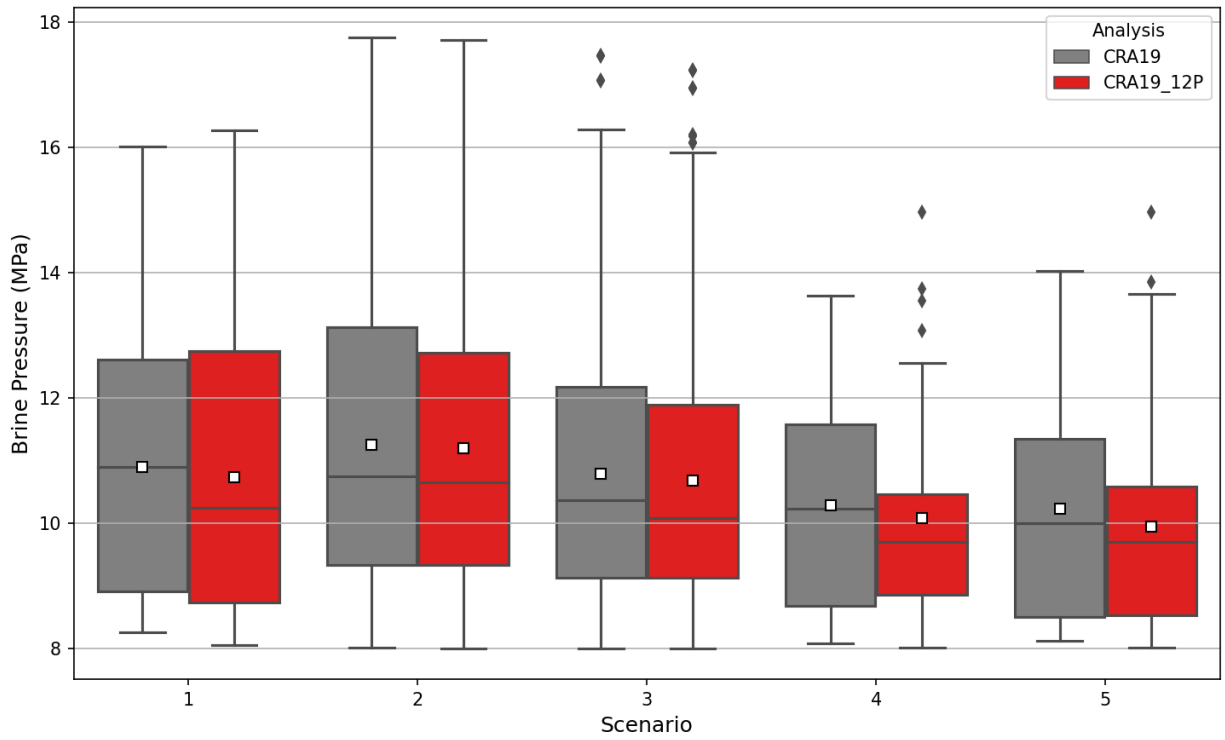

Figure 5-6: Initial Brine Pressure by Scenario; All Non-zero Releases

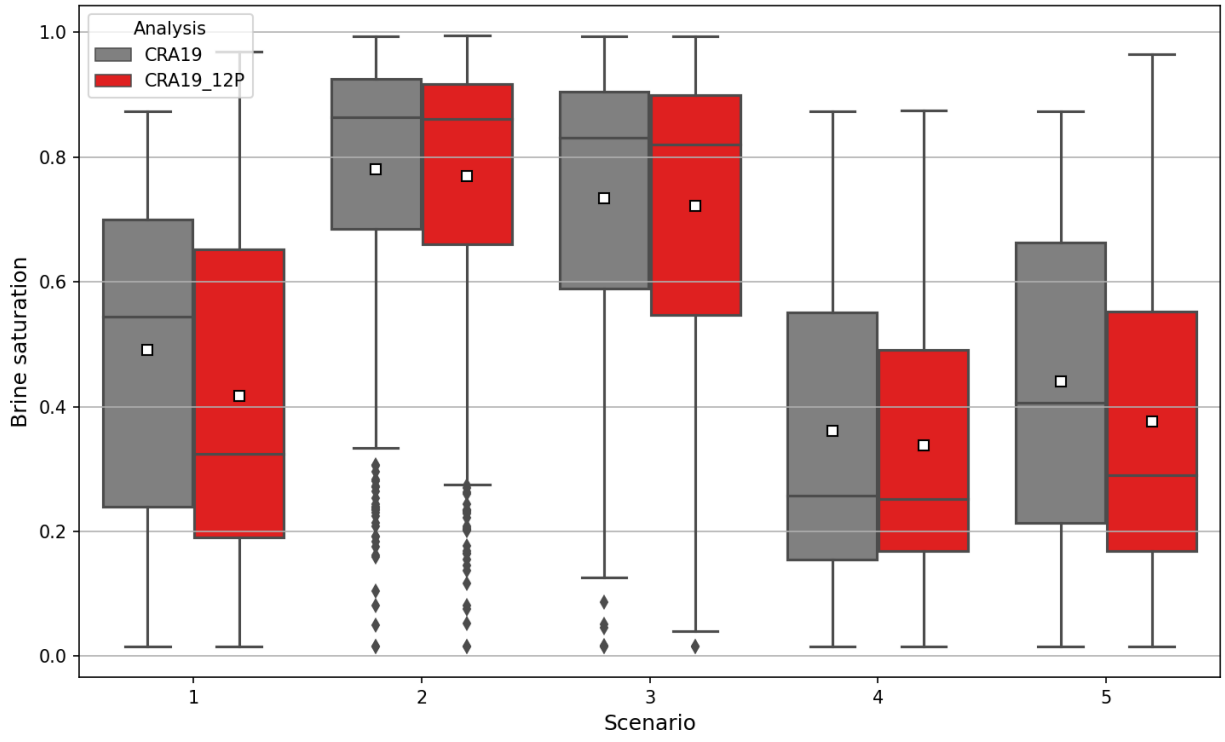

Figure 5-7: Initial Brine Saturation by Scenario; All Non-zero Releases

6 Solids Volume: CUTTINGS_S and DRSPALL Calculations

This section describes the calculations of the volume of solids releases from the WIPP repository from an intrusion borehole. The PA codes CUTTINGS_S and DRSPALL are used to calculate these volumes which include cuttings, cavings, and spallings. For more information on the solids release calculation methodology, see Kicker (2019).

6.1 Introduction

There were no changes to parameters associated with the cuttings and cavings processes in the CRA19_12P and therefore no changes to the cuttings and cavings input files used in CUTTINGS_S. Furthermore, cuttings and cavings volumes are independent of repository conditions so there are no changes between the CRA19 and the CRA19_12P.

Calculation of spalling release volumes involves hypothetical drilling intrusion scenarios and times. Spalling volume calculations use the same set of deterministic intrusions as direct brine release (DBR) volumes which include five different intrusion scenarios and 26 intrusion times (Table 5-1). For the CRA19, spallings volumes were calculated for three intrusion locations: 1) the Upper Region (which corresponds to the North Rest of Repository from BRAGFLO calculations); 2) the Middle Region (South Rest of Repository); and 3) Lower Region (South Waste Panel). For a single replicate this amounts to 7,800 total simulations (1 replicate × 100 vectors × 3 drilling locations × 26 intrusion times). To account for new waste area associated with the replacement panels, the CRA19_12P spallings volume numerical grid includes a fourth intrusion location: the Other Region (corresponding to the West Rest of Repository region from BRAGFLO calculations; Figure 2-3). The inclusion of the Other Region within the set of hypothetical deterministic intrusions increases total number of simulations per replicate to 10,400 (1 replicate × 100 vectors × 4 drilling locations × 26 intrusion times).

Spallings volumes are calculated based on pressure conditions in the repository waste areas. Time-dependent spallings volumes are determined by interpolating the spallings volumes calculated by DRSPALL to the time-dependent repository pressures calculated by BRAGFLO. DRSPALL uses sampled parameter values from the LHS code but has no dependencies on outputs of other PA codes (Lord and Rudeen 2003). It is for this reason that DRSPALL is not typically run during a PA calculation. Both the CRA19 and the CRA19_12P use DRSPALL outputs from a previous analysis (Kirchner et al. 2014; 2015).

Spallings releases are calculated by multiplying spallings volumes by the average concentration of radionuclides in CH waste at the time of intrusion. Concentrations of radionuclides are calculated by the PRECCDFGF code from EPAUNI output as the volume-weighted average concentration in all CH-TRU waste streams. The repository volume (REFCON:VREPOS; determined by the volume of waste panels) is increased in the CRA19_12P due to the inclusion of Panels 11 and 12. As a result, the repository-volume based spallings concentrations (i.e., in units of EPA Units per repository volume) have changed for the CRA19_12P. However, since the waste volume and inventory for the CRA19_12P are unchanged from the CRA19, waste-volume based spallings concentrations (i.e., in units of EPA Units per waste volume) are identical for the two analyses.

6.2 Results

Section 6.2.1 provides occurrence of non-zero spalling events by volume as well as aggregate and scenario-wise statistics of spallings volumes removed from the repository. Results from the CRA19_12P are compared to the results of the CRA19 for the 100 vectors of Replicate 1. Results for the other two replicates show the same trends. Section 6.2.2 provides repository-scale spallings concentrations from EPAUNI outputs.

6.2.1 Spallings Volume

Figure 6-1 and Figure 6-2 show the number of non-zero spalling events plotted by spallings volume for all scenarios, intrusion times, and vectors. Most spalling events have a spallings volume in the 0-1 m^3 range. Figure 6-1 compares spallings events located in the Lower, Middle, Upper, and Other (L, M, U, O) regions between analyses. The volume range bins 0-1 and 7-8 m^3 from the CRA19_12P show the largest increases in events relative to the CRA19. This increase can be attributed to the inclusion of results from the O region that represents the increased repository footprint in the CRA19_12P. Figure 6-2 compares spallings events located in the L, M, and U regions between analyses. Within the 0-1 and 7-8 m^3 range the CRA19_12P reports a more comparable number of events relative to the CRA19. The volume range bins 1-2, and 2-3 m^3 also report a lower number of events than their respective bin ranges in the L, M, U, and O locations.

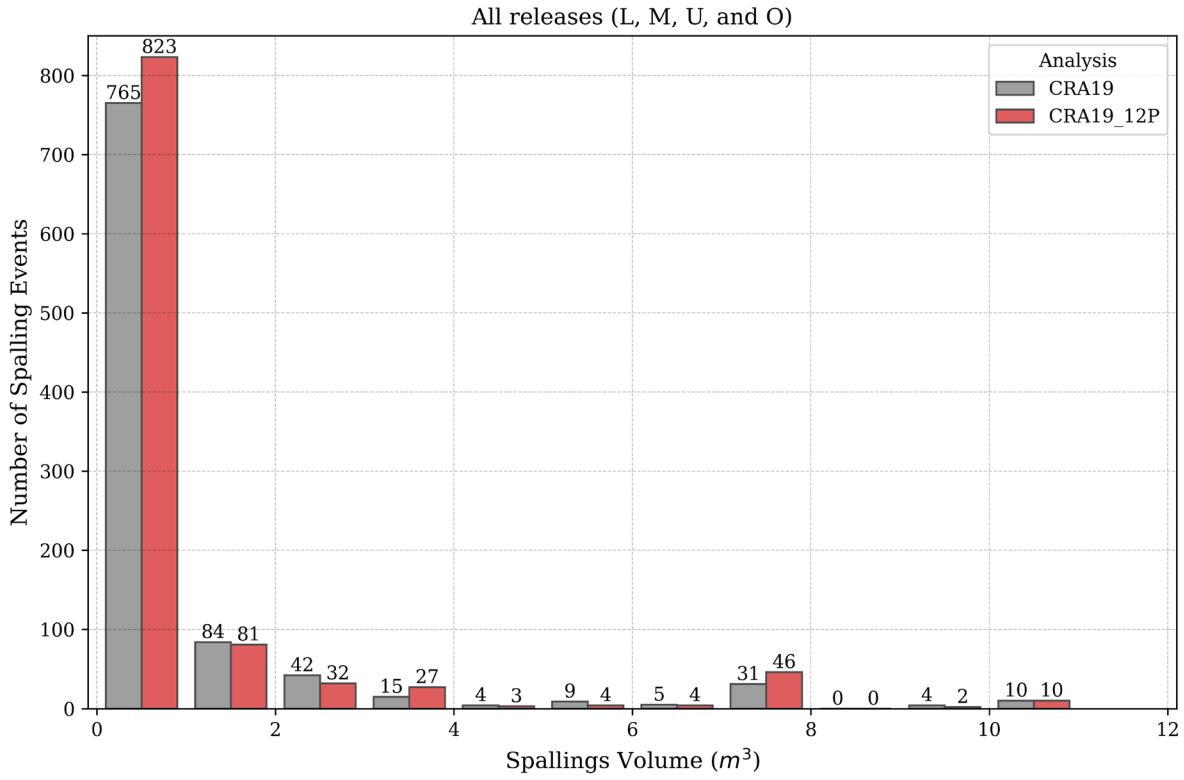

Figure 6-1: Number of Non-zero Spalling Events by Volume (All Intrusion Locations)

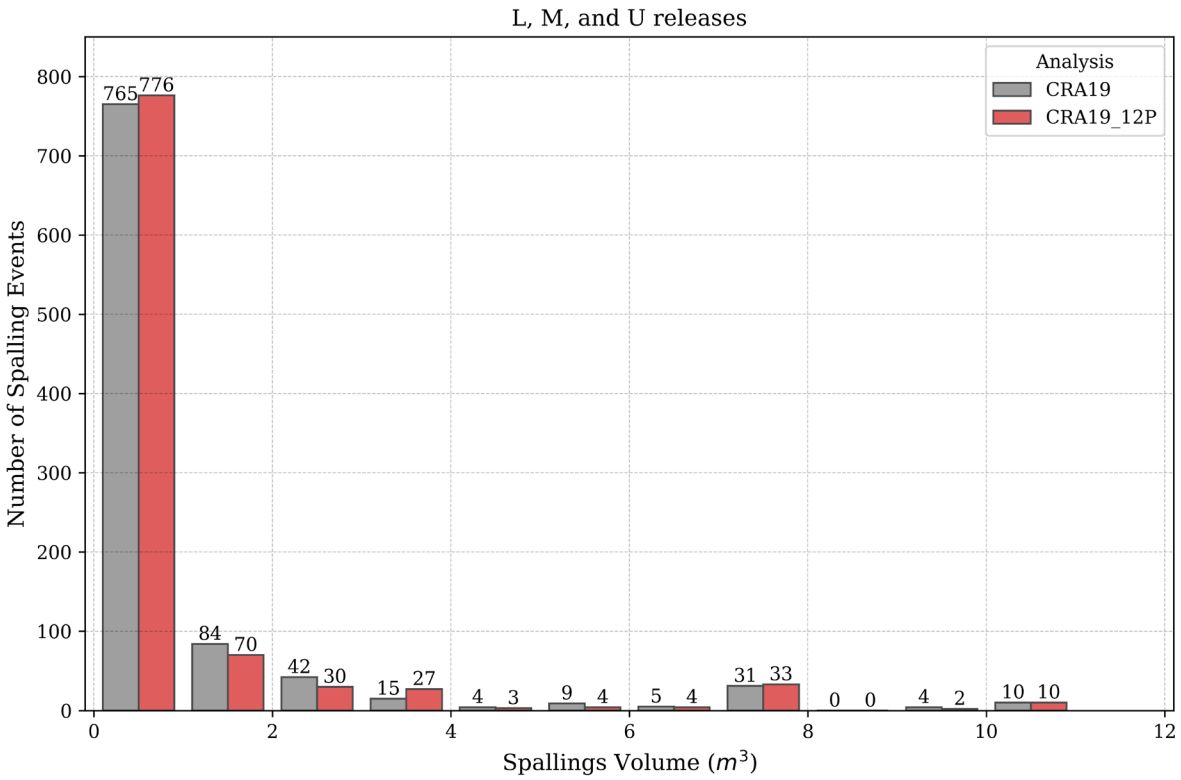

Figure 6-2: Number of Non-zero Spalling Events by Volume (L, M, and U Locations Only)

Summary statistics and box plots of non-zero spallings volumes over all scenarios, intrusion times, vectors, and drilling locations are given in Table 6-1 and Figure 6-3 respectively, for the CRA19 and the CRA19_12P. Maximum volumes are the same, and the means are nearly the same with the CRA19_12P slightly lower than the CRA19. While the number of non-zero realizations are slightly higher in the CRA19_12P due to the increased repository footprint, the non-zero realization fraction is lower relative to the CRA19.

Table 6-1: Non-Zero Spallings Volume Statistics

Maximum (m^3)	**Maximum (m^3)**	**Mean (m^3)**	**Mean (m^3)**	**Number of Realizations**	**Number of Realizations**
CRA19	**CRA19_12P**	**CRA19**	**CRA19_12P**	**CRA19**	**CRA19_12P**
10.229	10.229	1.000	0.996	969 (12.4%)	1032 (9.9%)

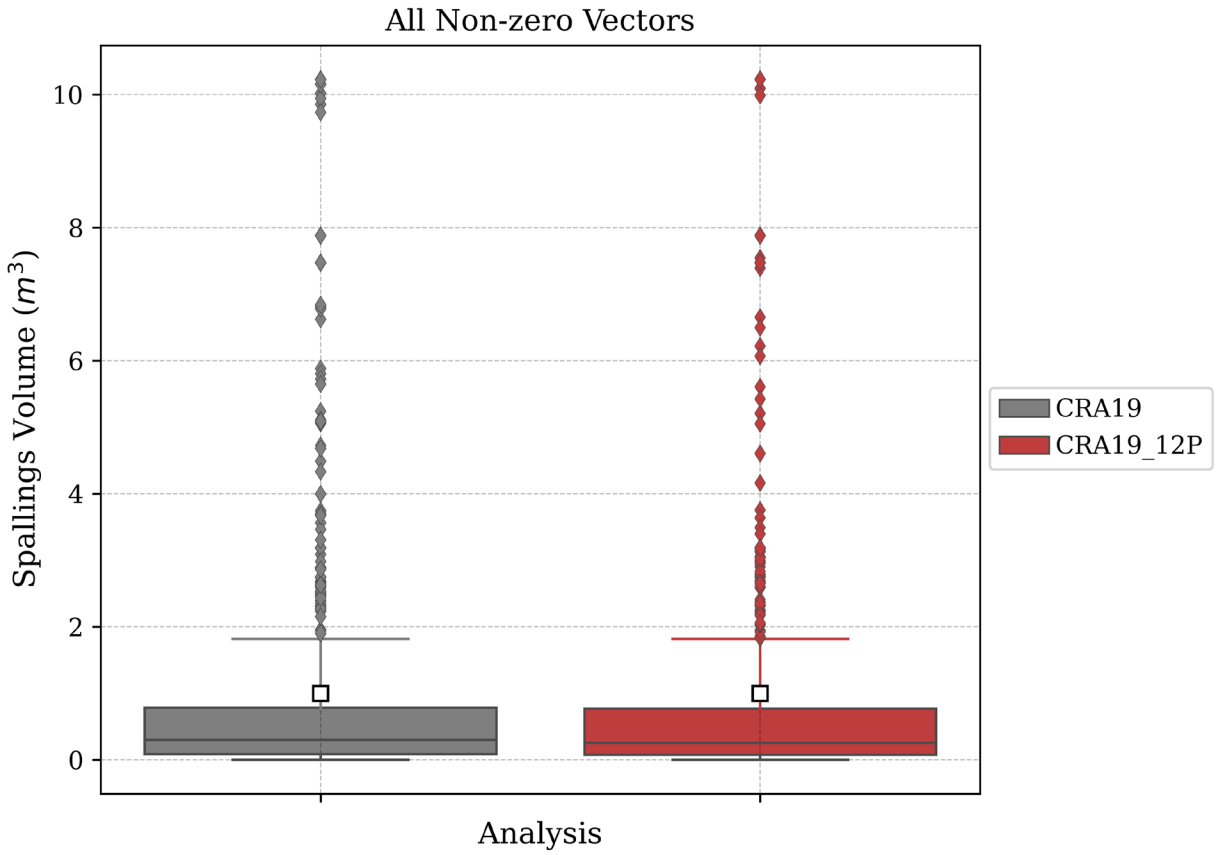

Figure 6-3: Non-Zero Spallings Volumes

Summary statistics and box plots of spallings volumes for each intrusion scenario are shown in Table 6-2 and Figure 6-4, respectively, for the CRA19 and the CRA19_12P. The maximum spallings volumes are the same in the CRA19 and the CRA19_12P and are highest in scenarios S2-DBR and S3-DBR, which also have the highest number of realizations that result in a non-zero spallings volume. While the fraction of realizations with non-zero spallings volume in scenarios S2-DBR and S3-DBR are comparable between analyses, the mean spallings volumes are slightly lower in the CRA19_12P. In general, spallings volume results are similar because there is little change in repository pressure between the CRA19 and CRA19_12P calculations (Section 4.2.1).

Table 6-2: Non-Zero Spallings Volume Statistics by Scenario

	Maximum (m^3)	Maximum (m^3)	Mean (m^3)	Mean (m^3)	Number of Realizations	Number of Realizations
Scenario	**CRA19**	**CRA19_12P**	**CRA19**	**CRA19_12P**	**CRA19**	**CRA19_12P**
S1-DBR	7.473	7.473	1.338	1.422	100 (5.6%)	119 (5.0%)
S2-DBR	10.229	10.229	1.000	0.918	421 (28.1%)	435 (21.8%)
S3-DBR	10.229	10.229	0.901	0.880	352 (23.5%)	343 (17.2%)
S4-DBR	7.473	7.473	1.079	1.243	41 (2.7%)	57 (2.9%)
S5-DBR	7.473	7.473	0.967	1.119	55 (3.7%)	78 (3.9%)

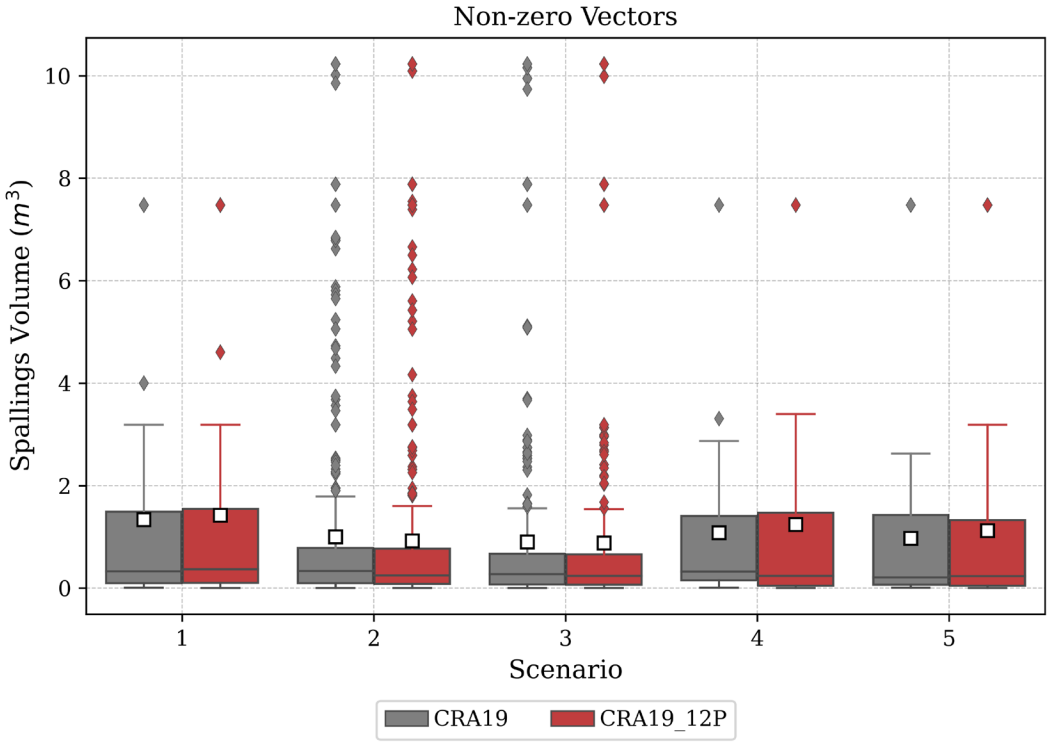

Figure 6-4: Non-Zero Spallings Volumes by Scenario

6.2.2 Spallings Concentration

The activity per solid waste volume in spallings releases has not changed in the CRA19_12P. However, increased repository volume results in decreased repository-volume concentrations (EPA Units per repository volume) in the CRA19_12P as shown in Figure 6-5. The activity concentration for a given spalling volume is therefore lower in the CRA19_12P.

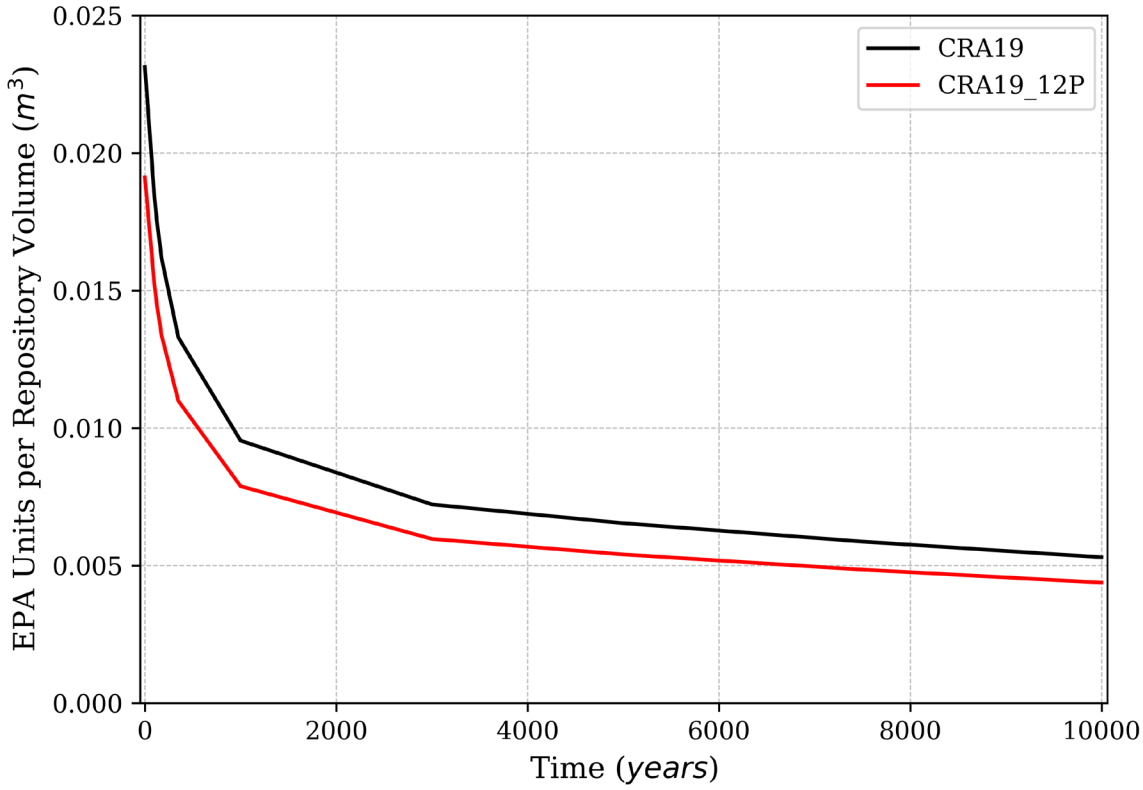

Figure 6-5: Repository Volume CH-Waste Concentration

7 Actinide Mobilization: PANEL Calculations

This section discusses the mobile (i.e., aqueous) actinide concentrations in the waste panels for the CRA19_12P PA. The calculated mobile actinide concentrations are used in conjunction with DBR volumes to estimate radionuclide releases due to DBR events. The Salado transport calculations, which also involve actinide concentrations, are discussed in Section 8. For more information on the actinide concentration calculation methodology, see Kim (2023).

7.1 Introduction

The code PANEL is used to simulate the radionuclide inventory in the waste panels as it decays and mixes with brine. Specifically, it performs four primary functions in the Waste Area (which consists of five interconnected waste panels):

1. PANEL calculates the radioactive decay and ingrowth of the radionuclide inventory in the waste panels. This calculation influences the amount of inventory available to be released at any time over the 10,000-year post-closure compliance period.
2. PANEL calculates the solubility each actinide of interest. Solubility as defined here consists of actinides either dissolved or associated with colloids in the aqueous phase. PANEL calculates the solubilities of colloids complexed with each actinide, where the complexed colloids are intrinsic colloid, microbial colloid, humic colloid, and mineral fragment.
3. PANEL calculates, as a function of time, the aqueous concentration of each radionuclide in brine that is in contact with the inventory in the waste panels. With the simplification that radionuclide mass in the repository is not reduced by brine flow out of the repository, this is a simple saturation-type calculation: the concentration is set to the lesser value of the solubility and the inventory available at the time divided by the volume of brine in the waste panel[5].
4. PANEL calculates the long-term discharge of radionuclide-contaminated brine from the repository waste panels to the Culebra in the E1E2 scenario (BRAGFLO scenario S6-BF). Discussion of these calculations is deferred to Section 8.

In the CRA19_12P PA calculations PANEL uses an updated value for the repository volume (REFCON:VREPOS). The DBR minimum brine volume (GLOBAL:DBRMINBV), inventory data, and actinide baseline solubilities are the same in the CRA19_12P as in the CRA19.

[5] The same calculation is made by the BRAGFLO code for the calculation of radiolytic gas generation. In the BRAGFLO code, brine volume changes with time while the PANEL code uses a fixed brine volume.

7.2 Results

The results of actinide mobilization calculations are presented in this section. Inventory at closure is presented. The lack of impact on radionuclide solubilities and mobilized actinide concentrations due to the increased repository volume is also discussed.

7.2.1 Inventory and Decay

PANEL models the decay and ingrowth of 30 radionuclides subject to decay chain reactions (Figure 2-1 in Kim (2023)) and performs mass balance calculations.[6] PANEL subsequently calculates concentrations of the 30 individual radionuclides, which are used for the DBR calculations.

PANEL performs a mass balance calculation over a group of "interconnected" waste panels rather than only a single waste panel. This is due to the expected lack of panel closures between waste panels in the southern portion of the repository. The five interconnected panels (Panels 3, 4, 5, 6, and 9) used in PANEL calculations are referred to as the Waste Area. Figure 7-1 shows the inventory at closure for the most prevalent radionuclides by activity in the Waste Area. The inventory in the WIPP repository is unchanged between the CRA19 and the CRA19_12P. However, the increase in repository volume due to the 12-panel repository layout in the CRA19_12P decreases the fractional footprint of a waste panel in the repository from 0.105 in the CRA19 to 0.087 in the CRA19_12P, leading to a corresponding decrease in the inventory at closure in the five interconnected waste panels. The relative inventories among the individual radionuclides at closure are unchanged from the CRA19.

[6] Note that because the CRA19_12P inventory is the same as the CRA19 inventory, no changes were made to inventory decay calculations performed by the EPAUNI code for the CRA19_12P. Although the results from the EPAUNI code are unaffected by the changes made for the CRA19_12P, for simplicity in the run control process, EPAUNI was rerun for the CRA19_12P PA using the same input as for the CRA19.

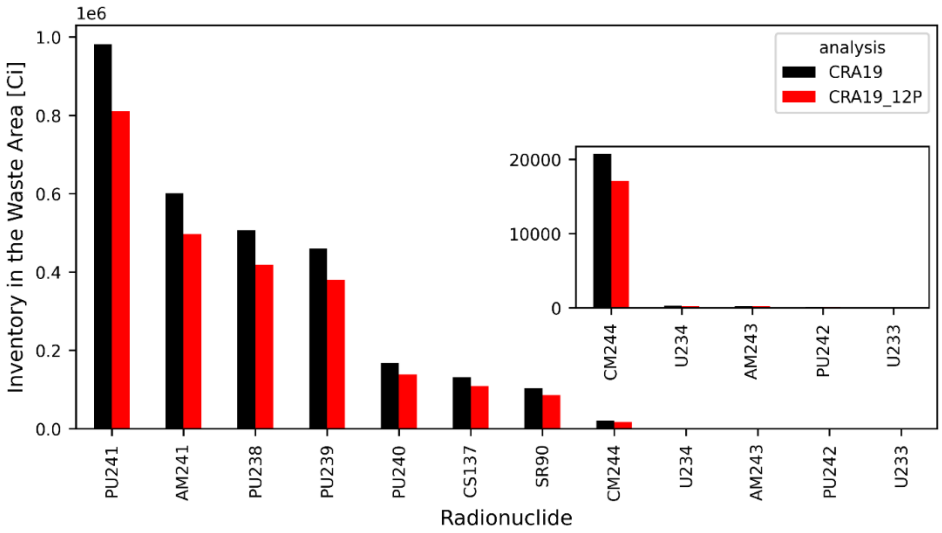

Figure 7-1: Inventory at Closure of the Significant Radionuclides in Five Waste Panels (Waste Area).

PANEL reports concentrations in terms of 30 individual radionuclides as well as five "lumped" radionuclides. A more detailed discussion of the selection and lumping methodology is given in Kicker (2023) and Kim (2023). PANEL performs this lumping procedure internally at each time step.

Radionuclides ^{137}Cs, ^{90}Sr, ^{244}Cm, and ^{243}Am, shown in Figure 7-1, are excluded in the lumping scheme. The fractions of initial inventory of these radionuclides with respect to 30 radionuclides modeled in PANEL are relatively small: 4.4% for ^{137}Cs, 3.5% for ^{90}Sr, 0.7% for ^{244}Cm, and 0.01% for ^{243}Am. However, ^{233}U (0.005%) and ^{234}U (0.007%) are included in the lumping scheme, though their inventory quantities are relatively small. This is because ^{233}U and ^{234}U are decay generation daughters of ^{241}Pu and ^{241}Am, and ^{242}Pu and ^{238}Pu, respectively.

The inventory of the five lumped radionuclides at closure in the Waste Area is shown in Figure 7-2. The fraction factor of the Waste Area volume to the repository volume is also used to calculate inventory at closure of lumped radionuclides in the Waste Area. Subsequently, the same trends are apparent as in the individual isotope inventory; PU239L and AM241L dominate.

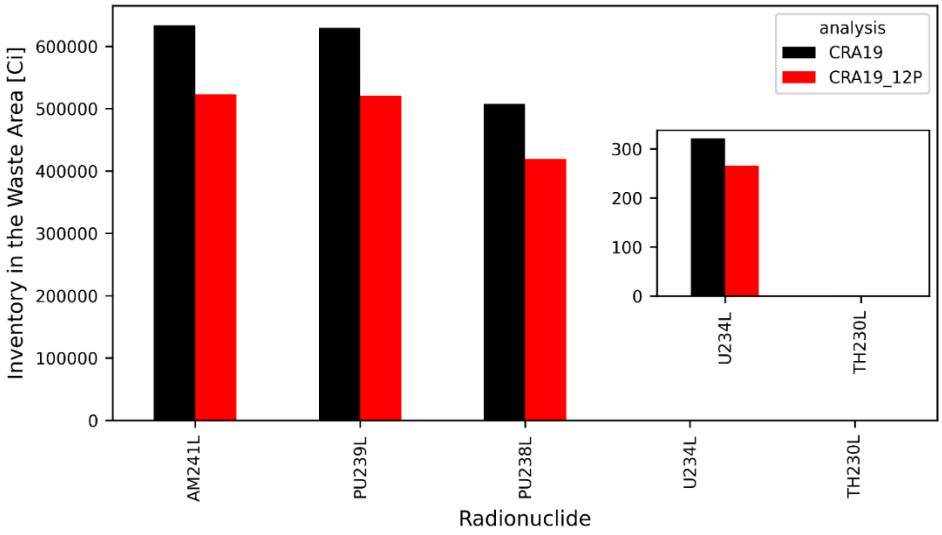

Figure 7-2: Inventory at Closure of Lumped Radionuclides in the Waste Area.

With inventory at closure of lumped radionuclides in Figure 7-2, inventory of the decaying lumped radionuclides in the Waste Area is calculated with increasing times for the CRA19 and the CRA19_12P, as shown in Figure 7-3. At early times, PU239L and AM241L impact the overall inventory activity, and AM241L is a significant contributor to total activity only at early times. PU239L dominates activity for most of the 10,000 years and thus would dominate the overall activity concentration in brine.

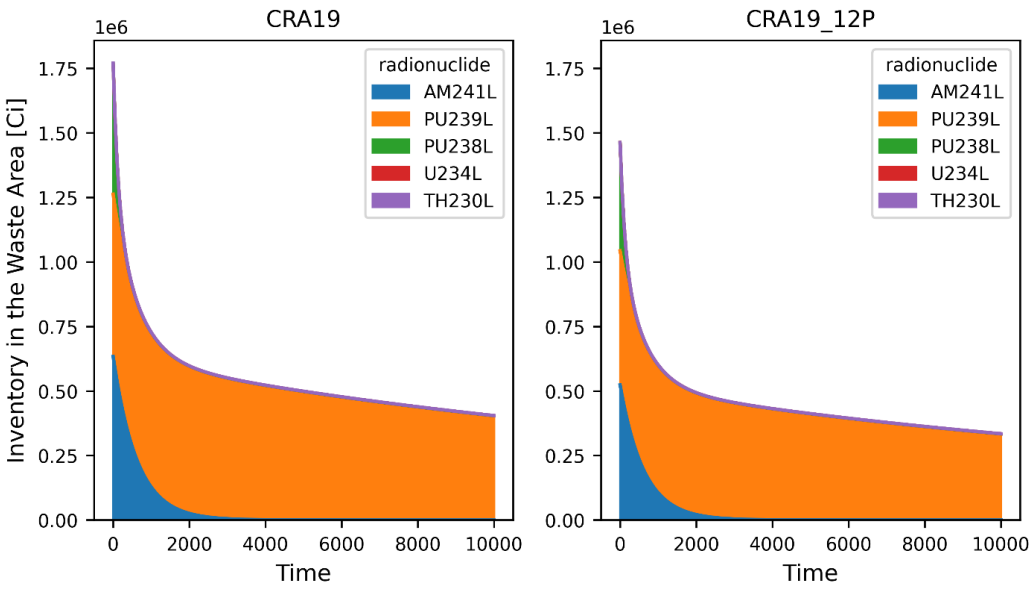

Figure 7-3: Inventory in the Waste Area of Lumped Radionuclides Over Time

7.2.2 Solubility Calculations

The CRA19_12P uses the same actinide baseline solubilities as the CRA19, since the introduction of Panels 11 and 12 result in no changes to the assumptions made for chemical thermodynamic property values or minimum brine volume. Similarly, the CRA19 solubility uncertainty factors and the colloid enhancement factors are used, resulting in no changes to the total mobilization potentials for Am, Pu, Th, U, and Np and no changes to the solubility limits of the lumped radionuclides.

7.2.3 Mobilized Actinide Concentrations in Waste Panel

The PANEL code calculates the mobilized concentration of each radionuclide in Salado and Castile brines in the Waste Area (consisting of five waste panels) as a function of time. The mobilized concentrations are combined with the DBR volumes (Section 5.2.1) to calculate DBRs. The inventory concentrations in the Waste Area are determined by a simple saturation-type calculation: each concentration is set to the lesser value of the solubility limit and the inventory limit (inventory at the time divided by the volume of brine in the Waste Area). The previous section demonstrates that the solubility limits are the same in the CRA19 and the CRA19_12P.

Figure 7-3 shows the inventory of five lumped radionuclides in the Waste Area, which is 0.525 (=0.105×5) of the repository inventory in the CRA19 and 0.435 (=0.087×5) in the CRA19_12P. The brine volume in the Waste Area is computed by multiplying the volume fraction of the Waste Area by the brine volume in the repository (DBRMINBV). Mobile concentrations are either limited by inventory or limited by solubility. When the entire radionuclide inventory is mobilized, the brine volume and the inventory are scaled by the same factor leading to the same mobile concentration for a given volume of brine in the repository. When the mobile concentration is limited by solubility, the mobile concentration remains at the solubility.

Therefore, as a function of the brine volume in the repository, mobile concentrations of radionuclides are the same in the CRA19 and in the CRA19_12P. Because homogeneous chemical conditions are assumed in the repository, at a given repository brine volume the Waste Area mobile concentration is the same as the repository mobile concentration and one panel mobile concentration.

However, when calculating mobile concentrations in brine for DBRs, the PA considers the brine volume in the intruded panel, not the entire repository. As the volume of the repository is larger in the 12-panel model with the same panel volume, the scaling from repository brine volume to panel brine volume has changed from 0.105 in the CRA19 to 0.087 in the CRA19_12P. The difference in one panel brine volume between the CRA19 and the CRA19_12P becomes (0.018)×(DBRMINBV)×(brine volume multiplier) at a given one panel concentration. Figure 7-4 shows the mean total mobilized radionuclide concentrations in Salado Brine at 100 and 10,000 years versus the intruded panel brine volume. This figure illustrates that the panel brine volume difference at a fixed concentration depends on the brine volume multiplier. As in the CRA19, the mean total concentration is dominated by the lumped quantities AM241L and PU239L at early times, and by PU239L at later times as AM241L decays away.

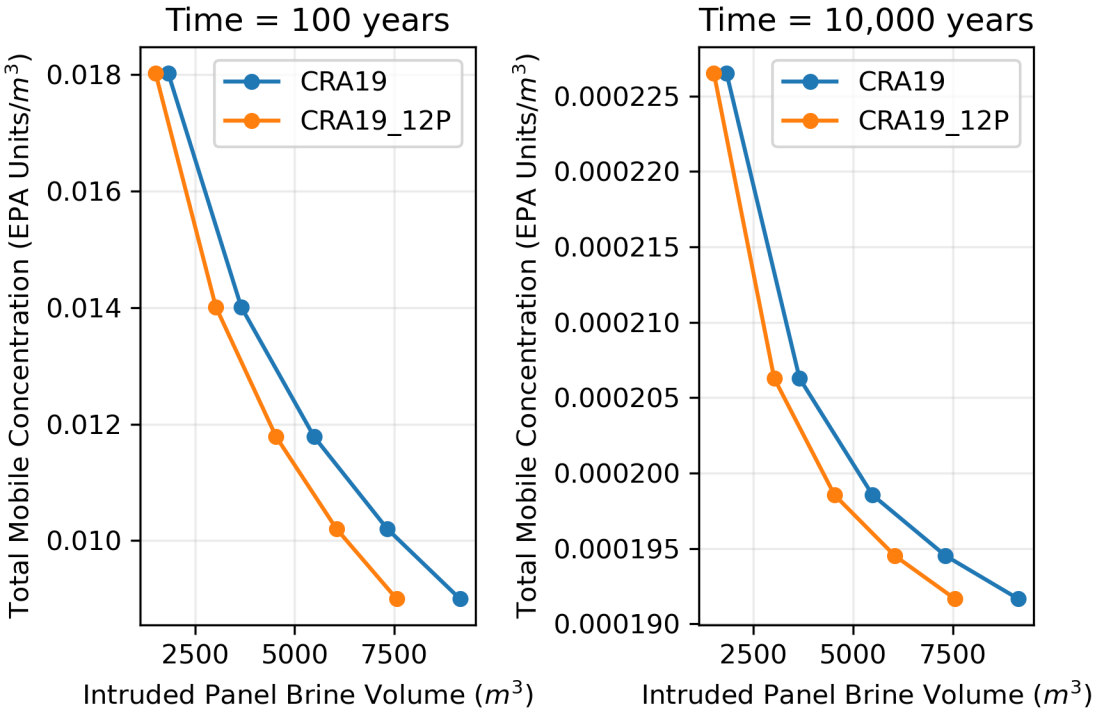

Figure 7-4: Mean Total Mobile Concentrations in Salado Brine at 100 and 10,000 years

8 Salado Transport: NUTS and PANEL Calculations

This section discusses the calculated long-term actinide discharges from the repository *to the Culebra* member of the Rustler formation. Transport through the Culebra is discussed in Section 10.

8.1 Introduction

The NUTS code performs decay and mass transport calculations in the Salado formation using only the five lumped radionuclides, whose inventories are input to NUTS. This contrasts with PANEL, which performs the decay and mass balance calculations on the full set of 30 individual radionuclides and five lumped radionuclides and reports the lumped values at each timestep. NUTS models three decay chains (Figure 2-2 in Kim (2023)), based on the assumption that the lumped isotopes inherit the properties of the named isotope.

NUTS uses the same two-dimensional grid as BRAGFLO (Figure 2-3) and relies on BRAGFLO results for the volumetric brine flow fields and other fluid and rock properties from scenarios S1-BF through S5-BF (Table 4-1). It models contaminant advection in the aqueous phase, dissolution and precipitation, and radioactive decay. It does not model diffusion, dispersion, adsorption, or gas-phase transport.

NUTS simulates transport of five lumped radionuclides between two-dimensional grid cells, while PANEL calculates releases by multiplying concentration and discharged brine volume at each time step. The intrusion times used with each code are shown in Table 8-1.

The PANEL code is used for transport calculations for the S6-BF scenario, which is the E1E2 multiple intrusion case. This code tabulates radionuclide advection at the intersection of the borehole and Marker Bed 138 (MB138) from the brine discharge volume calculated by BRAGFLO. In the S6-BF scenario, radionuclide advection to Marker Bed 138 is equated with advection to the Culebra. Thus, cumulative discharges *to the Culebra* are tabulated at the intersection of the borehole and MB138.

8.2 Results

This section describes the results of BRAGFLO, NUTS and PANEL calculations used for transport of radionuclides to the Culebra for Replicate 1. Results for the other two replicates show the same trends. Cumulative brine discharge to the Culebra is discussed. Radionuclide releases to the Culebra for various scenarios are also discussed.

8.2.1 Brine Releases to the Culebra

The cumulative brine discharges *to the Culebra* at 10,000 years are calculated by BRAGFLO in scenarios S1-BF to S6-BF and are shown in Figure 8-1. The cumulative brine discharges calculated by BRAGFLO exhibit a slight change in the CRA19_12P. Mean cumulative brine discharges are shown as a function of post closure time in Figure 8-2, where scenario S1-BF (undisturbed discharge case) is excluded because of negligibly small release compared to other scenarios. In scenarios S2-BF, S3-BF, and S6-BF (relevant to E1 intrusion) the cumulative brine

discharges are increased in the CRA19_12P. On the other hand, the cumulative brine discharges in scenarios S4-BF and S5-BF (relevant to E2 intrusion) are decreased in the CRA19_12P.

Table 8-1: Intrusion Times by NUTS (S2-BF through S5-BF) and PANEL (S6-BF)

BRAGFLO Scenarios	Intrusion Type	Intrusion Times (year) by NUTS and PANEL
S2-BF	E1	100, 350
S3-BF	E1	1000, 3000, 5000, 7000, 9000
S4-BF	E2	100, 350,
S5-BF	E2	1000, 3000, 5000, 7000, 9000
S6-BF[1]	E1E2	100, 350, 1000, 2000, 4000, 6000, 9000

Note:
1 – Intrusion time is for E1 intrusion.

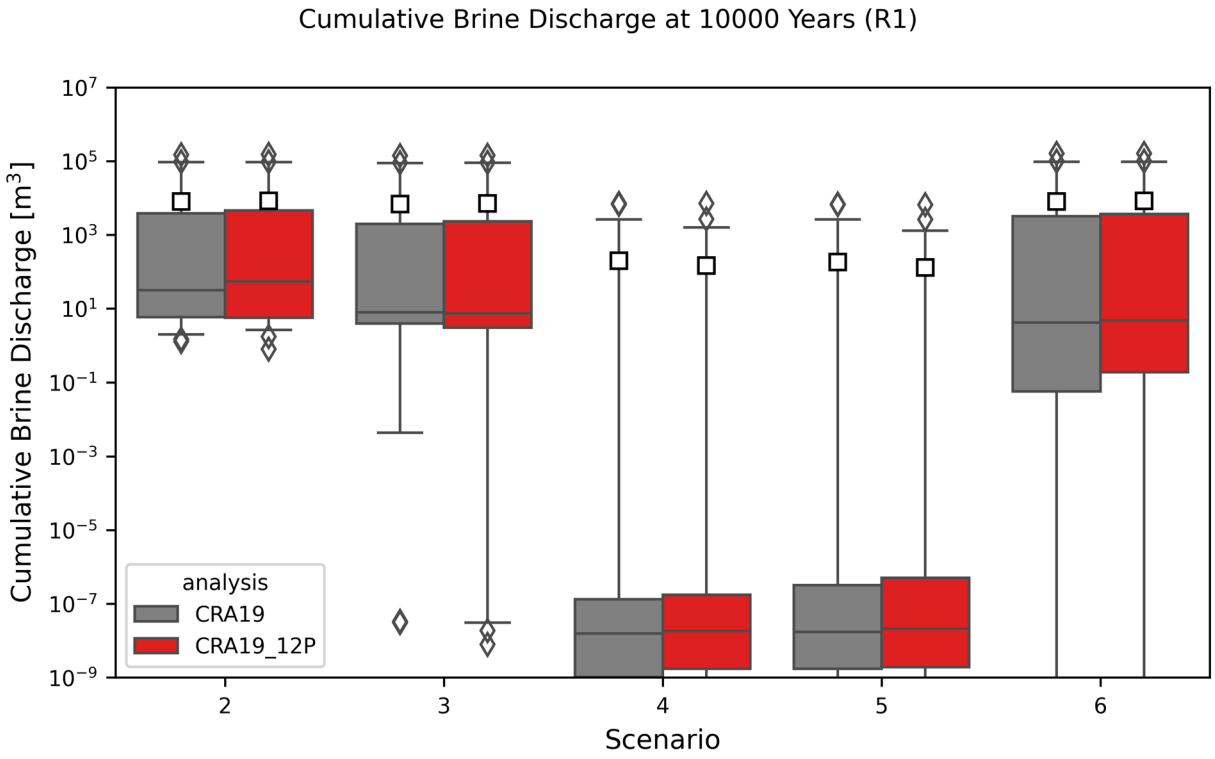

Figure 8-1: Cumulative Brine Volume Discharge to the Culebra at 10,000 Years from Scenarios S2-BF through S6-BF

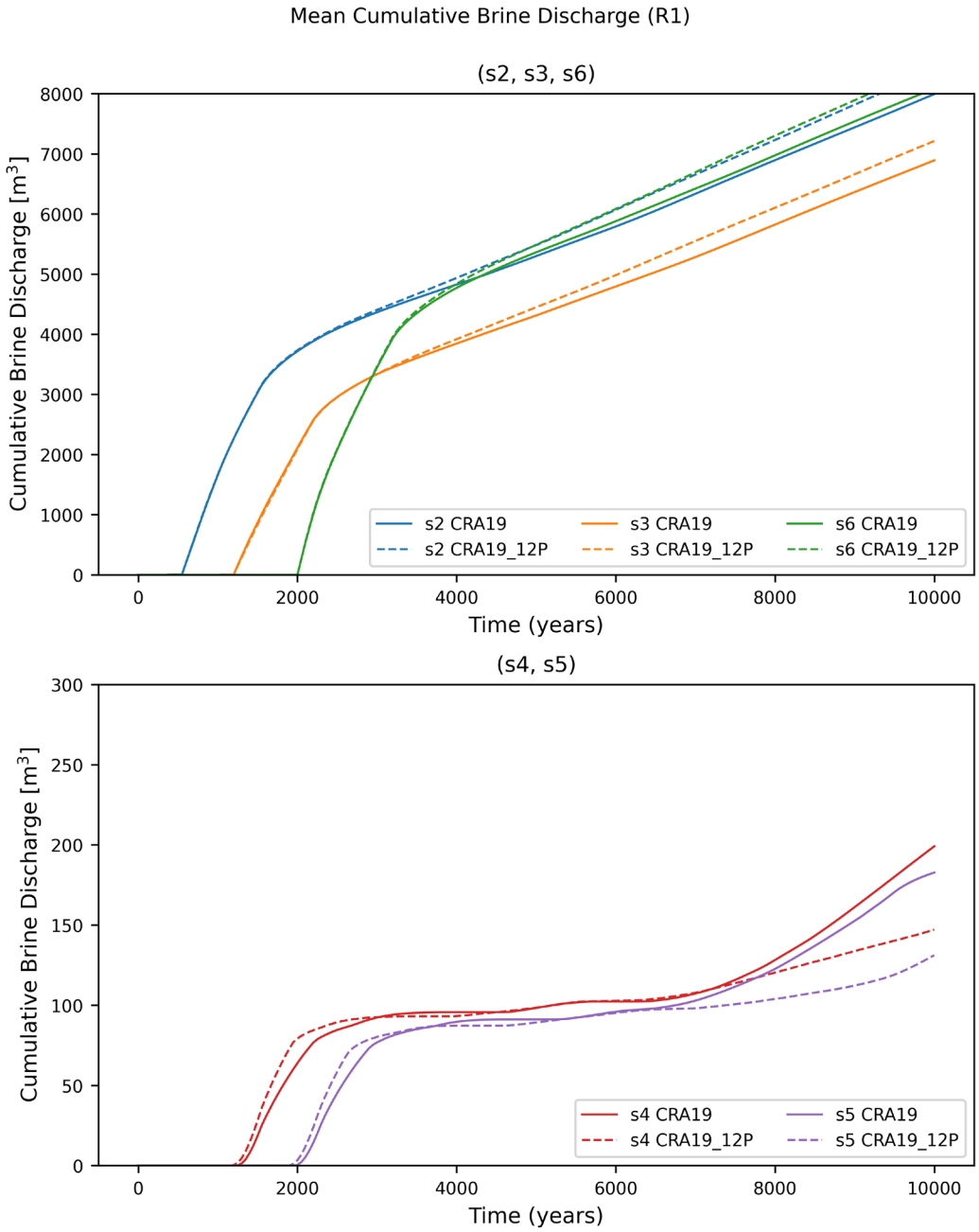

Figure 8-2: Cumulative Brine Volume Discharge to the Culebra vs Post-closure Time from Scenarios S2-BF through S6-BF.

8.2.2 Long Term Releases of Lumped Radionuclides

The NUTS calculations first utilize a non-decaying, non-reactive tracer for screening to eliminate calculations for realizations that transport insufficient quantities of radionuclides. In the CRA19_12P, the numbers of screened-in vectors are 205, 174, 25, and 26 out of 300 in S2-BF through S5-BF scenarios, compared to 207, 181, 22, and 21 in the CRA19. Cumulative total releases *to the Culebra* by Salado transport are not displayed for the undisturbed scenario S1-BF, because no discharge to the Culebra is greater than 10^{-14} EPA units. Cumulative discharges at

10,000 years for screened-out vectors are set to zero. Screened-out vectors and vectors with negligible radionuclide discharge, prevent the interquartile range from appearing for all but scenario S6-BF. For S4-BF and S5-BF scenarios, a whisker ranging values between the 75th and 98th percentiles is partially visible due to small numbers (less than 10% of 300 realization vectors) of screened-in vectors. Therefore, the mean discharges are heavily skewed by a few vectors with high radionuclide releases.

Due to common chemical properties, lumped radionuclide concentrations are the same in the CRA19_12P as in the CRA19. However, the cumulative brine discharges *to the Culebra* are changed (Figure 8-2) which impact long term lumped radionuclide releases *to the Culebra*. Assessed distributions of cumulative total radionuclide discharges *to the Culebra* at 10,000 years are slightly changed in the CRA19_12P, as shown in Figure 8-3. In this figure, a borehole intrusion occurs at intrusion times corresponding to BRAGFLO scenarios (Table 4-1).

Mean and median cumulative total releases to the Culebra at 10,000 years are tabulated at BRAGFLO-defined intrusion times as well as NUTS-defined intrusion times in Table 8-2. In this table median cumulative radionuclide discharges to the Culebra at 10,000 years are decreased except S4-BF at the E2 intrusion time of 100 years and S5-BF at the E2 intrusion time of 9,000 years, and S6-BF at the E1 intrusion times of 4,000 and 6,000 years. For scenarios S4-BF and S5-BF, median cumulative radionuclide discharges to the Culebra at 10,000 years are unchanged at 0.0 EPA Units because a limited numbers of vectors are screened in for Salado transport simulations in the CRA19 and the CRA19_12P.

Figure 8-3 shows mean and median cumulative discharges of total radionuclides *to the Culebra* at 10,000 years for intrusion times listed in Table 8-2. Mean cumulative total discharges show a similar trend between the CRA19 and the CRA19_12P except releases for an E2 intrusion at 9,000 years. Numerous screened-out vectors for E2 intrusion cases cause median cumulative discharges of total radionuclides at 10,000 years to remain at 0.0, resulting in no visible symbols in the right plot in Figure 8-4. A limited numbers of vectors govern the mean discharge values such that the resulting mean data are higher than the median data. Therefore, mean cumulative discharges of total radionuclides *to the Culebra* at 10,000 years are basically decreased in the CRA19_12P.

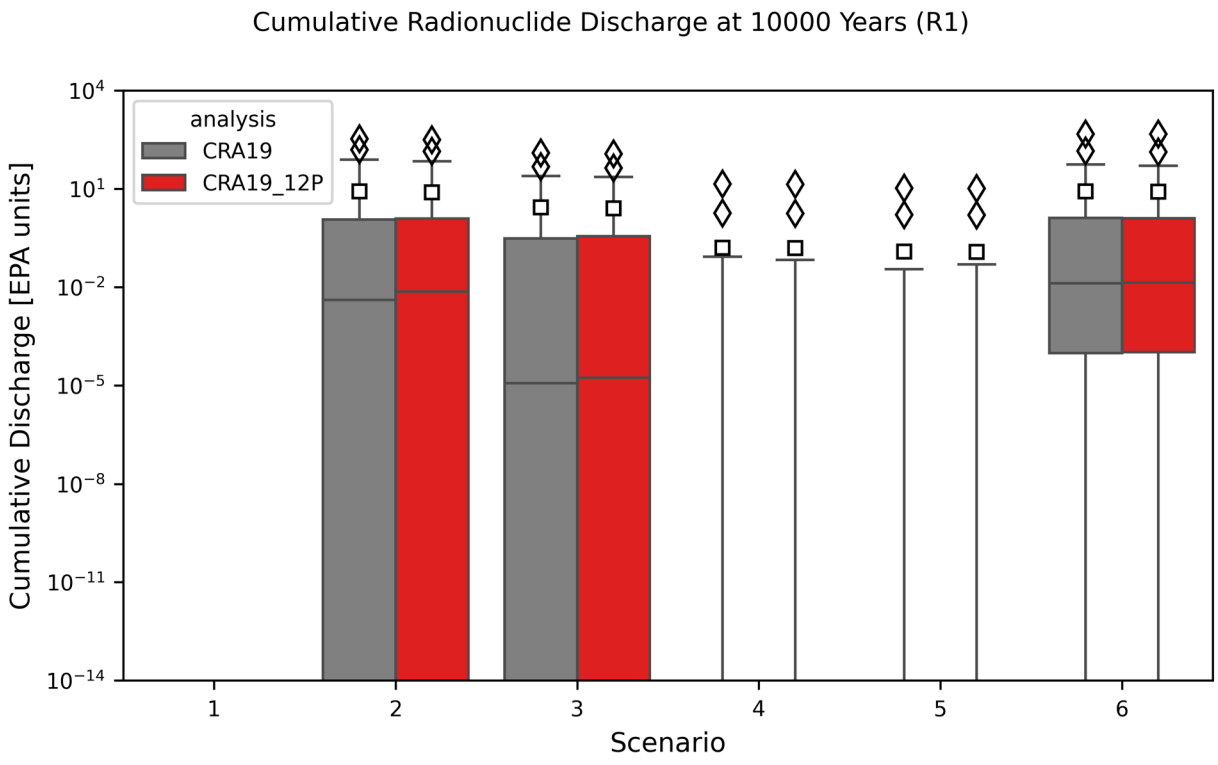

Figure 8-3: Cumulative Total Radionuclide Discharge to the Culebra at 10,000 Years for Scenarios S1-BF through S6-BF

Table 8-2: Cumulative Total Radionuclide Releases to the Culebra at 10,000 Years.

Intrusion Type	Scenario	Intrusion Time	Mean CRA19	Mean CRA19_12P	Median CRA19	Median CRA19_12P
E1	S2-BF	100	1.11E+01	1.02E+01	4.50E-03	8.28E-03
E1	S2-BF	350	8.38E+00	7.75E+00	4.00E-03	7.24E-03
E1	S3-BF	1000	2.68E+00	2.52E+00	1.15E-05	1.70E-05
E1	S3-BF	3000	1.13E+00	1.11E+00	4.23E-06	5.09E-06
E1	S3-BF	5000	9.76E-01	9.73E-01	7.47E-07	5.01E-07
E1	S3-BF	7000	9.07E-01	9.05E-01	3.63E-07	3.73E-08
E1	S3-BF	9000	6.57E-01	6.65E-01	3.54E-11	4.61E-10
E2	S4-BF	100	1.84E-01	1.81E-01	0.00E+00	0.00E+00
E2	S4-BF	350	1.58E-01	1.56E-01	0.00E+00	0.00E+00
E2	S5-BF	1000	1.21E-01	1.18E-01	0.00E+00	0.00E+00
E2	S5-BF	3000	8.99E-02	8.74E-02	0.00E+00	0.00E+00
E2	S5-BF	5000	8.54E-02	8.20E-02	0.00E+00	0.00E+00
E2	S5-BF	7000	8.48E-02	8.15E-02	0.00E+00	0.00E+00
E2	S5-BF	9000	1.23E-04	9.37E-04	0.00E+00	0.00E+00
E1E2	S6-BF	100	3.97E+01	3.58E+01	1.61E-02	1.68E-02
E1E2	S6-BF	350	3.08E+01	2.78E+01	1.60E-02	1.68E-02
E1E2	S6-BF	1000	1.65E+01	1.52E+01	1.57E-02	1.64E-02
E1E2	S6-BF	2000	8.37E+00	8.12E+00	1.29E-02	1.35E-02
E1E2	S6-BF	4000	4.94E+00	4.97E+00	2.55E-03	2.76E-03
E1E2	S6-BF	6000	3.96E+00	3.97E+00	2.64E-04	3.36E-04
E1E2	S6-BF	9000	2.31E+00	2.31E+00	1.52E-04	1.83E-04

Note:
Cells shaded in green represent the cumulative total radionuclide releases at 10,000 years calculated by the NUTS ISO mode in scenarios S2-BF through S5-BF, when a borehole intrusion occurs at a time defined corresponding to a BRAGFLO intrusion. Release values in other cells of these scenarios are calculated by the NUTS INT mode when a borehole intrusion occurs at time not corresponding to a BRAGFLO intrusion. Release values in cells of scenario S6-BF are calculated by the PANEL INT mode.

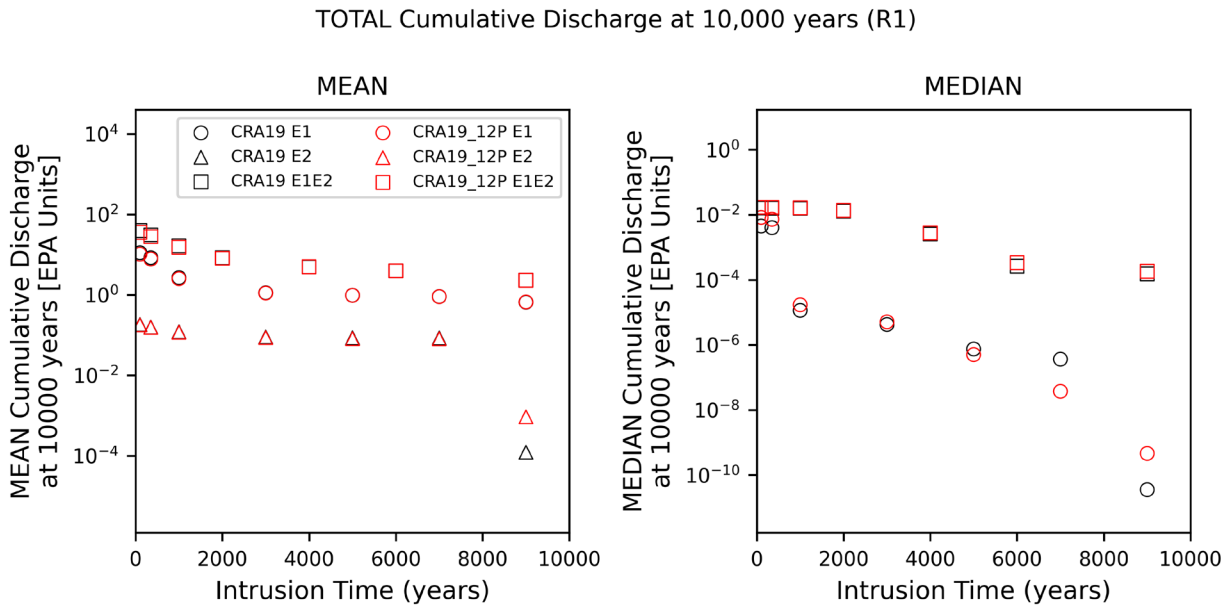

Figure 8-4: Mean and Median Cumulative Discharges of Total Radionuclides *to the Culebra* at 10,000 Years.

9 Culebra Flow and Transport: MODFLOW and SECOTP2D

This section describes the Culebra flow and transport models for the CRA19_12P analysis, and the results from these models. The Culebra flow model scenarios and inputs are the same as the CRA19 analysis; however, flow simulations are rerun using the updated groundwater flow software MODFLOW6. The model inputs and setup are briefly summarized below; otherwise, for a complete description of the Culebra flow model used in the CRA19 and the CRA19_12P, see the documentation for the 2009 Performance Assessment Baseline Calculation (Kuhlman 2010). A scenario is added to the Culebra transport calculation that simulates mass discharge into the Culebra from a point above the replacement panels region, identified as Culebra Release Point 2 (CRP-2). The scenario with mass discharge into a point above the centroid of the existing waste panels (CRP-1) is retained from the CRA19 calculations. Analysis results are presented for CRP-1 and CRP-2.

9.1 Introduction

The Culebra is modeled as a single horizontal layer of uniform 7.75 m vertical thickness discretized into 100-m square cells, yielding a model that is 284 cells or 28.4 km wide by 307 cells or 30.7 km tall (Figure 9-1). The model boundary conditions along straight-line portions of the north, west, and south edges of the domain are specified head determined from the initial head surface. The constant-head region associated with the halite-sandwiched portion of the Culebra is set to the land surface elevation. The piecewise-linear boundary in the northwest corner is a no-flow boundary parallel to the Nash Draw groundwater divide.

It is hypothesized that subsidence due to collapse of the underground voids created by potash mining may increase permeability in the Culebra. The impact of mining is modeled as a constant multiplier on transmissivity on cells within the angle of draw of mined potash areas. The scaling factor for each T-field is sampled uniformly between 1 to 1,000 by the LHS software. The range of this factor is set by the EPA in regulation 40 CFR 194.32(b) (U.S. EPA 1996). Culebra flow calculations are performed for a “partial mining” scenario in which all potash outside of the LWB is mined, and a “full mining” scenario in which all potash in the model domain is mined.

Particle tracks are computed using DTRKMF (WIPP PA 2024) to characterize the flow fields in terms of advective pathway and travel time taken by a marked water particle from each release point to the WIPP LWB. DTRKMF was modified to read output from MODFLOW6 and run simulations of CRP-1 and CRP-2, but otherwise the model setup and assumptions are as documented in Kuhlman (2010).

Radionuclide transport through the Culebra is simulated with the WIPP PA software SECOTP2D, which assumes parallel plate fracturing wherein fluid flow is restricted to the advective continuum (fractures), and mass is transferred between the advective and diffusive (matrix) continua via molecular diffusion. Transport simulations are run for both full- and partial-mining flow scenarios. In each simulation, 1 kg of each of ^{241}Am, ^{239}Pu, ^{234}U, and ^{230}Th are released at a single location during the first 50 years after repository closure and the cumulative mass discharge at the WIPP LWB over the 10,000-year regulatory period is reported. The ^{234}U decay product ^{230}Th is tracked and reported separately. Releases from the ^{234}U decay

product are reported as ^{230}Th and releases from the ^{230}Th mass released into the Culebra are reported as ^{230}ThA.

The Culebra transport calculation is augmented from the CRA19 analysis with an additional scenario that simulates mass discharge into the Culebra from the replacement panels region. In the CRA19, mass is released at the centroid of Panels 1 through 10 (CRP-1 on Figure 9-1). The CRA19_12P analysis retains these simulations and additionally simulates mass release into the centroid of the replacement panels Panel 11 and Panel 12 (CRP-2 on Figure 9-1).

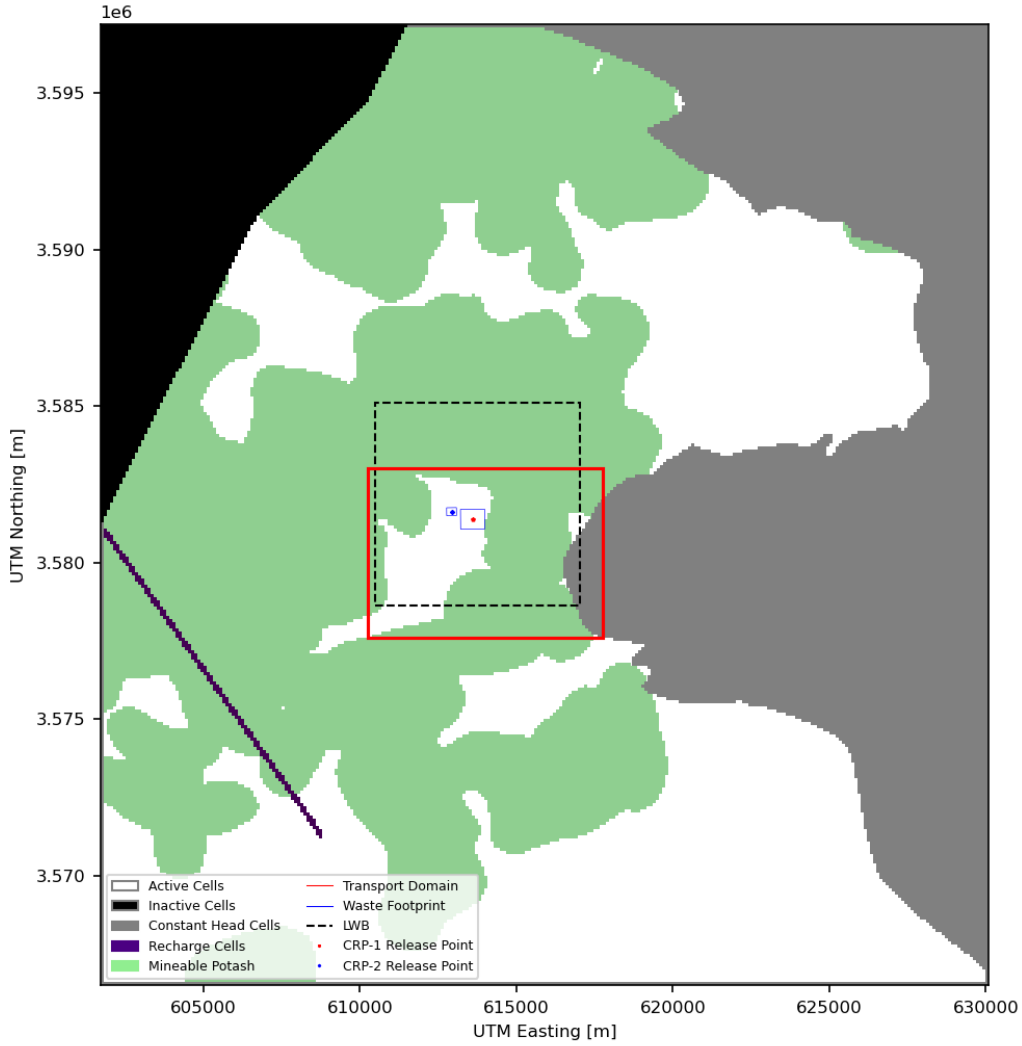

Figure 9-1: Culebra Flow and Transport Model Domain

9.2 Results

This section presents results of the Culebra flow model as characterized by the DTRKMF output particle tracks, and the Culebra radionuclide transport model resulting cumulative mass discharge to the LWB. Results are presented for all simulations, including two mining scenarios impacting the flow fields, and two release point scenarios impacting the transport. The full

analysis includes three replicates of 100 LHS samples. Figures in this section display results from one LHS replicate ("Replicate 1") to characterize the results across different scenarios, while tables in this section display results from all three replicates to verify the similarity across replicates. The CRA19 analysis is represented by the CRA19_12P CRP-1 results. Quantities below a reporting threshold of 10^{-24} kg are tabulated as 0.0.

The particle tracks from each release point and replicate are plotted for the full mining scenario and partial mining scenario (Figure 9-2 and Figure 9-3, respectively), with the mining-impacted area shown in gray. In the full mining scenario, particles released at both CRP-1 and CRP-2 generally move toward the mining impacted area to the southeast, and then deflect to the south following the interface with the mining affected region to the southern extent of the LWB. Because CRP-2 is farther upstream, i.e., to the northwest of CRP-1, particles released at this point must travel farther to reach the LWB. The partial mining particle tracks are more broadly distributed across the east-west direction (i.e., not focused by any persistent features across realizations) from both CRP-1 and CRP-2 but are also generally directed toward the south.

The cumulative distribution function (CDF) of the time taken for a particle to reach the LWB along each particle track is plotted for each replicate, mining scenario, and release point (Figure 9-4). These plots describe the likelihood of a particle crossing the LWB by the indicated x-axis travel time. Mean, median, and minimum particle travel times are summarized in Table 9-1. Particle travel times to the LWB are higher from the CRP-2 than the CRP-1 release point across all probability levels for both mining scenarios and in all replicates.

Complementary Cumulative Distribution Function (CCDF) plots of the cumulative mass reaching the LWB by t=10,000 years model time are provided in Figure 9-5. These plots describe the likelihood of a simulation exceeding the indicated mass discharge on the x-axis for each replicate, mining scenario, and release point. Despite the extremely low limit on the x-axis (10^{-9} kg), less than 50% and 20% of the full mining and partial mining scenario simulation results, respectively, plot on the visible range for all isotopes and release points. Consistent with the higher particle travel times, mass discharge from CRP-2 is lower for all scenarios and isotopes across the visible range of probability levels. Cumulative mass transported to the LWB is highest for ^{234}U, lowest for ^{241}Am, with ^{230}ThA and ^{239}Pu values in-between for both CRP-1 and CRP-2 simulations.

Summary statistics of the cumulative mass reaching the LWB by t=10,000 years are provided in Table 9-2 through Table 9-7. Table 9-2 and Table 9-3 show the mean cumulative mass transported to the LWB by 10,000 years in the full and partial mining conditions, respectively. Table 9-4 and Table 9-5 show the median cumulative mass transported to the LWB by 10,000 years in the full and partial mining conditions, respectively. Median mass values in all partial mining simulations are also below the reporting criterion of 10^{-24} kg. Table 9-6 and Table 9-7 show the count of vectors (n=100) exceeding 10^{-9} kg cumulative mass transported to the LWB by 10,000 years in the full and partial mining conditions, respectively. Cumulative mass discharge results in CRP-1 simulations are generally consistent with the CRA19 results (Kuhlman 2010), with minor differences likely resulting from the change from the MODFLOW-2000 to MODFLOW6 flow simulation software.

The results show that mass discharged above the replacement panels region consistently reaches the LWB later and in lower amounts across both the full and partial mining scenarios than mass discharged above the original waste panels.

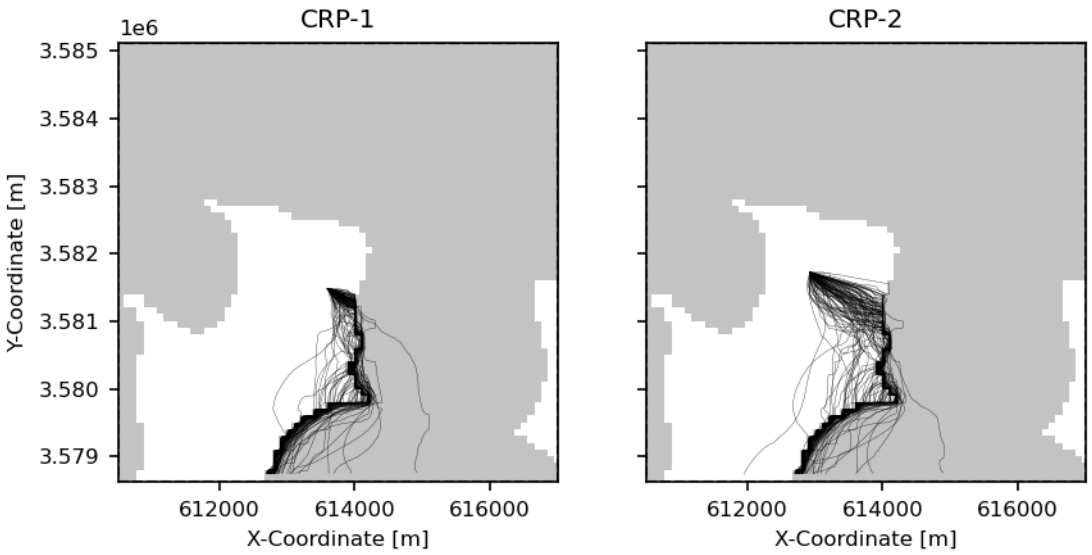

Figure 9-2: DTRKMF Particle Tracks, Full Mining Scenario

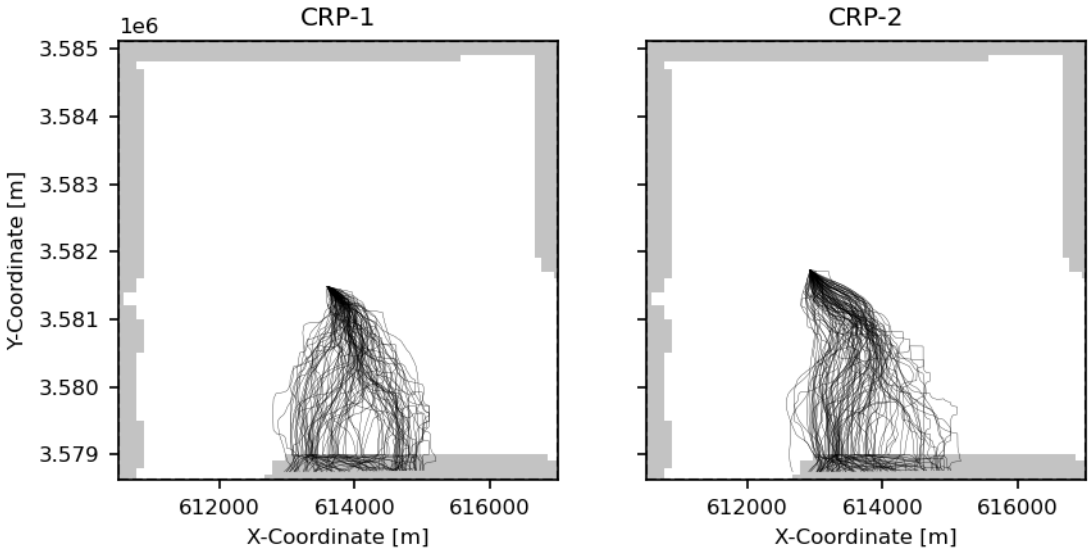

Figure 9-3: DTRKMF Particle Tracks, Partial Mining Scenario

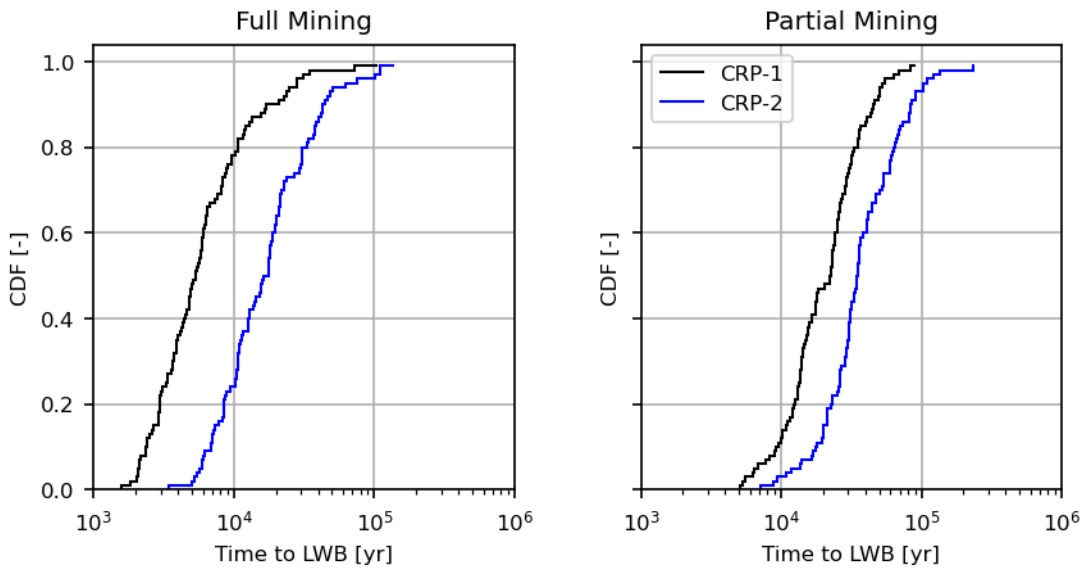

Figure 9-4: DTRKMF travel times to the WIPP LWB

Table 9-1: Particle Travel Time Summary

	Replicate 1 CRP-1	**Replicate 1 CRP-2**	**Replicate 2 CRP-1**	**Replicate 2 CRP-2**	**Replicate 3 CRP-1**	**Replicate 3 CRP-2**
Full Mining						
Mean	9.10E+03	2.33E+04	9.36E+03	2.35E+04	8.33E+03	2.74E+04
Median	5.30E+03	1.69E+04	5.11E+03	1.53E+04	5.26E+03	1.61E+04
Minimum	1.58E+03	3.46E+03	1.41E+03	3.78E+03	1.41E+03	3.93E+03
Partial Mining						
Mean	2.47E+04	4.66E+04	2.49E+04	4.36E+04	2.55E+04	4.49E+04
Median	2.26E+04	3.49E+04	2.23E+04	3.59E+04	2.20E+04	3.93E+04
Minimum	5.11E+03	7.21E+03	5.07E+03	7.58E+03	4.47E+03	6.78E+03

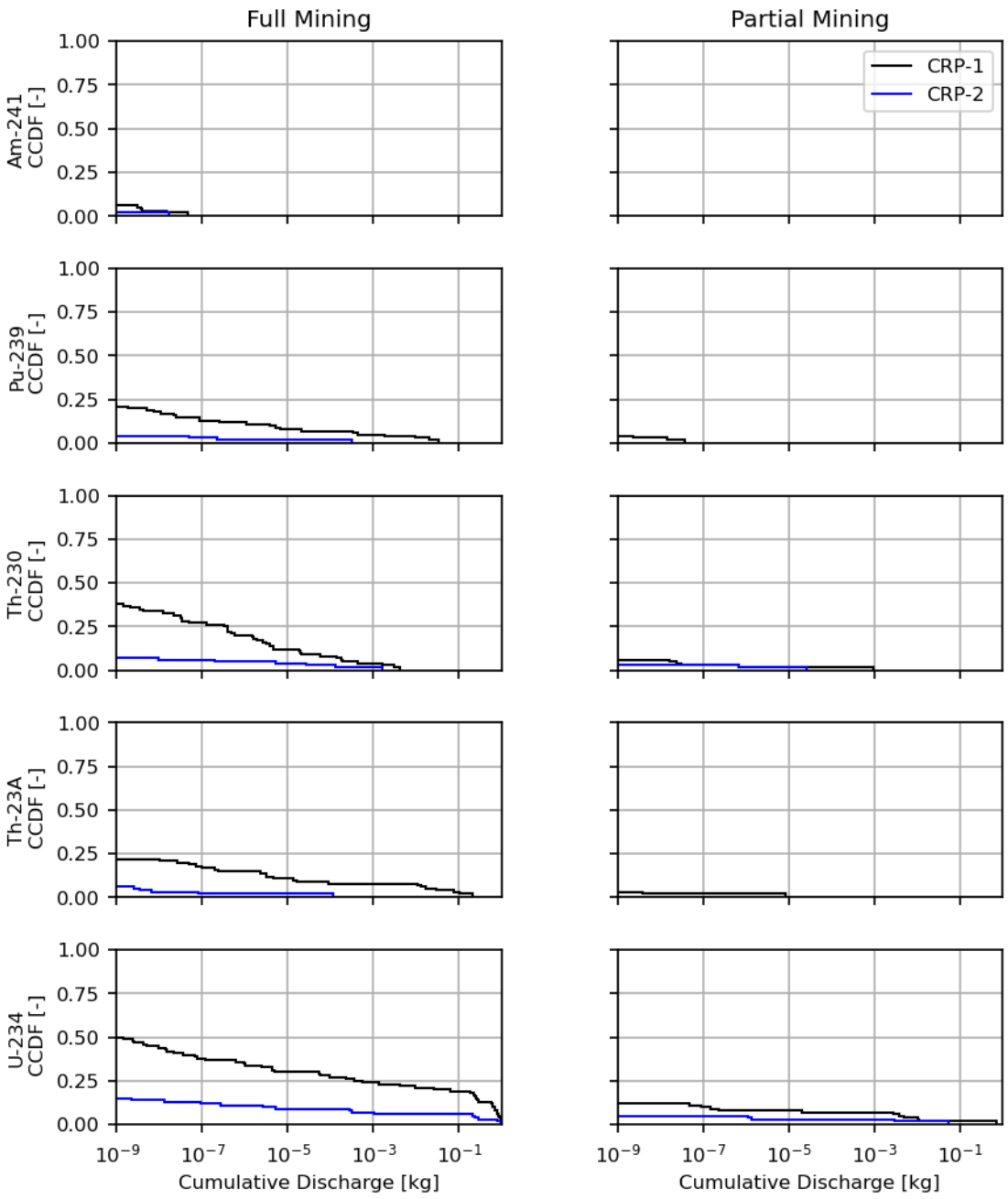

Figure 9-5: Cumulative Mass Discharge to the LWB by t=10,000yrs

Table 9-2: Mean Radionuclide Mass Transported to LWB [kg], Full Mining

	Replicate 1 CRP-1	**Replicate 1 CRP-2**	**Replicate 2 CRP-1**	**Replicate 2 CRP-2**	**Replicate 3 CRP-1**	**Replicate 3 CRP-2**
^{241}Am	8.74E-10	1.72E-10	8.79E-08	3.90E-11	6.72E-11	3.33E-12
^{239}Pu	6.44E-04	3.14E-06	3.98E-03	3.81E-07	1.63E-03	2.81E-09
^{230}Th	9.98E-05	1.77E-05	1.55E-04	4.48E-06	4.12E-05	2.38E-06
^{230}ThA	4.53E-03	1.16E-06	5.14E-03	1.27E-07	1.65E-03	2.48E-08
^{234}U	1.08E-01	2.46E-02	1.41E-01	2.00E-02	8.97E-02	1.44E-02

Table 9-3: Mean Radionuclide Mass Transported to LWB [kg], Partial Mining

	Replicate 1 CRP-1	**Replicate 1 CRP-2**	**Replicate 2 CRP-1**	**Replicate 2 CRP-2**	**Replicate 3 CRP-1**	**Replicate 3 CRP-2**
^{241}Am	0.00E+00	0.00E+00	1.18E-23	7.62E-24	0.00E+00	0.00E+00
^{239}Pu	5.55E-10	1.73E-14	3.30E-07	4.81E-11	5.69E-09	3.78E-19
^{230}Th	9.94E-06	2.67E-07	2.53E-06	3.29E-10	2.17E-08	6.01E-12
^{230}ThA	8.53E-08	2.05E-14	9.55E-06	2.35E-12	4.04E-14	8.41E-21
^{234}U	7.43E-03	5.94E-04	1.32E-02	6.79E-06	2.51E-03	1.76E-06

Table 9-4: Median Radionuclide Mass Transported to LWB [kg], Full Mining

	Replicate 1 CRP-1	**Replicate 1 CRP-2**	**Replicate 2 CRP-1**	**Replicate 2 CRP-2**	**Replicate 3 CRP-1**	**Replicate 3 CRP-2**
^{241}Am	1.67E-17	0.00E+00	2.19E-17	0.00E+00	3.55E-17	0.00E+00
^{239}Pu	1.14E-13	5.61E-24	2.03E-14	0.00E+00	1.04E-13	0.00E+00
^{230}Th	3.13E-11	6.65E-22	4.61E-11	1.83E-21	2.82E-11	6.03E-22
^{230}ThA	3.32E-13	1.41E-22	6.36E-15	3.28E-24	1.33E-13	0.00E+00
^{234}U	3.97E-10	1.72E-19	1.53E-09	2.77E-19	9.90E-10	4.10E-20

Table 9-5: Median Radionuclide Mass Transported to LWB [kg], Partial Mining

	Replicate 1 CRP-1	**Replicate 1 CRP-2**	**Replicate 2 CRP-1**	**Replicate 2 CRP-2**	**Replicate 3 CRP-1**	**Replicate 3 CRP-2**
^{241}Am	0.00E+00	0.00E+00	0.00E+00	0.00E+00	0.00E+00	0.00E+00
^{239}Pu	0.00E+00	0.00E+00	0.00E+00	0.00E+00	0.00E+00	0.00E+00
^{230}Th	0.00E+00	0.00E+00	0.00E+00	0.00E+00	0.00E+00	0.00E+00
^{230}ThA	0.00E+00	0.00E+00	0.00E+00	0.00E+00	0.00E+00	0.00E+00
^{234}U	0.00E+00	0.00E+00	0.00E+00	0.00E+00	0.00E+00	0.00E+00

Table 9-6: Number of Vectors Exceeding 1e-9 kg Transported to LWB, Full Mining

	Replicate 1 CRP-1	**Replicate 1 CRP-2**	**Replicate 2 CRP-1**	**Replicate 2 CRP-2**	**Replicate 3 CRP-1**	**Replicate 3 CRP-2**
^{241}Am	6	1	9	1	2	0
^{239}Pu	20	4	30	6	25	3
^{230}Th	38	7	41	10	43	8
^{230}ThA	22	5	33	6	32	4
^{234}U	49	15	51	17	50	11

Table 9-7: Number of Vectors Exceeding 1e-9 kg Transported to LWB, Partial Mining

	Replicate 1 CRP-1	**Replicate 1 CRP-2**	**Replicate 2 CRP-1**	**Replicate 2 CRP-2**	**Replicate 3 CRP-1**	**Replicate 3 CRP-2**
^{241}Am	0	0	0	0	0	0
^{239}Pu	3	0	1	1	1	0
^{230}Th	5	2	10	2	6	0
^{230}ThA	2	0	3	0	0	0
^{234}U	11	4	14	5	12	4

This page intentionally left blank.

10 CCDF Normalized Releases

This section describes the results of calculations performed using the CCDFGF code, which uses the output of the other WIPP PA codes to produce complementary cumulative distribution functions (CCDFs) of releases in EPA units. For a full description of CCDFGF in the CRA19, see Brunell (2019).

10.1 Introduction

The performance assessment methodology accommodates both aleatory (i.e., stochastic) and epistemic (i.e., subjective) uncertainty in its constituent models (DOE 2019, Appendix PA). Aleatory uncertainty pertains to unknowable future events, such as intrusion times and locations, that may affect repository performance. It is accounted for by the generation of random sequences of future events, such as inadvertent drilling intrusions. Epistemic uncertainty concerns parameters that are assumed to have constant values, but the true values are uncertain due to a lack of knowledge.

In WIPP PA, the PA models are executed for three replicates of 100 vectors, each vector comprising a fixed set of randomly sampled parameter values. For each vector, 10,000 random futures are independently generated, which define the timing and location of intrusion events and the occurrence of potash mining (DOE 2019, Appendix PA). CCDFs of releases are generated for each release mechanism, along with CCDFs of total releases,. Overall means are obtained by forming the average over all three replicates and a 95 percent confidence interval is computed from the mean CCDFs for the three replicates.

For the CRA19_12P, the CCDGF code is updated to extend panel neighboring relationships (Section 2.1.2.5), as well as for the additional “O” intrusion location and the additional Culebra release point associated with Panels 11 and 12 (Section 2.1.4).

10.2 Results

Discussions of the four primary release mechanisms, i.e., 1) cuttings and cavings; 2) spallings; 3) DBRs; and 4) releases from the Culebra, are found in subsections below. Intermediate results that provide input into CCDFGF calculations have been discussed in Sections 3 through 9. The results for the CRA19_12P analysis are compared to results from the CRA19 (Brunell 2019) and the APPA (Brunell et al. 2021). Plots of releases for individual release mechanisms include means and their corresponding 95 percent confidence intervals. Total normalized releases and a summary table of means and confidence intervals for total releases at probabilities of 0.1 and 0.001 are presented in Section 10.2.5.

10.2.1 Cuttings and Cavings Releases

Cuttings and cavings releases depend on cuttings and cavings volumes and sampled waste stream concentrations. The assumed cuttings and cavings concentration for a given intrusion is based on waste stream volumes (which determine the probability of selecting a given waste stream) as well as waste stream concentrations over time (Kicker 2019). Figure 10-1 compares the overall mean CCDF and 95 percent confidence intervals for this release mechanism for the CRA19, APPA, and CRA19_12P analyses.

As discussed in Section 6, the cuttings and cavings parameters and volumes for individual boreholes are identical between the three analyses. The larger repository footprint results in a greater number of boreholes per future in the APPA and in the CRA19_12P as compared to the CRA19. As the number of intrusions increases while the value of FVW decreases proportionally (Section 2.1.5), the cumulative releases from individual futures will derive from a larger sample of the waste streams and thus releases from each future will converge toward a mean value (Brunell et al. 2021).

Overall, as seen in Figure 10-1, the mean CCDF for cuttings and cavings releases in the CRA19_12P are in between the CCDFs for mean releases in the CRA19 and the APPA, at all probabilities. Statistics on the mean cuttings and cavings releases are shown in Table 10-1. Cuttings and cavings releases in the CRA19_12P are overall similar to those in the CRA19 and the APPA, demonstrating that the additional repository volume has a minor effect on the cuttings and cavings releases.

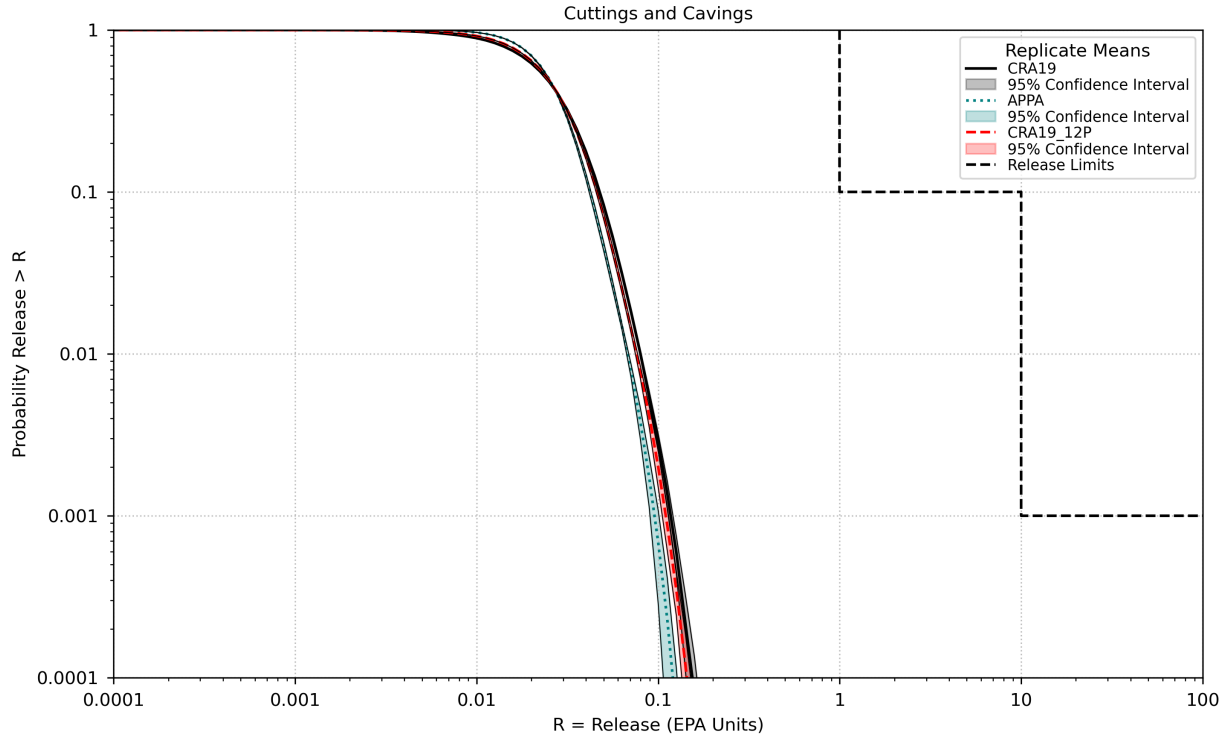

Figure 10-1: Overall Mean CCDFs for Cuttings and Cavings Releases

Table 10-1: Statistics on the Mean Cuttings and Cavings Releases

Probability	Analysis	Mean Total Release	Lower 95% CL	Upper 95% CL	Release Limit
0.1	CRA19	0.0479	0.0475	0.0483	1
0.1	APPA	0.0425	0.0420	0.0429	1
0.1	CRA19_12P	0.0462	0.0457	0.0467	1
0.001	CRA19	0.1187	0.1143	0.1220	10
0.001	APPA	0.0967	0.0909	0.1015	10
0.001	CRA19_12P	0.1108	0.1068	0.1149	10

10.2.2 Spallings Releases

Spallings releases depend on spallings volumes (which are a function of waste area pressure at the time of intrusion, discussed in Section 4.2.1) and spallings concentrations (which are calculated as the average CH waste concentration at the time of intrusion, discussed in Section 6.2.2).

While mean spallings volumes from individual intrusions have decreased (Section 6.2.1), the increased footprint of the repository has led to similar mean spallings volumes in the CRA19_12P, the APPA, and the CRA19 (Figure 10-2). Spallings concentrations in terms of EPA Units per unit waste volume are identical between the CRA19, the CRA19_12P, and the APPA, so spallings releases follow the decreasing trend of the FVW scaling parameter (Brunell et al. 2021). The overall mean spallings releases in the CRA19_12P lie between the mean releases in the CRA19 and the APPA analysis, at all probabilities (Figure 10-3). Statistics on the mean spallings releases are shown in Table 10-2.

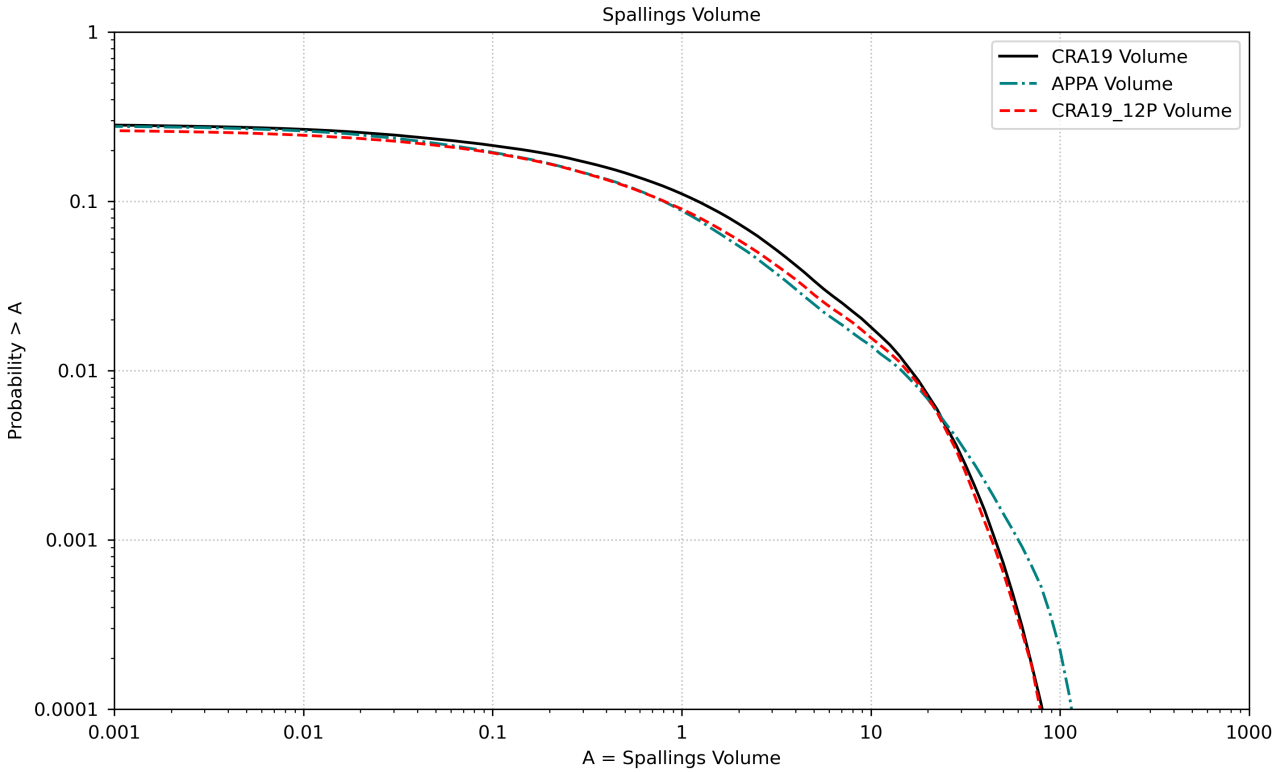

Figure 10-2: Overall Mean CCDFs for Spallings Volumes

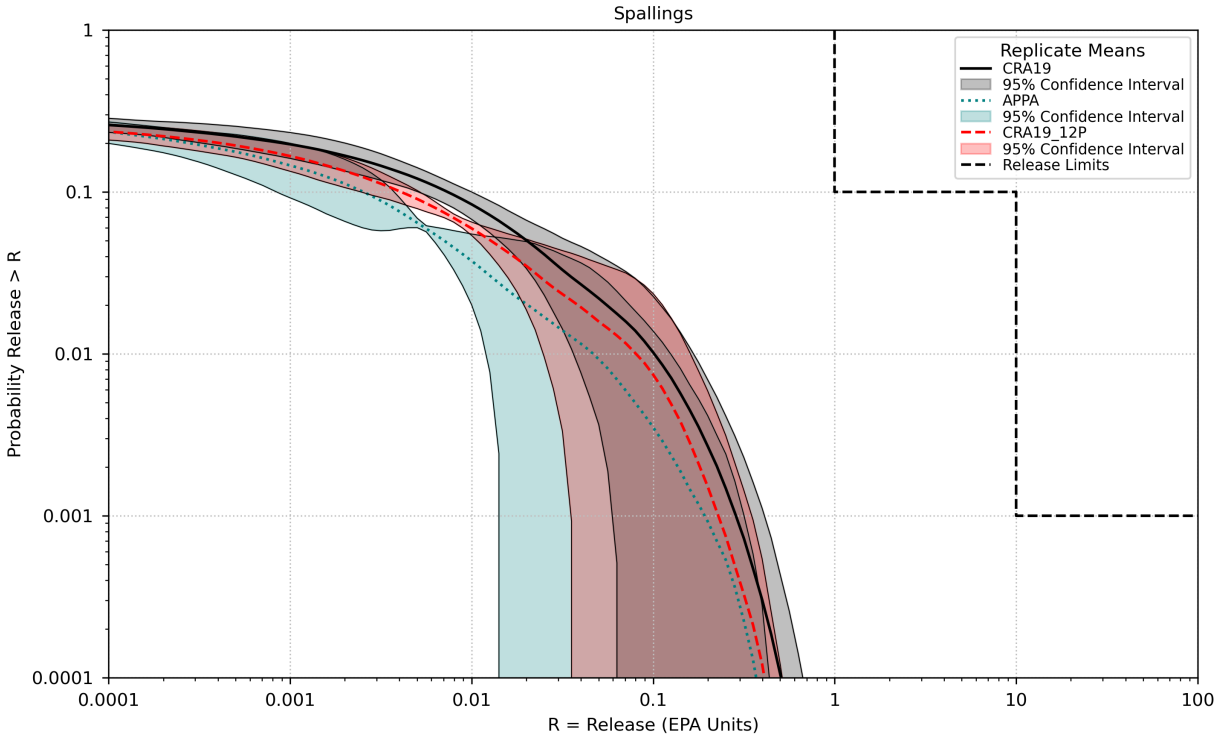

Figure 10-3: Overall Mean CCDFs for Spallings Releases

Table 10-2: Statistics on Mean Spallings Releases

Probability	Analysis	Mean Total Release	Lower 95% CL	Upper 95% CL	Release Limit
0.1	CRA19	0.0074	0.0051	0.0100	1
0.1	APPA	0.0025	0.0008	0.0038	1
0.1	CRA19_12P	0.0041	0.0025	0.0052	1
0.001	CRA19	0.2862	0.0607	0.4125	10
0.001	APPA	0.1929	0.0147	0.3167	10
0.001	CRA19_12P	0.2292	0.0354	0.3502	10

10.2.3 Direct Brine Releases

Direct brine releases (DBRs) depend on direct brine release volumes (Section 5) and radionuclide concentrations in the brine (Section 7). Figure 10-4 shows the resulting overall mean CCDFs of DBRs for the CRA19, APPA, and CRA19_12P analyses. Statistics on mean DBRs are shown in Table 10-3. Compared to the CRA19, mean DBRs in the CRA19_12P decreased at all probabilities. As discussed in Section 5, this decrease is due to smaller initial saturation and initial pressure driving a shift towards lower direct brine release volumes for individual intrusions, and lower direct brine release volumes overall (Figure 10-5). Compared to the APPA, DBRs in the CRA19_12P are decreased at high probabilities and increased at lower probabilities. The larger repository footprint modeled in the APPA results in a greater excavated area in contact with the disturbed rock zone (DRZ), which leads to an increase in brine saturation. This increase contributes to a rise in high-probability (smaller volume) releases while simultaneously decreasing lower-probability (larger volume) releases (Brunell et al. 2021). The shift towards smaller releases is less pronounced in the CRA19_12P compared to the APPA due to smaller excavated area in the CRA19_12P.

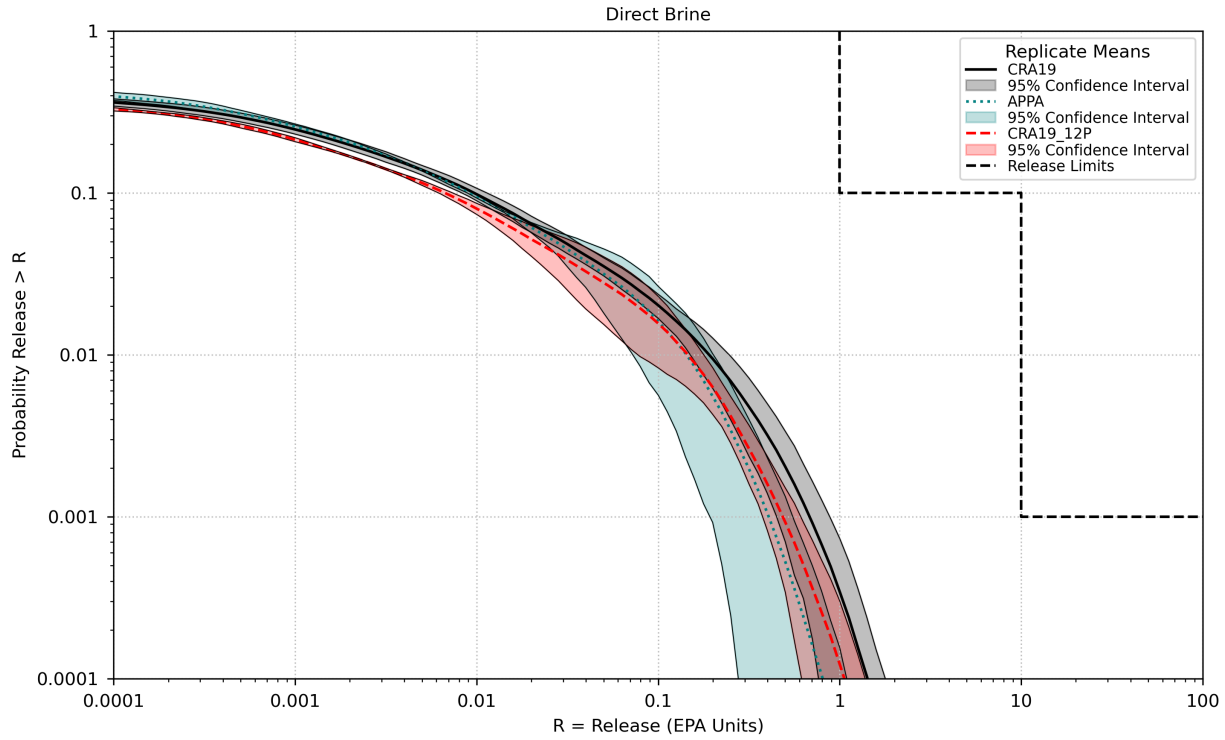

Figure 10-4: Overall Mean CCDF for Direct Brine Releases

Table 10-3: Statistics on Mean Direct Brine Releases

Probability	Analysis	Mean Total Release	Lower 95% CL	Upper 95% CL	Release Limit
0.1	CRA19	0.0097	0.0083	0.0114	1
0.1	APPA	0.0092	0.0089	0.0095	1
0.1	CRA19_12P	0.0067	0.0062	0.0074	1
0.001	CRA19	0.6855	0.4495	0.8828	10
0.001	APPA	0.4078	0.1934	0.5532	10
0.001	CRA19_12P	0.4875	0.3784	0.6126	10

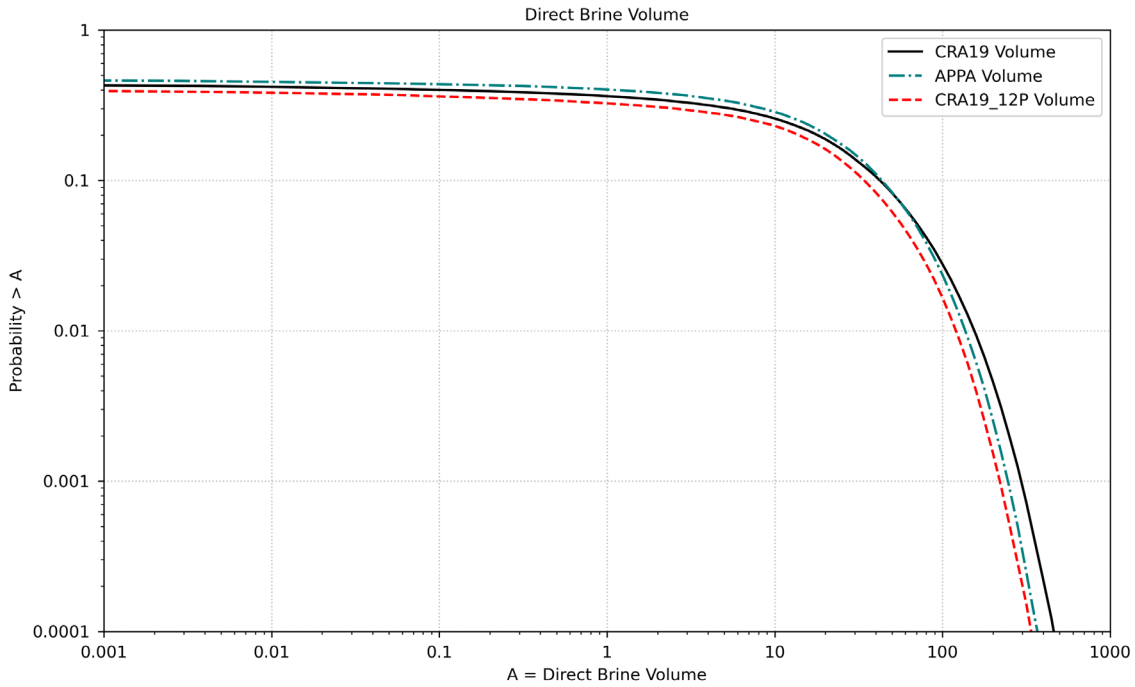

Figure 10-5: Overall Mean CCDFs for Direct Brine Release Volumes

10.2.4 Releases from the Culebra

Releases by transport through the Culebra to the LWB result from radionuclides transported to the Culebra via the borehole. The results of the Culebra transport calculations are described in Section 9.

Figure 10-6 shows the total radionuclide transport to the Culebra, while Figure 10-7 shows total releases from the Culebra. Table 10-4 contains statistics on mean releases from the Culebra. As discussed in Section 9, the CRA19 and the APPA are modeled with a single release point (CRP-1), while the CRA19_12P is modeled with two release points (CRP-1 and CRP-2). As seen in Figure 10-6, releases from the Culebra are highest at all probabilities in the APPA. Compared to the CRA19, Culebra releases are similar in the CRA19_12P at high probabilities, and slightly higher at lower probabilities.

Figure 10-8 (CRA19), Figure 10-9 (APPA), and Figure 10-10 (CRA19_12P) show total transport to and releases from the Culebra for the four radionuclides tracked in the Culebra transport model. Although radionuclide transport to the Culebra is dominated by ^{241}Am and ^{239}Pu, releases from the Culebra are dominated by ^{234}U, followed by ^{239}Pu and ^{230}Th. On a per-radionuclide basis, transport to and releases from the Culebra are very similar across the three analyses.

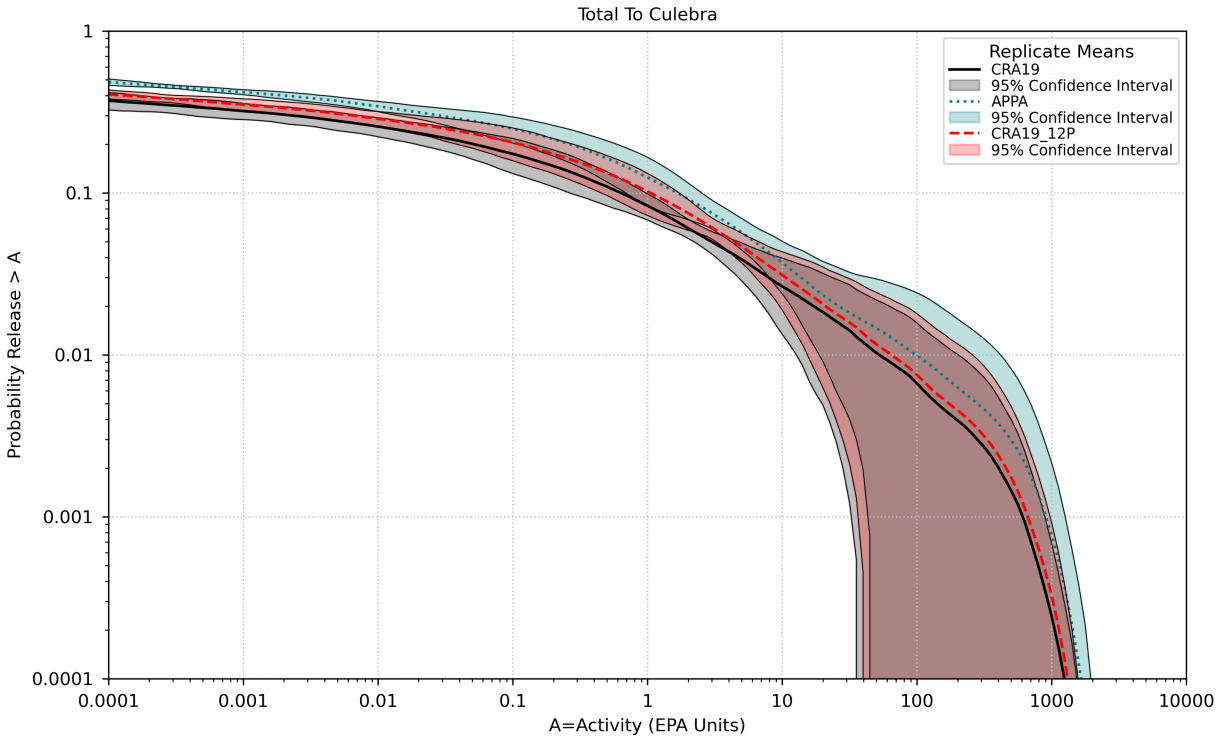

Figure 10-6: Overall Mean CCDF for Radionuclide Transport to the Culebra

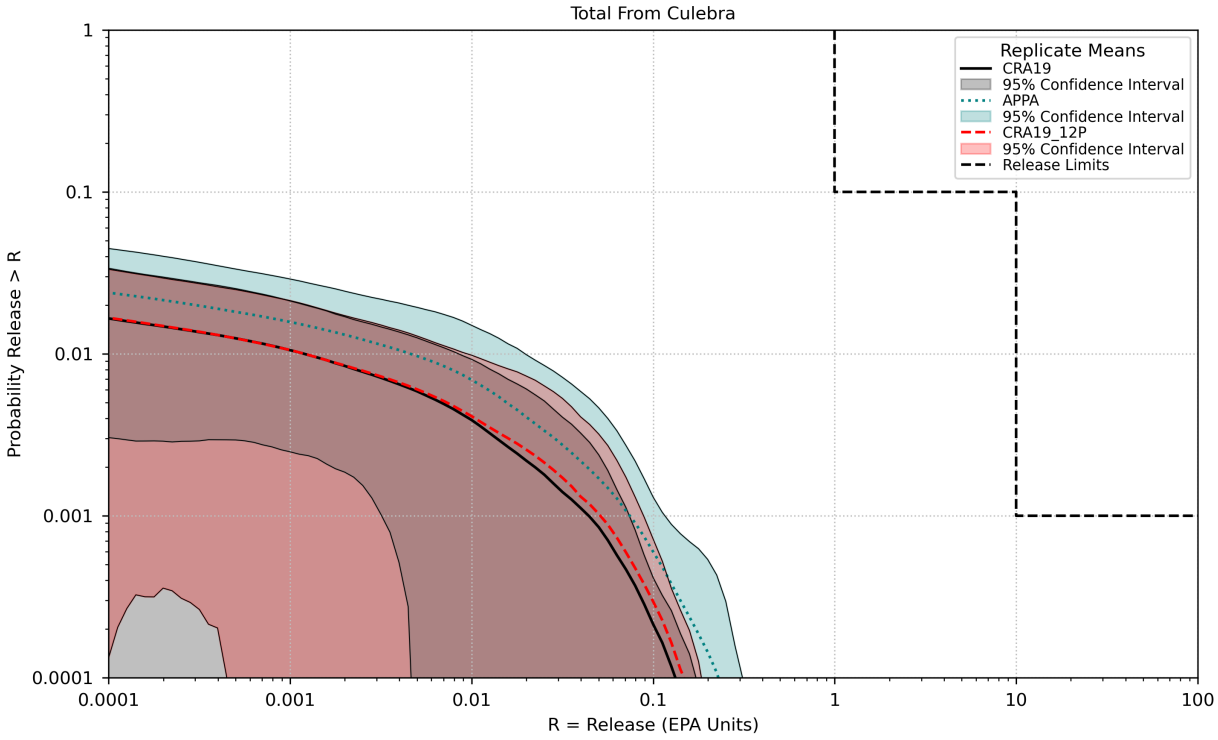

Figure 10-7: Overall Mean CCDF for Releases from the Culebra

Table 10-4: Statistics on Mean Releases from the Culebra

Probability	Analysis	Mean Total Release	Lower 95% CL	Upper 95% CL	Release Limit
0.1	CRA19	0.0	0.0	0.0	1
0.1	APPA	0.0	0.0	0.0	1
0.1	CRA19_12P	0.0	0.0	0.0	1
0.001	CRA19	0.0441	0.0	0.0743	10
0.001	APPA	0.0745	0.0032	0.1163	10
0.001	CRA19_12P	0.0512	0.0	0.0886	10

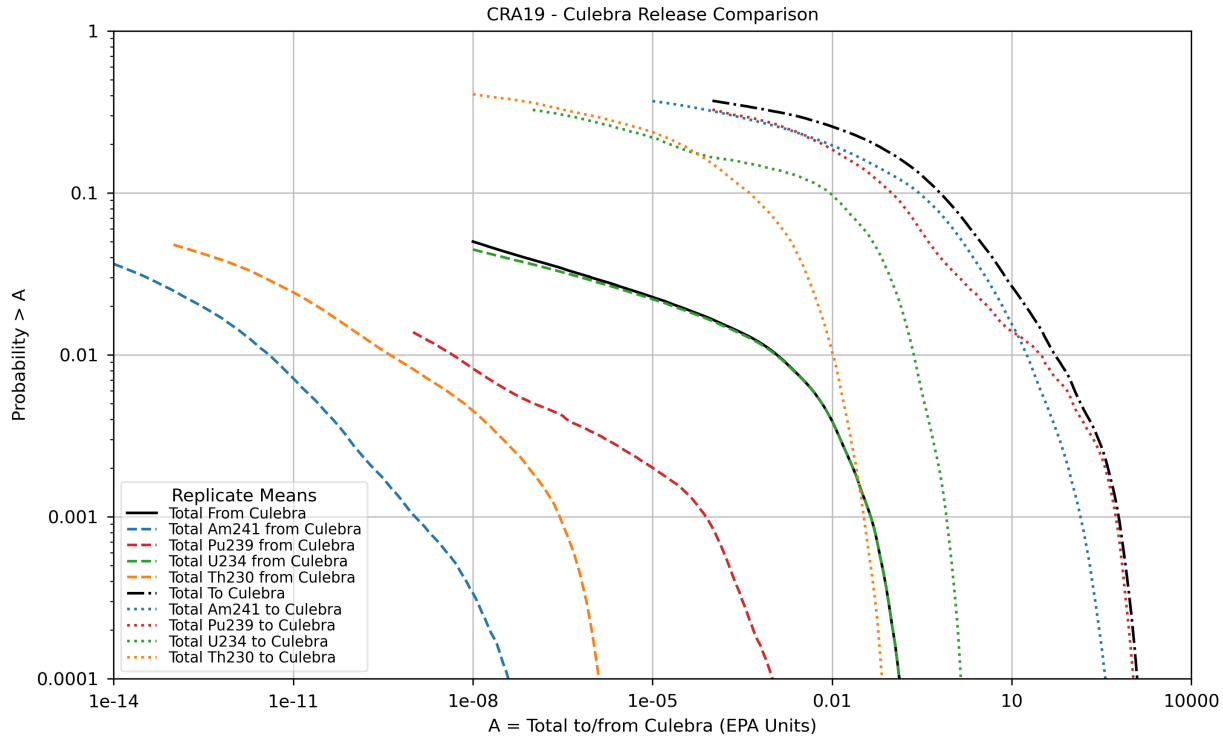

Figure 10-8: Mean CCDFs for Releases to and from the Culebra by Radionuclide – CRA19

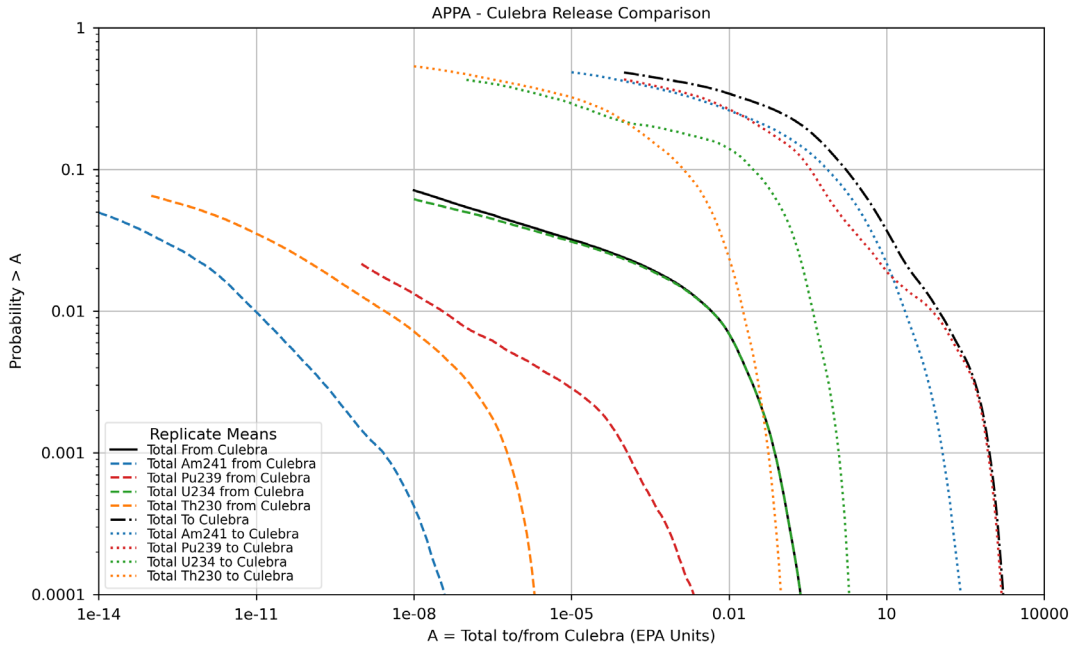

Figure 10-9: Mean CCDFs for Releases to and from the Culebra by Radionuclide – APPA

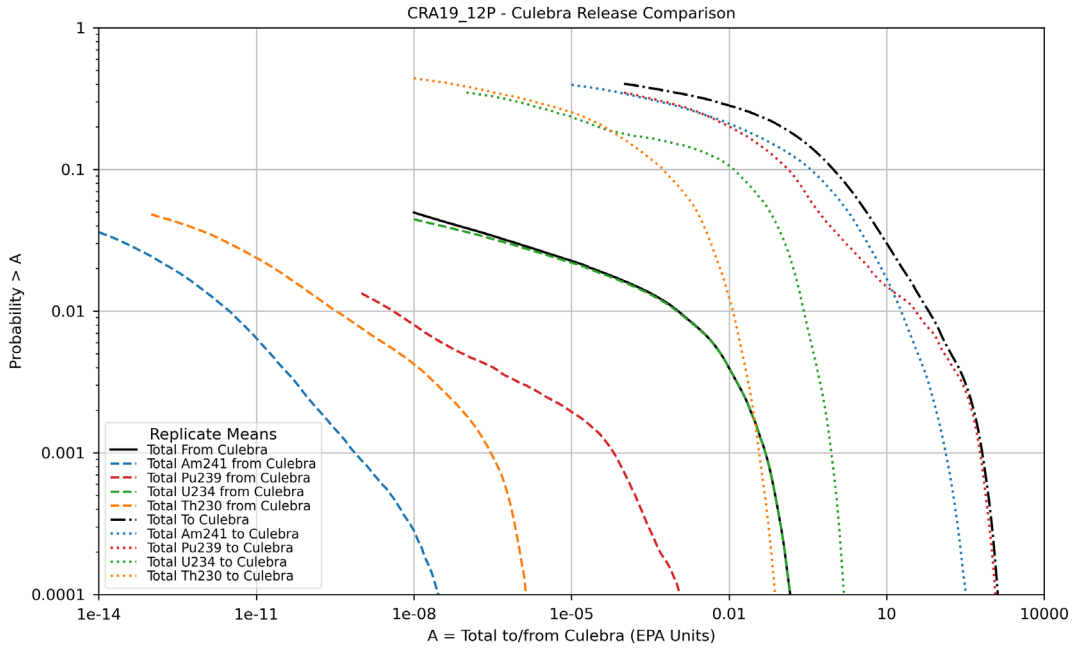

Figure 10-10: Mean CCDFs for Releases to and from the Culebra by Radionuclide – CRA19_12P

10.2.5 Total Releases

For each future in a realization, total releases are calculated by summing the releases from each release pathway: cuttings and cavings releases, spallings releases, DBRs, and transport releases.

CCDFs for total releases obtained in the 100 realizations (vectors) comprising Replicate 1, Replicate 2, and Replicate 3 of the CRA19_12P analysis are plotted in Figure 10-11, Figure 10-12, and Figure 10-13, respectively – each CCDF curve represents the distribution of total releases from 10,000 individual futures conditional on the values of parameters sampled for a single realization.

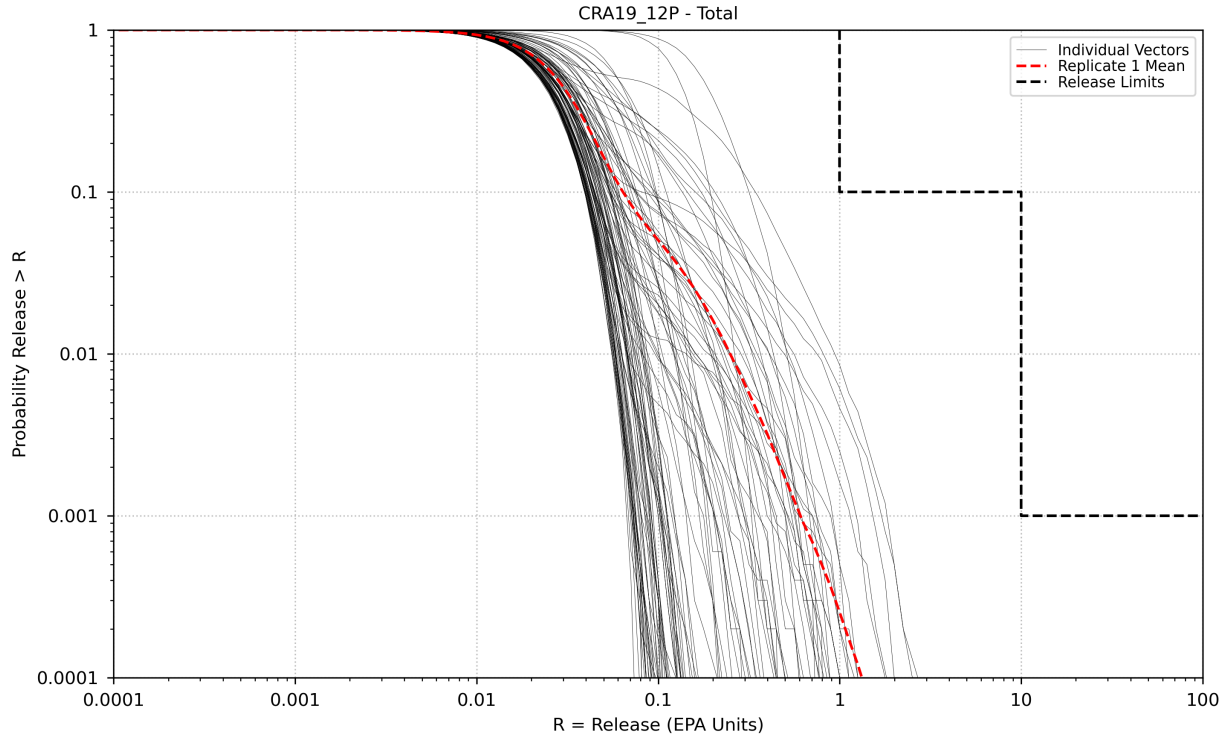

Figure 10-11: Total Normalized Releases, Replicate 1

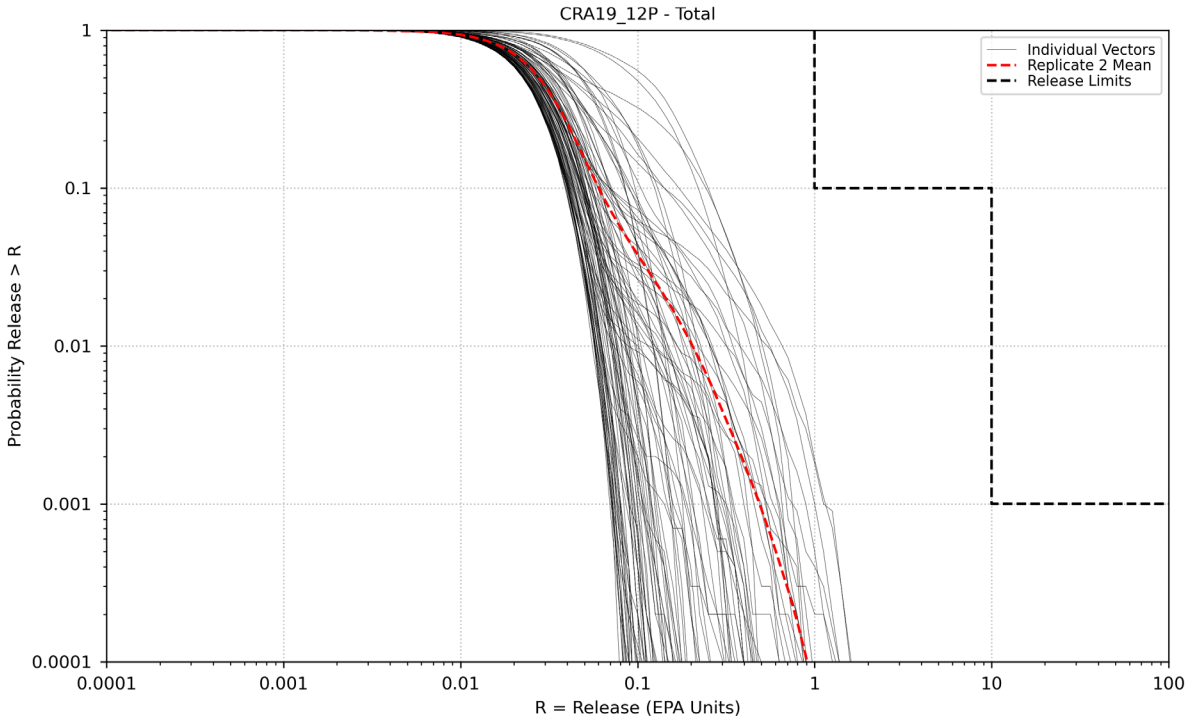

Figure 10-12: Total Normalized Releases, Replicate 2

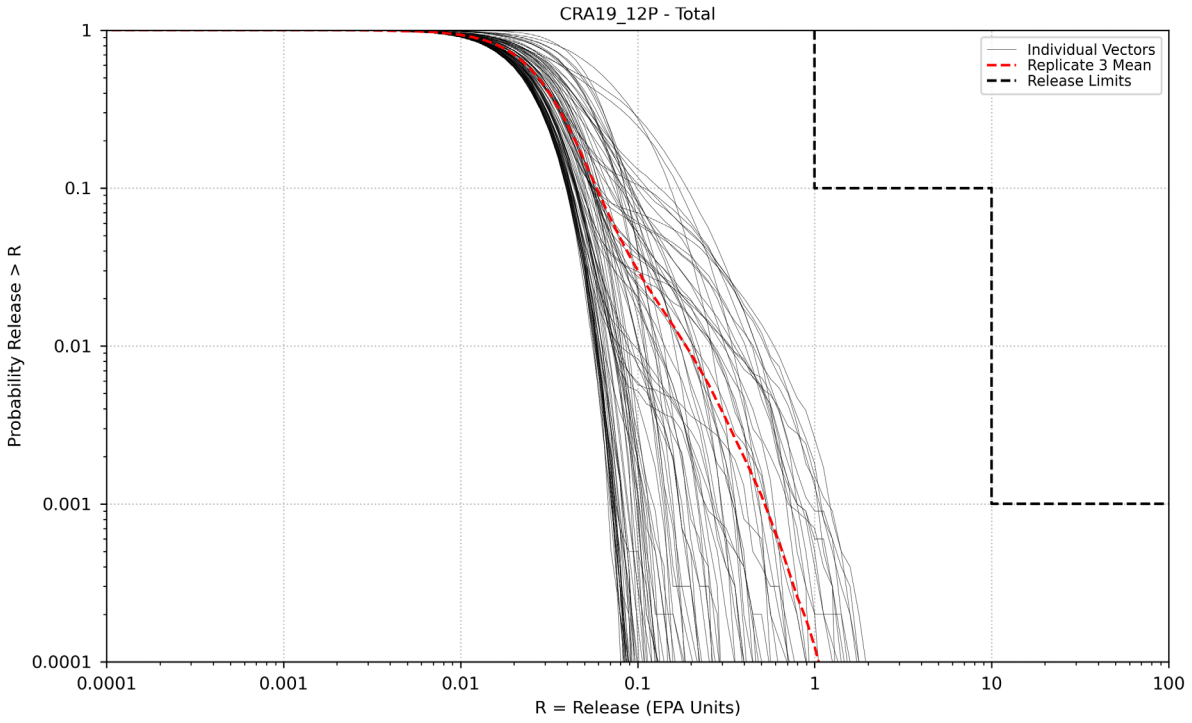

Figure 10-13: Total Normalized Releases, Replicate 3

Mean CCDFs of the individual release mechanisms that comprise total normalized releases, as well as the mean CCDF for the total release (average over all three replicates), for each analysis are plotted in Figure 10-14 (CRA19), Figure 10-15 (APPA), and Figure 10-16 (CRA19_12P). As seen in these figures, total normalized releases are dominated in each analysis by cuttings and cavings and direct brine releases. Contributions to total releases from spallings releases and Culebra transport are not dominant.

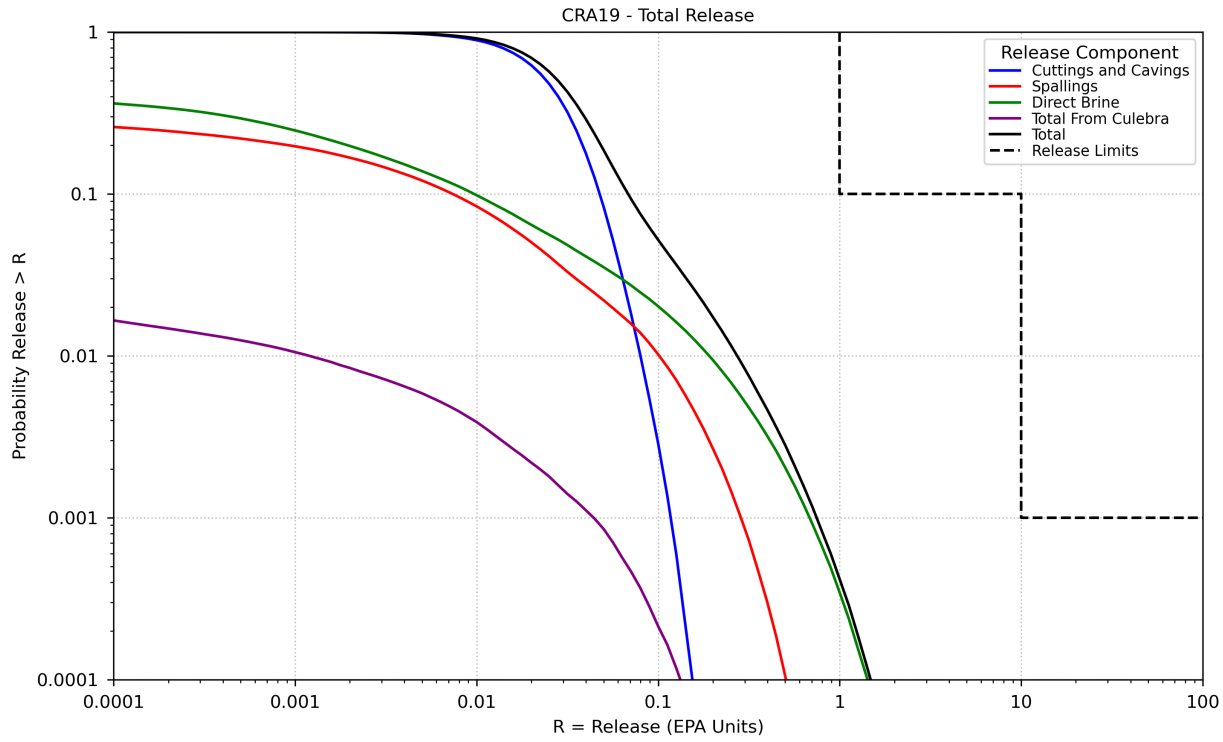

Figure 10-14: Comparison of Overall Means for Release Components – CRA19

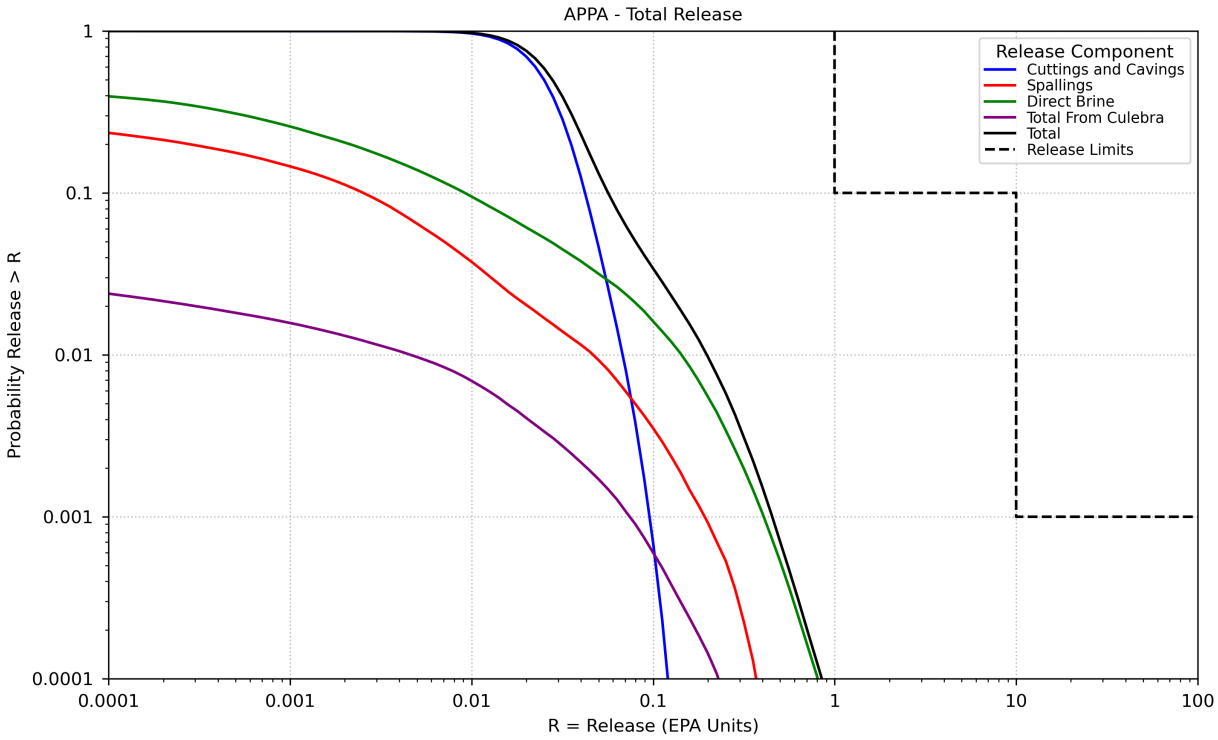

Figure 10-15: Comparison of Overall Means for Release Components – APPA

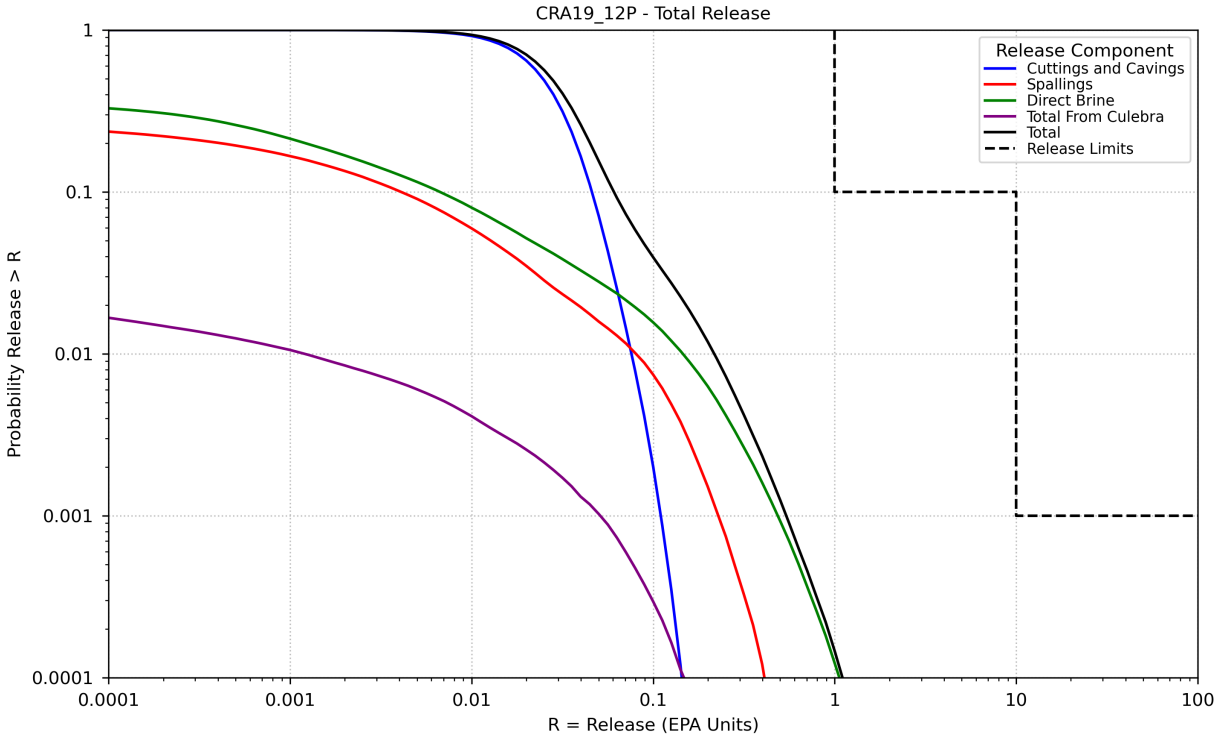

Figure 10-16: Comparison of Overall Means for Release Components – CRA19_12P

The overall mean CCDF is computed as the arithmetic mean of the mean CCDFs from each replicate. Figure 10-17 compares the overall mean CCDF for total releases between the three analyses, while Figure 10-18 includes the 95% confidence interval about the overall mean, computed using the Student's t-distribution and the mean CCDFs from each replicate (Helton et al. 1998, Section 6.4). Table 10-5 summarizes the statistics on the overall mean CCDF for total normalized releases and 95% confidence interval. As seen in Figure 10-18 and Table 10-5, total mean normalized releases are similar among the analyses at the highest probabilities. At lower probabilities, releases are slightly higher in the CRA19 than in the CRA19_12P, and slightly lower in the APPA than in the CRA19_12P. The total mean normalized releases are shown to be less than the release limits specified by the Certification Criteria in Title 40 CFR Part 194 for all three analyses.

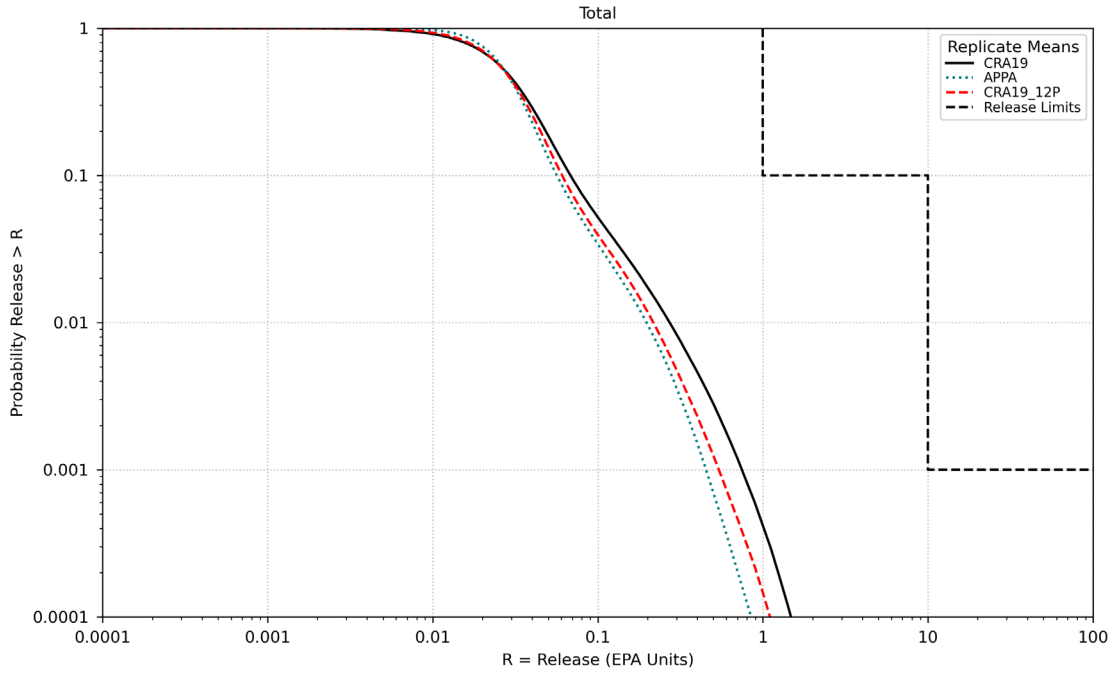

Figure 10-17: Overall Mean CCDF for Total Normalized Releases

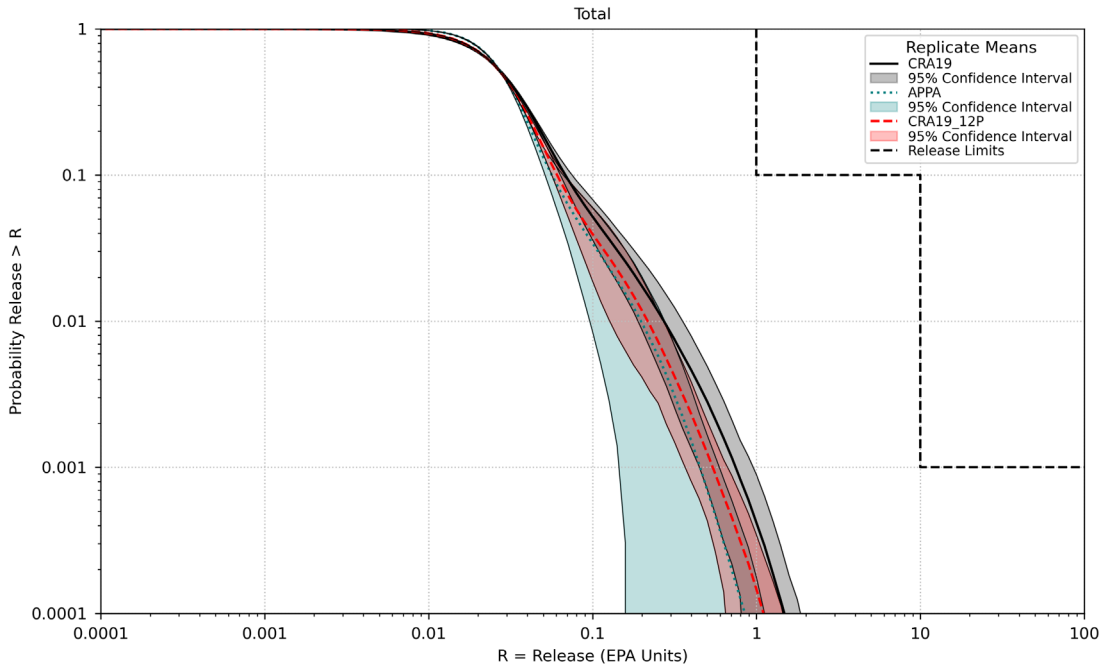

Figure 10-18: Overall Mean CCDF for Total Normalized Releases with Confidence Intervals

Table 10-5: Statistics on the Overall Mean for Total Normalized Releases

Probability	Analysis	Mean Total Release	Lower 95% CL	Upper 95% CL	Release Limit
0.1	CRA19	0.0685	0.0636	0.0753	1
0.1	APPA	0.0564	0.0515	0.0665	1
0.1	CRA19_12P	0.0610	0.0564	0.0680	1
0.001	CRA19	0.7505	0.4487	0.9595	10
0.001	APPA	0.4540	0.1475	0.5970	10
0.001	CRA19_12P	0.5436	0.3687	0.6691	10

11 Sensitivity Analysis

The WIPP PA employs stepwise linear multiple ranked regression to evaluate the relative importance of the various sampled parameters to uncertainty in the estimates of potential releases. The sensitivity analysis is used to address the question of which sampled parameters contribute most to the variability (uncertainty) observed in the mean releases by vector. In this section the results of the sensitivity analysis for the CRA19_12P are compared to the results of the sensitivity analysis for the CRA19. The sensitivity analysis approach and the CRA19 results are documented by Zeitler (2019).

11.1 Introduction

The STEPWISE code is used to perform a stepwise linear multiple regression analysis for the WIPP PA. In the forward stepwise approach, a sequence of regression models is constructed, beginning with the input parameter that exhibits the strongest simple correlation with the output variable. Subsequently, partial correlations between the output and the remaining variables are calculated, which account for the linear effects of variables already included in the model. The variable with the largest significant partial correlation coefficient is then added, and the partial correlations for the remaining input variables are recalculated.

Significance is assessed using an F-test, with the significance level for adding an input variable to the model set to 1 - α_{in}, where α_{in} is the significance level for a Type I error, determined by the analyst. The F-test compares the variability contributed by the variable to the unexplained variability, i.e., the residuals' variability. In this analysis α_{in} is set to a value of 0.05, indicating a 95% confident that there is a partial correlation between the input and output variables.

The process of adding the variable with the largest significant partial correlation coefficient is repeated until no remaining variables have significant correlations with the output variable. Variables excluded from the regression model do not significantly contribute to the unexplained variability, rendering the results relatively insensitive to those parameters. The method does not guarantee that the relative contributions of model parameters to the R^2 (coefficient of determination) will consistently decrease as the rank increases, although this is frequently observed.

Input variables added to the regression model are not necessarily retained. For an input variable to be retained, its regression coefficient (i.e. the linear contribution of an input to the prediction of the output variable) must be statistically distinguishable from zero. A t-test is used to determine whether a regression coefficient is significantly different than zero. The t-test evaluates the null hypothesis that the regression coefficient is zero. The hypothesis is not rejected when random effects can give rise to the observed regression coefficient with probability α_{out}. The random effects are caused by the stochastic variability contributed by the input variables not in the regression model. In other words, the hypothesis is rejected, and the variable is included in the model when the 1 - α_{out} confidence interval of the regression coefficient does not encompass zero.

The α_{out} value used by the STEPWISE code for allowing a variable to enter the regression model is 0.05. With this value, one is 95% confident that the input variables make a linear contribution to the response of the output variable.

11.2 Results

This section describes the results of the stepwise ranked regression analysis for the sampled parameters used in the CRA19_12P analysis as they impact total releases. The results are presented in tables that indicate those parameters that contribute most significantly to the total variation of observed releases. These tables contain the steps in the stepwise analysis, the variable names listed in the order of selection, the cumulative R^2 value with entry of each variable into the regression model, and the Standardized Rank Regression Coefficient (SRRC), for both the CRA19 and CRA19_12P calculations.

To aid in interpretation and discussion of the results, parameters with ΔR^2 values (the difference in R^2 between the current step and the previous step) greater than 0.05 are highlighted in the tables below. While this threshold is somewhat arbitrary, those highlighted parameters are clearly influential and tend to have a more consistent ranking.

The results of the stepwise ranked regression analysis for mean total releases for replicate 1, 2, and 3 are shown in Table 11-1, Table 11-2, and Table 11-3, respectively. In all three replicates, the grey highlighting indicates variables that contribute a ΔR^2 greater than 0.05 in the CRA19, and also contribute a ΔR^2 greater than 0.05 in the CRA19_12P. In the instances where these variables are ordered differently between the CRA19 and the CRA19_12P, the contribution to R^2 of each variable is similar in both orderings. In general, the differences between the results for the CRA19 and the CRA19_12P are minor. That is, the two replacement panels have very little impact on the sampled parameters which contribute to uncertainty in releases.

Table 11-1: Stepwise Ranked Regression Analysis for Mean Total Releases, Replicate 1 of the CRA19 and CRA19_12P Analyses

	CRA19			CRA19_12P		
Step	Variable	R^2	SRRC	Variable	R^2	SRRC
1	SOLMOD3:SOLVAR	0.23	0.51	SOLMOD3:SOLVAR	0.20	0.47
2	BOREHOLE:TAUFAIL	0.35	-0.35	BOREHOLE:TAUFAIL	0.35	-0.38
3	CASTILER:PRESSURE	0.44	0.31	CASTILER:PRESSURE	0.45	0.33
4	BH_SAND:PRMX_LOG	0.50	-0.27	BH_SAND:PRMX_LOG	0.50	-0.22
5	STEEL:CORRMCO2	0.53	-0.19	S_HALITE:POROSITY	0.53	0.17
6	WAS_AREA:PROBDEG	0.56	0.17	S_HALITE:COMP_RCK	0.56	-0.16
7				STEEL:CORRMCO2	0.58	-0.15
8				WAS_AREA:PROBDEG	0.60	0.16

Table 11-2: Stepwise Ranked Regression Analysis for Mean Total Releases, Replicate 2 of the CRA19 and CRA19_12P Analyses

	CRA19			CRA19_12P		
Step	Variable	R^2	SRRC	Variable	R^2	SRRC
1	SOLMOD3:SOLVAR	0.23	0.48	BOREHOLE:TAUFAIL	0.23	-0.48
2	BOREHOLE:TAUFAIL	0.38	-0.40	SOLMOD3:SOLVAR	0.40	0.42
3	CASTILER:PRESSURE	0.47	0.28	CASTILER:PRESSURE	0.48	0.28
4	GLOBAL:PBRINE	0.54	0.28	GLOBAL:PBRINE	0.55	0.26
5	BH_SAND:PRMX_LOG	0.62	-0.27	BH_SAND:PRMX_LOG	0.61	-0.24
6	S_HALITE:POROSITY	0.65	0.19	S_HALITE:POROSITY	0.65	0.19
7	SHFTU:SAT_RGAS	0.67	-0.12	STEEL:CORRMCO2	0.66	-0.13
8	STEEL:CORRMCO2	0.68	-0.12			

Table 11-3: Stepwise Ranked Regression Analysis for Mean Total Releases, Replicate 3 of the CRA19 and CRA19_12P Analyses

	CRA19			CRA19_12P		
Step	Variable	R^2	SRRC	Variable	R^2	SRRC
1	BH_SAND:PRMX_LOG	0.17	-0.39	BOREHOLE:TAUFAIL	0.18	-0.41
2	SOLMOD3:SOLVAR	0.34	0.39	BH_SAND:PRMX_LOG	0.32	-0.37
3	BOREHOLE:TAUFAIL	0.45	-0.34	SOLMOD3:SOLVAR	0.45	0.36
4	GLOBAL:PBRINE	0.53	0.28	GLOBAL:PBRINE	0.54	0.28
5	CASTILER:PRESSURE	0.59	0.24	CASTILER:PRESSURE	0.58	0.22
6	DRZ_1:PRMX_LOG	0.62	-0.19	DRZ_1:PRMX_LOG	0.61	-0.18
7	SPALLMOD:PARTDIAM	0.64	-0.17	SPALLMOD:PARTDIAM	0.63	-0.15
8	CASTILER:COMP_RCK	0.67	0.13			
9	S_HALITE:PRESSURE	0.69	-0.14			
10	CULEBRA:MINP_FAC	0.70	0.13			
11	S_MB139:RELP_MOD	0.72	-0.15			
12	WAS_AREA:SAT_RBRN	0.74	-0.13			

12 Summary

The CRA19_12P PA analysis is performed to supplement the Replacement Panels Planned Change Request (RPPCR) analysis submitted by the DOE to the Environmental Protection Agency (EPA). CRA19_12P PA calculations differ from the CRA19 calculations by considering two additional panels for waste disposal by increasing the assumed repository waste disposal volume and footprint. The CRA19_12P PA was performed in accordance with the SNL WIPP QA procedure NP 9-1.

WIPP PA calculations estimate the probability and consequence of potential radionuclide releases from the repository to the accessible environment for a regulatory period of 10,000 years after facility closure. Total mean normalized releases are similar between the CRA19 and CRA19_12P analyses at the highest probabilities. At lower probabilities, releases are slightly lower in the CRA19_12P than in the CRA19. The total mean normalized releases are shown to be less than the release limits specified by the Certification Criteria in Title 40 CFR Part 194. In general, the differences between the results for the CRA19 and the CRA19_12P are minor.

This page intentionally left blank.

13 References

Bollinger, M. 2024. Letter to Lee Ann B. Veal. Subject: Planned Change Request for the use of Replacement Panels 11 and 12. March 12, 2024. U.S. Department of Energy Waste Isolation Pilot Plant, Carlsbad Field Office.

Brunell, S. 2019. Analysis Package for Normalized Releases in the 2019 Compliance Recertification Application Performance Assessment (CRA-2019 PA). ERMS 571373. Carlsbad, NM: Sandia National Laboratories.

Brunell, S., C. Hansen, D. Kicker, S. Kim, S. King, and J. Long, 2021. Summary Report for the 2020 Additional Panels Performance Assessment (APPA). ERMS 574494. Carlsbad, NM: Sandia National Laboratories.

Brunell, S., J. Bethune, P. Docherty, D. Kicker, S. Kim, S. King, J. Long, and T. Zeitler. 2024. Summary Report for the 2023 Replacement Panels Planned Change Request Performance Assessment. Revision 1. ERMS 581044. Carlsbad, NM: Sandia National Laboratories.

Casey, S., R. Patterson, M. Gross, K. Lickliter, J. Stein. 2003. Regulatory Considerations of Waste Emplacement within the WIPP Repository: Random versus Non-Random Distributions. Tucson, AZ: Waste Management 2003 Conference. February 23-27, 2003.

Clayton, D. J. 2008. Memorandum to Larry Brush. Subject: Update to the Calculation of the Minimum Brine Volume for a Direct Brine Release. April 2, 2008. ERMS 548522. Carlsbad, NM: Sandia National Laboratories.

Clayton, D. J., S. Dunagan, J.W. Garner, A.E. Ismail, T.B. Kirchner, G.R. Kirkes, M.B. Nemer. 2008. Summary Report of the 2009 Compliance Recertification Application Performance Assessment. ERMS 548862. Carlsbad, NM: Sandia National Laboratories.

Day, B. 2019. Analysis Package for Salado Flow in the 2019 Compliance Recertification Application Performance Assessment (CRA-2019 PA). ERMS 571368. Carlsbad, NM: Sandia National Laboratories.

Falta, R., M. Hu, E. M. Kwicklis, C. I. Steefel, S. C. Williams-Stroud, and J. A. Thies. 2021. Additional Panels Performance Assessment (APPA) Changed Conceptual Models Peer Review Report. Carlsbad, NM: U.S. Department of Energy, Carlsbad Field Office.

Hansen, C. W., Brush, L. H. Gross, M. G., Hansen, F. D., Park, B. Y., Stein, J. S., and Thompson, T. W. 2003. Effects of Supercompacted Waste and Heterogeneous Waste Emplacement on Repository Performance. Carlsbad, NM: Sandia National Laboratories. ERMS 532475.

Hansen, C., S. Brunell, and S. King. 2023. Estimation of Releases from a 12-Panel Repository. ERMS 578831. Carlsbad, NM: Sandia National Laboratories.

Helton, J. C., J. E. Bean, J. W. Berglund, F. J. Davis, K. Economy, J. W. Garner, J. D. Johnson, R. J., MacKinnon, J. Miller, D. G. O'Brien, J.L. Ramsey, J. D. Schreiber, A. Shinta, L. N. Smith, D. M. Stoelzel, C. Stockman, and P. Vaughn. 1998. Uncertainty and Sensitivity Analysis Results

Obtained in the 1996 Performance Assessment for the Waste Isolation Pilot Plant. SAND98-0365. ERMS 252619. Albuquerque, NM: Sandia National Laboratories.

Kicker, D. 2019. Analysis Package for Cuttings, Cavings, and Spallings in the 2019 Compliance Recertification Application Performance Assessment (CRA-2019 PA). ERMS 571369. Carlsbad, NM: Sandia national Laboratories.

Kicker, D. C. 2023. Radionuclide Inventory Screening Analysis for the Replacement Panels Planned Change Request Performance Assessment (RPPCR PA). ERMS 578878. Carlsbad, NM: Sandia National Laboratories.

Kim, S. 2023. Analysis Report for Actinide Mobilization and Salado Transport in the Replacement Panels Planned Change Request (RPPCR). ERMS 579726. Carlsbad, NM: Sandia National Laboratories.

King, S. 2021. Analysis Package for Direct Brine Release in the Additional Panels Performance Assessment (APPA). ERMS 574498. Carlsbad, NM: Sandia National Laboratories.

King, S., P. Docherty, and C. Hansen. 2024. Impact Analysis of High Plutonium Loading in a Single WIPP Waste Panel. Revision 1. ERMS 581045. Carlsbad, NM: Sandia National Laboratories.

Kirchner, T., A. Gilkey, and J. Long. 2014. Summary Report on the Migration of the WIPP PA Codes from VMS to Solaris, Rev. 1. ERMS 561757. Carlsbad, NM: Sandia National Laboratories.

Kirchner, T., A. Gilkey, and J. Long. 2015. Addendum to the Summary Report on the Migration of the WIPP PA Codes. ERMS 564675. Carlsbad, NM: Sandia National Laboratories.

Kirkes, G. R. 2019. Features, Events, and Processes Assessment for the 2019 Compliance Recertification Application Performance Assessment (CRA-2019 PA). ERMS 571366. Carlsbad, NM: Sandia National Laboratories.

Kirkes, G. R. 2021. Features, Events, and Processes Assessment for the Additional Panels Performance Assessment. ERMS 574493. Carlsbad, NM: Sandia National Laboratories.

Kuhlman, K. 2010. Analysis Report for the CRA-2009 PABC Culebra Flow and Transport Calculations. ERMS 552951. Carlsbad, NM: Sandia National Laboratories.

Lord, D. L., and D. K. Rudeen. 2003. Sensitivity Analysis Report: Parts I and II: DRSPALL Version 1.00: Report for Conceptual Model Peer Review July 7–11. ERMS 524400. Carlsbad, NM: Sandia National Laboratories.

New Mexico Environment Department (NMED). 2023. WIPP Hazardous Waste Facility Permit. November 2023. Santa Fe, NM: New Mexico Environment Department Hazardous Waste Bureau.

Nielsen, S. 2024. Nuclear Waste Management Procedure NP 9-1 Analyses. Revision 12. Carlsbad, NM: Sandia National Laboratories.

Sjomeling, D. 2019. "2:30 Meeting Information," an email to Paul Shoemaker with the attachment "West Mains and Panels peer review info Final 091219.pdf." Nuclear Waste Partnership LLC, Carlsbad, New Mexico. October 17, 2019. ERMS 572682.

Stoelzel, D. M., and D. G. O'Brien. 1996. Analysis Package for the BRAGFLO Direct Release Calculations (Task 4) of the Performance Assessment Calculations Supporting the Compliance Certification Application (CCA), AP-029, Brine Release Calculations. ERMS 417870. Albuquerque, NM: Sandia National Laboratories.

U.S. Department of Energy (DOE) 2019. Title 40 CFR Part 191 Subparts B and C Compliance Recertification Application 2019 for the Waste Isolation Pilot. Carlsbad, NM: U.S. Department of Energy Waste Isolation Pilot Plant, Carlsbad Field Office.

Van Soest, G. D. 2018. Performance Assessment Inventory Report – 2018. LA-UR-18-31882, Revision 0. Los Alamos National Laboratory, Carlsbad, NM.

Ward, A. 2024a. Email to Steve Wagner. Subject: [EXTERNAL] RE: 12-panel PA to EPA by mid-February. Dated October 2, 2024. Carlsbad, NM: U.S. Department of Energy, Carlsbad Field Office.

Ward, A. 2024b. Email to Steve Wagner. Subject: [EXTERNAL] FW: EPA letter and the 12-panel PA for the PCR. Dated December 4, 2024. Carlsbad, NM: U.S. Department of Energy, Carlsbad Field Office.

WIPP Performance Assessment. 2024. Design Document and User Manual for DTRKMF, Version 2.00. ERMS 582254. Carlsbad, NM: Sandia National Laboratories.

Zeitler, T. R. 2019. Analysis Package for the Sensitivity of Releases to Input Parameters in the 2019 Compliance Recertification Application Performance Assessment (CRA-2019 PA). ERMS 571374. Carlsbad, NM: Sandia National Laboratories.

Zeitler, T. R. 2024. Planning Document for the CRA19 12-Panel (CRA19_12P) PA. Carlsbad, NM: Sandia National Laboratories.